# **ESTEC** and **NPL**
# GNSS stations relative calibration
# G1/G2 #1017-2024

**Michel Abgrall, Baptiste Chupin**

Observatoire de Paris

michel.abgrall@obspm.fr, baptiste.chupin@obspm.fr, caroline.lim@obspm.fr

February 4, 2025
Issue 1.1

## 1 Introduction.

### 1.1 General informations.

This calibration report released by LNE-SYRTE is about the G1/G2 relative calibration campaign of GNSS stations located in ESTEC and NPL. This campaign took place from 9 July 2024 (MJD 60500) to 30 October 2024 (MJD 60613). The report is built according to the Annex 4 of the document "BIPM guidelines for GNSS calibration" [1] and contains all the required informations, data, plots and results either required by BIPM in the frame of the CCTF Working Group on GNSS, or by BIPM and EURAMET in the frame of the Group1/Group2 calibration scheme. It also contains the uncertainty budget computation according to the Guidelines, which is showing whether the calibrated links used in the frame of the TAI computation would be in line with the conventional values.
This report is consistent with the capabilities that are included in Appendix C of the CIPM MRA drawn up by the CIPM. Under the CIPM MRA, all participating institutes recognize the validity of each other's calibration and measurement certificates for the quantities, ranges and measurement uncertainties specified in the KCDB (for details see `https://www.bipm.org/kcdb/`).
The first section of this document gives the introduction, the document structure, the list of acronyms and of the reference documents. Section 2 contains a summary of the results. Section 3 describes the equipment and operations during the calibration campaign. Section 4 provides all informations about data handling and calibration processing. Section 5 is about the calibration results between stations, and Section 6 is devoted to the uncertainty budgets computation. This document finish with an assessment of the stability of the GNSS reference station and of the traveling ones during this campaign in Section 7.
Annex A provides the required BIPM information sheets for all GNSS stations involved. Annex B shows the plots of the raw data together with the related TDEV. Annex C describes all the terms appearing in the uncertainty budgets.

### 1.2 Calibration report changes.

This is Issue 1.1 of the calibration report

### 1.3 Acronym list.

| | |
|---|---|
| ADEV: | Allan deviation, square root of AVAR |
| AVAR: | Allan variance or Two-sample variance |
| Beidou: | Chinese GNSS |
| BIPM: | Bureau International des Poids et Mesures |
| CCTF: | Consultative Committee on Time and Frequency |
| CGGTTS: | CCTF Global GNSS Time Transfer Standard format |
| CIPM: | Comité International des Poids et Mesures |
| CV: | Common-view |
| Galileo: | European Union GNSS |
| GFZ: | Geoforschungszentrum, Germany |
| GLONASS: | Russian GNSS |
| GNSS: | Global Navigation Satellite System |
| GPS: | United States of America GNSS |
| IGS: | International GNSS Service |
| LNE: | Laboratoire National de Métrologie et d'Essais, France |
| LNE-SYRTE: | French designated laboratory in charge of time and frequency units |
| MDEV: | Modified Allan deviation, square root of MVAR |
| MVAR: | Modified Allan variance |
| NA: | Not Applicable |
| NMI: | National Metrology Institute |
| NRCan: | National Resources Canada |
| OP: | Observatoire de Paris, France |
| PPP: | Precise Point Positioning |
| PPS: | Pulse per second |
| RINEX: | Receiver international exchange format for Geodesy |
| SYRTE: | Systèmes de Référence Temps-espace, OP laboratory where LNE-SYRTE is located |
| TDEV: | Time Allan deviation, square root of TVAR |
| TIC: | Time Interval Counter |
| TVAR: | Time Allan variance |

### 1.4 Reference documents.


[1] BIPM. *"BIPM guidelines for GNSS calibration"*. Version V4.0. 05/08/2021.

[2] G. D. Rovera, M. Abgrall, P. Uhrich, P. Defraigne, and B. Bertrand. "GNSS antenna multipath effects". In: *Proc. of the 31$^{st}$ European Frequency and time Forum (EFTF)*. Torino, Italy, 2018.

[3] G. D. Rovera, M. Siccardi, S. Römisch, and M. Abgrall. "Time delay measurements: estimation of the error budget". In: *Metrologia* 56.3 (2019).

[4] G. D. Rovera, M. Abgrall, P. Uhrich, and M. Siccardi. "Techniques of antenna cable delay measurement for GPS time transfer". In: *Proc. of the 5$^{th}$ International Colloquium on Scientific and Fundamental Aspects of the Galileo Programme*. Braunschweig, Germany, 27-29 October 2015.

[5] P. Uhrich and D. Valat. "GPS receiver relative calibration campaign preparation for Galileo In-Orbit Validation". In: *Proc. of the 24$^{th}$ European Frequency and time Forum (EFTF)*. Noordwijk, The Netherlands, April 2010.

[6] G. D. Rovera, J.-M. Torre, R. Sherwood, M. Abgrall, C. Courde, M. Laas-Bourez, and P. Uhrich. "Link calibration against receiver calibration: an assessment of GPS time transfer uncertainties". In: *Metrologia* 51.5 (2014), pp. 476–490.


## 2 Summary of the results.

This Section is a summary of the station relative calibration results. Table 1 provides the GPS P1-code and P2-code calibrated delays for ESTEC and NPL stations, from where the ionosphere-free linear combination P3 delays are computed, together with their related uncertainties according to the conventional values. Table 2 provides the corresponding results for Galileo E1-code, E5a-code calibrated and ionosphere-free combination E3. Table 3 provides the corresponding results for Beidou B1C-code, B2a-code calibrated and ionosphere-free combination B3. These results are fully valid for the period of the calibration campaign.
For ESTEC stations, if we compare the current results to the previous calibration performed by PTB, we find that the total delays are in agreement to better than 500 ps in P3 and to better than 1.3 ns in E3. For NPL stations, if we compare

the current results to the previous calibration performed by ROA, we find that the total delays are in agreement to better than 1.2 ns in P3 and to better than 1.3 ns in E3

Table 1: Summary of the stations GPS delays (all values in ns)

| **Station** | Measurement period | P1 delays | Combined uncertainty | P2 delays | Combined uncertainty | P3 delays | Combined uncertainty | Combined uncertainty [*] |
|---|---|---|---|---|---|---|---|---|
| ES07 | 60522–60527 | 28.062 | 0.7 | 24.720 | 0.7 | 33.228 | 0.7 | 2.5 |
| ES08 | 60522–60527 | 29.464 | 0.7 | 27.655 | 0.7 | 32.260 | 0.7 | 2.5 |
| ES09 | 60522–60527 | 19.240 | 0.7 | 16.202 | 0.7 | 23.936 | 0.7 | 2.5 |
| TR01 | 60522–60527 | 24.739 | 0.7 | 22.036 | 0.7 | 28.917 | 0.7 | 2.5 |
| NPL1 | 60571–60585 | -35.723 | 0.7 | -26.902 | 0.7 | -49.360 | 0.7 | 2.5 |
| NPL3 | 60571–60585 | 21.622 | 0.7 | 21.596 | 0.7 | 21.662 | 0.7 | 2.5 |
| NPL4 | 60571–60585 | 27.235 | 0.7 | 27.920 | 0.7 | 26.176 | 0.7 | 2.5 |
| NPL5 | 60571–60585 | 11.806 | 0.7 | 10.714 | 0.7 | 13.494 | 0.7 | 2.5 |

Table 2: Summary of the stations Galileo delays (all values in ns)

| **Station** | Measurement period | E1 delays | Combined uncertainty | E5a delays | Combined uncertainty | E3 delays | Combined uncertainty | Combined uncertainty [*] |
|---|---|---|---|---|---|---|---|---|
| ES07 | 60522–60527 | 30.410 | 0.7 | 30.098 | 0.6 | 30.803 | 0.7 | 2.5 |
| ES08 | 60522–60527 | 32.078 | 0.7 | 34.705 | 0.6 | 28.766 | 0.7 | 2.5 |
| ES09 | 60522–60527 | 19.822 | 0.7 | 22.875 | 0.7 | 15.973 | 0.7 | 2.5 |
| TR01 | 60522–60527 | 27.149 | 0.7 | 27.268 | 0.6 | 26.999 | 0.7 | 2.5 |
| NPL3 | 60571–60585 | 24.319 | 0.7 | 26.184 | 0.7 | 21.968 | 0.7 | 2.5 |
| NPL4 | 60571–60585 | 30.618 | 0.7 | 29.275 | 0.7 | 32.311 | 0.7 | 2.5 |
| NPL5 | 60571–60585 | 12.648 | 0.7 | 11.890 | 0.7 | 13.604 | 0.7 | 2.5 |

Table 3: Summary of the stations Beidou delays (all values in ns)

| **Station** | Measurement period | B1C delays | Combined uncertainty | B2a delays | Combined uncertainty | B3 delays | Combined uncertainty | Combined uncertainty [*] |
|---|---|---|---|---|---|---|---|---|
| ES07 | 60522–60527 | 30.214 | 0.7 | 29.528 | 0.6 | 31.079 | 0.7 | 2.5 |
| ES08 | 60522–60527 | 31.912 | 0.7 | 34.126 | 0.6 | 29.121 | 0.7 | 2.5 |
| ES09 | 60522–60527 | 19.295 | 0.7 | 21.952 | 0.7 | 15.946 | 0.7 | 2.5 |
| TR01 | 60522–60527 | 26.844 | 0.7 | 26.723 | 0.6 | 26.997 | 0.7 | 2.5 |
| NPL3 | 60571–60585 | 23.961 | 0.7 | 25.604 | 0.7 | 21.890 | 0.7 | 2.5 |
| NPL5 | 60571–60585 | 11.542 | 0.7 | 10.874 | 0.7 | 12.384 | 0.7 | 2.5 |

[*] Conventional combined uncertainty value for G1/G2 calibration, including the OP reference station combined uncertainty.

# 3 Description of equipment.

## 3.1 OP GNSS equipment.

OP73 is currently made of a Septentrio multichannel multi-GNSS PolaRx5-TR, a high quality 30 m antenna cable and a SepChoke B3/E6 multi-GNSS choke-ring antenna. This station was part of the last G1 calibration campaign (# 1001-2022), its delays having been computed by BIPM with P3, E3 and B3 time transfer conventional combined uncertainties of 1.8 ns for GPS and 1.5 ns for Galileo and Beidou, respectively.
The OP GNSS traveling equipment is made of two multi-GNSS Septentrio PolaRx5-TR main units called OP72 and OP74, connected to one single 50 m long antenna cable thanks to a power splitter, and to one single multi-GNSS Veraphase 6000 antenna.
All the OP PolaRx5-TR receivers involved in this calibration are operated with the PPS-In delay compensation disabled: the PPS-Out connectors define their reference point for refdelay measurements.

### 3.2 UTC(k) GNSS equipment.

The UTC(k) GNSS equipment to calibrate was depending on the visited site. The receiver main units were either Septentrio PolaRx5TR, or Dicom (company name today is Mesit) GTR50, GTR51 or GTR55. There were also different antennas. At ESTEC, ES08 and ES09 shared the same antenna. All the UTC(k) PolaRx5-TR receivers involved in this calibration are operated with the PPS-In delay compensation enabled: the PPS-In connectors define their reference point for refdelay measurements. Annex A contains the details about the local implementations in the visited stations. These stations were calibrated as G2 GNSS stations according to the BIPM Guidelines for the delays computations including the related combined uncertainties. We mention that the ESA TR01 station is a traveling equipment of ESOC, another center of ESA. This station is not used in the TAI network.

### 3.3 Summary of the involved equipment and planning.

Table 4 summarizes the equipment involved in the GNSS relative calibration campaign with highlighted traveling station measurement periods on each site.

Table 4: Description of equipment

| **Institute** | Status of equipement | MJD of measurement | Receiver type | BIPM code | RINEX name |
|---|---|---|---|---|---|
| OP | Traveling | NA – NA | Septentrio PolaRx5TR | OP72 | OP72 |
| OP | Traveling | NA – NA | Septentrio PolaRx5TR | OP74 | OP74 |
| OP | Groupe 1 Reference | 60500 – 60508 | Septentrio PolaRx5TR | OP73 | OP73 |
| OP | Groupe 1 Reference | 60605 – 60613 | Septentrio PolaRx5TR | OP73 | OP73 |
| ESTEC | Groupe 2 | 60522 – 60527 | Septentrio PolaRx5TR | ES07 | ES07 |
| ESTEC | Groupe 2 | 60522 – 60527 | Septentrio PolaRx5TR | ES08 | ES08 |
| ESTEC | Groupe 2 | 60522 – 60527 | Mesit GTR55 | ES09 | ES09 |
| ESTEC | Groupe 2/traveling ESOC | 60522 – 60527 | Septentrio PolaRx5TR | TR01 | TR01 |
| NPL | Groupe 2 | 60571 – 60585 | DICOM GTR50 | NPL1 | NPL1 |
| NPL | Groupe 2 | 60571 – 60585 | Septentrio PolaRx5TR | NPL3 | NPL3 |
| NPL | Groupe 2 | 60571 – 60585 | DICOM GTR51 | NPL4 | NPL4 |
| NPL | Groupe 2 | 60571 – 60585 | DICOM GTR55 | NPL5 | NPL5 |

## 4 Data and processing.

All OP collected raw Septentrio binary files (SBF) data are transformed into GNSS RINEX 3 format by using the Septentrio proprietary SBF2RIN software. Local receivers SBF and/or RINEX 3 and/or RINEX 2 data, together with CGGTTS files when they exist, are provided by the visited institution/laboratory. The calibration is consisting in building differential 30 s sampled CGGTTS data for each P1- and P2- codes for GPS, for each E1- and E5a- codes for Galileo and for each B1C- and B2a- codes for Beidou between pairs of receivers, for which we partly use the R2CGGTTS software developed by P. Defraigne (ORB). Another part of the calibration software is an original development by LNE-SYRTE. These CGGTTS differences are corrected by the known reference delay (REFDLY) and antenna cable delay (CABDLY) when available. In this case, the calibrated delays are for the ensemble receiver main unit plus antenna.
For each location, the coordinates of the antenna phase centers are especially computed for the calibration period from RINEX 2 files by using the NRCan PPP software. Unfortunately, this computation is limited to GPS phase center for L1 and L2 carrier frequencies. Galileo E1 carrier and Beidou B1C being equal to L1, we assume the phase centers are identical. But it is not the case for Galileo E5a and Beidou B2a compared to L2, and we can only approximate the Galileo E5a and Beidou B2a phase centers by using L2 one. The geometric correction between pairs of antenna phase centers for receivers in common-clock set-up is computed by using Rapid BRDC files provided by IGS.
Reference delays are measured against either the local UTC(k) physical reference point or the local time scale reference point at the trigger level currently used in the involved laboratories. The trigger level in LNE-SYRTE is 1.0 V. Antenna

cable delay is either obtained from dedicated measurements or included in the P1 and P2 delays, in the E1 and E5a delays and in the B1C and B2a delays when no value is available for this parameter. In this latter case, the CABDLY value is set to 0 in the parameter file, and the calibrated delays are for the ensemble receiver main unit plus antenna cable plus antenna.
For validation purposes, ionosphere-free linear combinations P3, E3 and B3 CGGTTS files are computed by using the R2CGGTTS software provided by P. Defraigne (ORB), and CV are built between pairs of receivers. This is more especially the case when we are using two traveling receivers in a visited location, in order to better assess the stability of this traveling ensemble all over the calibration campaign. The conservative estimated value for the traveling equipment stability during such a campaign is typically chosen for each code as the maximum between the misclosure between the start and the end of the campaign and the average offset between both traveling receivers as measured in each location.
As conservative estimate, the noise of the P1 and P2 differences, of the E1 and E5a differences and of the B1C and B2a differences is obtained from the highest value of the one-sigma statistical uncertainty of the TDEV at 1 d, issued from a linear interpolation between consecutive TDEV points when required. In the case there is not enough data to compute a TDEV at 1 d, the upper limit of the last error bar available is considered as noise of the raw differences. The noise of P3, E3 and B3 data is issued from a similar analysis on TDEV data.

# 5 Results of raw data processing.

Table 5, table 6 and table 7 provide a summary of all the delays involved in the GPS codes, in the Galileo codes and in the Beidou codes, respectively. The tables provide first the calibration of the traveling stations OP72 and OP74 against the reference station OP73 at the start and the end of the campaign, from which we estimate, from an average, the internal delays to be accounted for during measurements at the remote site. Then the tables show the calibration of the visited stations against these traveling receivers. The calibration results summarized in tables 1, 2 and 3 are computed from the average delays of both traveling receivers. The misclosure was found at 170 ps or below for each GPS, Galileo and Beidou codes which demonstrates the good stability of the traveling equipment during the campaign. As typically expected, the noise estimates from the TDEVs are about or below 200 ps, and are hence remaining low enough in the uncertainty budgets (see Section 6). All the plots of P1, P2, E1, E5a, B1C and B2a differences are provided in Annex B, together with the related TDEV analysis. The P3, E3 and B3 computed by using the results of the calibration and the related TDEV are also made available in Annex B.

Table 5: Summary of **GPS** delays (all values in ns)

| Receiver | Reference | MJD of Measurement | REFDLY | CABDLY | P1 DLY | TDEV | P2 DLY | TDEV | P3 DLY | TDEV |
|---|---|---|---|---|---|---|---|---|---|---|
| OP73 | Ref | 60500 – 60508 | 85.2 | 129.6 | 29.550 | NA | 26.020 | NA | 35.006 | NA |
| OP72 | OP73 | 60500 – 60508 | 93.3 | 0.0 | 224.238 | 0.030 | 222.135 | 0.035 | 227.489 | 0.107 |
| OP74 | OP73 | 60500 – 60508 | 111.3 | 0.0 | 224.913 | 0.029 | 222.872 | 0.035 | 228.068 | 0.105 |
| OP73 | Ref | 60605 – 60613 | 85.2 | 129.6 | 29.550 | NA | 26.020 | NA | 35.006 | NA |
| OP72 | OP73 | 60605 – 60613 | 93.4 | 0.0 | 224.145 | 0.025 | 221.990 | 0.041 | 227.476 | 0.071 |
| OP74 | OP73 | 60605 – 60613 | 111.4 | 0.0 | 224.789 | 0.024 | 222.693 | 0.042 | 228.029 | 0.072 |
| OP72 | Ref | 60522 – 60527 | 50.1 | 0.0 | 224.191 | NA | 222.062 | NA | 227.482 | NA |
| ES07 | OP72 | 60522 – 60527 | 16.1 | 210.3 | 28.038 | 0.019 | 24.689 | 0.027 | 33.215 | 0.055 |
| ES08 | OP72 | 60522 – 60527 | 16.1 | 251.0 | 29.441 | 0.025 | 27.624 | 0.020 | 32.250 | 0.077 |
| ES09 | OP72 | 60522 – 60527 | 20.8 | 253.3 | 19.216 | 0.047 | 16.172 | 0.083 | 23.921 | 0.093 |
| TR01 | OP72 | 60522 – 60527 | 11.3 | 358.6 | 24.715 | 0.031 | 22.006 | 0.075 | 28.902 | 0.136 |
| OP74 | Ref | 60522 – 60527 | 34.7 | 0.0 | 224.851 | NA | 222.782 | NA | 228.049 | NA |
| ES07 | OP74 | 60522 – 60527 | 16.1 | 210.3 | 28.086 | 0.019 | 24.751 | 0.027 | 33.241 | 0.056 |
| ES08 | OP74 | 60522 – 60527 | 16.1 | 251.0 | 29.488 | 0.026 | 27.686 | 0.020 | 32.273 | 0.073 |
| ES09 | OP74 | 60522 – 60527 | 20.8 | 253.3 | 19.263 | 0.045 | 16.233 | 0.083 | 23.947 | 0.088 |
| TR01 | OP74 | 60522 – 60527 | 11.3 | 358.6 | 24.763 | 0.030 | 22.067 | 0.074 | 28.930 | 0.138 |
| OP72 | Ref | 60571 – 60585 | 111.4 | 0.0 | 224.191 | NA | 222.062 | NA | 227.482 | NA |
| NPL1 | OP72 | 60571 – 60585 | 68.4 | 251.5 | -35.770 | 0.033 | -26.935 | 0.043 | -49.429 | 0.125 |
| NPL3 | OP72 | 60571 – 60585 | 73.3 | 294.7 | 21.575 | 0.067 | 21.562 | 0.058 | 21.595 | 0.163 |
| NPL4 | OP72 | 60571 – 60585 | 63.5 | 336.2 | 27.188 | 0.037 | 27.887 | 0.076 | 26.108 | 0.107 |
| NPL5 | OP72 | 60571 – 60585 | 65.4 | 261.2 | 11.759 | 0.070 | 10.681 | 0.116 | 13.425 | 0.095 |
| OP74 | Ref | 60571 – 60585 | 129.2 | 0.0 | 224.851 | NA | 222.782 | NA | 228.049 | NA |
| NPL1 | OP74 | 60571 – 60585 | 68.4 | 251.5 | -35.675 | 0.032 | -26.869 | 0.043 | -49.289 | 0.122 |
| NPL3 | OP74 | 60571 – 60585 | 73.3 | 294.7 | 21.669 | 0.067 | 21.629 | 0.059 | 21.731 | 0.161 |
| NPL4 | OP74 | 60571 – 60585 | 63.5 | 336.2 | 27.282 | 0.036 | 27.954 | 0.076 | 26.243 | 0.104 |
| NPL5 | OP74 | 60571 – 60585 | 65.4 | 261.2 | 11.853 | 0.070 | 10.747 | 0.115 | 13.563 | 0.092 |

Table 6: Summary of **Galileo** delays (all values in ns)

| Receiver | Reference | MJD of Measurement | REFDLY | CABDLY | E1 DLY | TDEV | E5a DLY | TDEV | E3 DLY | TDEV |
|---|---|---|---|---|---|---|---|---|---|---|
| OP73 | Ref | 60500 – 60508 | 85.2 | 129.6 | 31.780 | NA | 31.520 | NA | 32.108 | NA |
| OP72 | OP73 | 60500 – 60508 | 93.3 | 0.0 | 226.595 | 0.036 | 225.976 | 0.047 | 227.375 | 0.073 |
| OP74 | OP73 | 60500 – 60508 | 111.3 | 0.0 | 227.412 | 0.035 | 226.730 | 0.046 | 228.272 | 0.073 |
| OP73 | Ref | 60605 – 60613 | 85.2 | 129.6 | 31.780 | NA | 31.520 | NA | 32.108 | NA |
| OP72 | OP73 | 60605 – 60613 | 93.4 | 0.0 | 226.528 | 0.028 | 226.017 | 0.035 | 227.172 | 0.076 |
| OP74 | OP73 | 60605 – 60613 | 111.4 | 0.0 | 227.313 | 0.028 | 226.744 | 0.034 | 228.030 | 0.077 |
| OP72 | Ref | 60522 – 60527 | 50.1 | 0.0 | 226.561 | NA | 225.997 | NA | 227.272 | NA |
| ES07 | OP72 | 60522 – 60527 | 16.1 | 210.3 | 30.387 | 0.036 | 30.068 | 0.044 | 30.789 | 0.097 |
| ES08 | OP72 | 60522 – 60527 | 16.1 | 251.0 | 32.054 | 0.025 | 34.675 | 0.041 | 28.750 | 0.047 |
| ES09 | OP72 | 60522 – 60527 | 20.8 | 253.3 | 19.799 | 0.065 | 22.845 | 0.100 | 15.959 | 0.076 |
| TR01 | OP72 | 60522 – 60527 | 11.3 | 358.6 | 27.125 | 0.030 | 27.238 | 0.044 | 26.983 | 0.080 |
| OP74 | Ref | 60522 – 60527 | 34.7 | 0.0 | 227.363 | NA | 226.737 | NA | 228.152 | NA |
| ES07 | OP74 | 60522 – 60527 | 16.1 | 210.3 | 30.434 | 0.035 | 30.128 | 0.044 | 30.820 | 0.094 |
| ES08 | OP74 | 60522 – 60527 | 16.1 | 251.0 | 32.102 | 0.025 | 34.735 | 0.041 | 28.783 | 0.047 |
| ES09 | OP74 | 60522 – 60527 | 20.8 | 253.3 | 19.846 | 0.065 | 22.905 | 0.099 | 15.990 | 0.076 |
| TR01 | OP74 | 60522 – 60527 | 11.3 | 358.6 | 27.173 | 0.031 | 27.299 | 0.043 | 27.014 | 0.080 |
| OP72 | Ref | 60571 – 60585 | 111.4 | 0.0 | 226.561 | NA | 225.997 | NA | 227.272 | NA |
| NPL3 | OP72 | 60571 – 60585 | 73.3 | 294.7 | 24.269 | 0.056 | 26.174 | 0.108 | 21.868 | 0.114 |
| NPL4 | OP72 | 60571 – 60585 | 63.5 | 336.2 | 30.568 | 0.054 | 29.264 | 0.059 | 32.212 | 0.139 |
| NPL5 | OP72 | 60571 – 60585 | 65.4 | 261.2 | 12.598 | 0.076 | 11.880 | 0.133 | 13.503 | 0.098 |
| OP74 | Ref | 60571 – 60585 | 129.2 | 0.0 | 227.363 | NA | 226.737 | NA | 228.152 | NA |
| NPL3 | OP74 | 60571 – 60585 | 73.3 | 294.7 | 24.369 | 0.056 | 26.195 | 0.108 | 22.067 | 0.116 |
| NPL4 | OP74 | 60571 – 60585 | 63.5 | 336.2 | 30.667 | 0.053 | 29.286 | 0.058 | 32.408 | 0.138 |
| NPL5 | OP74 | 60571 – 60585 | 65.4 | 261.2 | 12.698 | 0.076 | 11.901 | 0.133 | 13.703 | 0.094 |

Table 7: Summary of **Beidou** delays (all values in ns)

| Receiver | Reference | MJD of Measurement | REFDLY | CABDLY | B1C DLY | TDEV | B2a DLY | TDEV | B3 DLY | TDEV |
|---|---|---|---|---|---|---|---|---|---|---|
| OP73 | Ref | 60500 – 60508 | 85.2 | 129.6 | 31.630 | NA | 30.930 | NA | 32.512 | NA |
| OP72 | OP73 | 60500 – 60508 | 93.3 | 0.0 | 226.375 | 0.040 | 225.409 | 0.035 | 227.593 | 0.081 |
| OP74 | OP73 | 60500 – 60508 | 111.3 | 0.0 | 227.283 | 0.039 | 226.165 | 0.034 | 228.692 | 0.080 |
| OP73 | Ref | 60605 – 60613 | 85.2 | 129.6 | 31.630 | NA | 30.930 | NA | 32.512 | NA |
| OP72 | OP73 | 60605 – 60613 | 93.4 | 0.0 | 226.308 | 0.029 | 225.436 | 0.029 | 227.407 | 0.069 |
| OP74 | OP73 | 60605 – 60613 | 111.4 | 0.0 | 227.186 | 0.028 | 226.164 | 0.029 | 228.474 | 0.065 |
| OP72 | Ref | 60522 – 60527 | 50.1 | 0.0 | 226.341 | NA | 225.422 | NA | 227.499 | NA |
| ES07 | OP72 | 60522 – 60527 | 16.1 | 210.3 | 30.191 | 0.028 | 29.499 | 0.040 | 31.063 | 0.093 |
| ES08 | OP72 | 60522 – 60527 | 16.1 | 251.0 | 31.889 | 0.027 | 34.097 | 0.034 | 29.106 | 0.069 |
| ES09 | OP72 | 60522 – 60527 | 20.8 | 253.3 | 19.271 | 0.075 | 21.922 | 0.098 | 15.929 | 0.201 |
| TR01 | OP72 | 60522 – 60527 | 11.3 | 358.6 | 26.820 | 0.025 | 26.693 | 0.066 | 26.980 | 0.089 |
| OP74 | Ref | 60522 – 60527 | 34.7 | 0.0 | 227.235 | NA | 226.164 | NA | 228.585 | NA |
| ES07 | OP74 | 60522 – 60527 | 16.1 | 210.3 | 30.236 | 0.030 | 29.558 | 0.040 | 31.091 | 0.094 |
| ES08 | OP74 | 60522 – 60527 | 16.1 | 251.0 | 31.935 | 0.028 | 34.156 | 0.034 | 29.135 | 0.075 |
| ES09 | OP74 | 60522 – 60527 | 20.8 | 253.3 | 19.319 | 0.076 | 21.982 | 0.097 | 15.962 | 0.201 |
| TR01 | OP74 | 60522 – 60527 | 11.3 | 358.6 | 26.867 | 0.026 | 26.753 | 0.065 | 27.011 | 0.094 |
| OP72 | Ref | 60571 – 60585 | 111.4 | 0.0 | 226.341 | NA | 225.422 | NA | 227.499 | NA |
| NPL3 | OP72 | 60571 – 60585 | 73.3 | 294.7 | 23.912 | 0.062 | 25.593 | 0.096 | 21.793 | 0.117 |
| NPL5 | OP72 | 60571 – 60585 | 65.4 | 261.2 | 11.492 | 0.113 | 10.863 | 0.146 | 12.285 | 0.186 |
| OP74 | Ref | 60571 – 60585 | 129.2 | 0.0 | 227.235 | NA | 226.164 | NA | 228.585 | NA |
| NPL3 | OP74 | 60571 – 60585 | 73.3 | 294.7 | 24.010 | 0.063 | 25.614 | 0.095 | 21.988 | 0.121 |
| NPL5 | OP74 | 60571 – 60585 | 65.4 | 261.2 | 11.593 | 0.114 | 10.885 | 0.146 | 12.486 | 0.190 |

# 6 Uncertainty budgets.

Tables 8 to 27 are providing the uncertainty budget for the computed internal delays of the ESTEC and NPL stations for GPS, Galileo and Beidou, respectively. All the values are given in ns. See Annex C for detailed explanations about the different terms.
The Type A uncertainty on measured codes is estimated from the high value of the 1 sigma statistical uncertainty of the TDEV(1 d). To be conservative, we take the largest value obtained within the two traveling receivers. The Type A uncertainty of the difference between codes is the quadratic sum between both estimations. The P3, E3 and B3 Type A uncertainties are estimated from the high value of the 1 sigma statistical uncertainty of the related TDEV(1 d). All TDEV plots are in Annex B.
To estimate the misclosure, we first compute the deviation from closure between the traveling stations OP72 and OP74, and the reference station OP73 for each GNSS code. We then calculate the average of these values, taken as positive.
The GPS P3 misclosure is estimated by applying to the misclosure values computed for P1- and P2- code the ionosphere-free linear combination formula: P3 = P1 + 1.546 × (P1 - P2)
The Galileo E3 misclosure is estimated by applying to the misclosure values computed for E1- and E5a- code the ionosphere-free linear combination formula:
E3 = E1 + 1.261 × (E1 - E5a)
The Beidou B3 misclosure is estimated by applying to the misclosure values computed for B1C- and B2c- code the ionosphere-free linear combination formula:
B3 = B1C + 1.261 × (B1C - B2a)
It was not necessary to measure separately the antenna cable delays (CABDLY) of the traveling equipment which remained in the same configuration at OP and at the visited site. Therefore the corresponding uncertainties are expected to be negligible.
The delay of the antenna cables of the ESTEC and NPL stations has not been measured. Calibration was done using prior antenna cable delay measurement values, provided by the visited laboratories. There is therefore no uncertainty associated with the antenna cable. The uncertainty of the calibrations correspond to that of the overall calibrations (internal delay + antenna + antenna cable).

Table 8: **ES07** uncertainty budget for **GPS** calibrated delays (all values in ns)

| Uncertainty type | P1 | P2 | P1-P2 | P3 | Description |
|---|---|---|---|---|---|
| $u_a$(Reference) | 0.030 | 0.042 | 0.051 | 0.107 | Largest TDEV(1 d) sigma between the start and the end of OP72 or OP74 against OP73 |
| $u_a$(ES07) | 0.019 | 0.027 | 0.034 | 0.056 | Largest TDEV(1 d) sigma of offset between visited station and OP72 or OP74 |
| Type A uncertainties | | | | | |
| $u_a$ | 0.036 | 0.050 | 0.062 | 0.121 | Visited against reference |
| Misclosure | | | | | |
| $u_{b,1}$ | 0.110 | 0.163 | 0.054 | 0.027 | Actual misclosure offset |
| Systematic components related to RAWDIF | | | | | |
| $u_{b,11}$ | 0.200 | 0.200 | 0.200 | 0.200 | Position error at OP |
| $u_{b,12}$ | 0.200 | 0.200 | 0.200 | 0.200 | Position error at visited site |
| $u_{b,13}$ | 0.200 | 0.200 | 0.200 | 0.200 | Multipaths at OP |
| $u_{b,14}$ | 0.200 | 0.200 | 0.200 | 0.200 | Multipaths at visited site |
| Link of the traveling system to local time scale | | | | | |
| $u_{b,21}$ | 0.220 | 0.220 | | 0.220 | REFDLY at OP |
| $u_{b,22}$ | 0.220 | 0.220 | | 0.220 | REFDLY at visited site |
| $u_{b,TOT}$ | 0.519 | 0.533 | 0.404 | 0.508 | |
| Link of the reference system to UTC(OP) | | | | | |
| $u_{b,31}$ | 0.220 | 0.220 | | 0.220 | REFDLY at OP |
| Link of the visited system to its local time scale | | | | | |
| $u_{b,32}$ | 0.220 | 0.220 | | 0.220 | REFDLY at visited site |
| Antenna cable delays | | | | | |
| $u_{b,41}$ | 0.000 | 0.000 | | 0.000 | CABDLY at OP |
| $u_{b,42}$ | 0.000 | 0.000 | | 0.000 | CABDLY at visited site |
| Type B uncertainties | | | | | |
| $u_{b,SYS}$ | 0.606 | 0.618 | | 0.596 | Quadratic sum of $u_b$ |
| Combined uncertainties | | | | | |
| $u_{CAL0}$ | 0.608 | 0.621 | | 0.609 | Composed of $u_a$ and $u_{b,SYS}$ |

Table 9: **ES08** uncertainty budget for **GPS** calibrated delays (all values in ns)

| Uncertainty type | P1 | P2 | P1-P2 | P3 | Description |
|---|---|---|---|---|---|
| $u_a$(Reference) | 0.030 | 0.042 | 0.051 | 0.107 | Largest TDEV(1 d) sigma between the start and the end of OP72 or OP74 against OP73 |
| $u_a$(ES08) | 0.026 | 0.020 | 0.033 | 0.077 | Largest TDEV(1 d) sigma of offset between visited station and OP72 or OP74 |
| Type A uncertainties | | | | | |
| $u_a$ | 0.040 | 0.047 | 0.061 | 0.132 | Visited against reference |
| Misclosure | | | | | |
| $u_{b,1}$ | 0.110 | 0.163 | 0.054 | 0.027 | Actual misclosure offset |
| Systematic components related to RAWDIF | | | | | |
| $u_{b,11}$ | 0.200 | 0.200 | 0.200 | 0.200 | Position error at OP |
| $u_{b,12}$ | 0.200 | 0.200 | 0.200 | 0.200 | Position error at visited site |
| $u_{b,13}$ | 0.200 | 0.200 | 0.200 | 0.200 | Multipaths at OP |
| $u_{b,14}$ | 0.200 | 0.200 | 0.200 | 0.200 | Multipaths at visited site |
| Link of the traveling system to local time scale | | | | | |
| $u_{b,21}$ | 0.220 | 0.220 | | 0.220 | REFDLY at OP |
| $u_{b,22}$ | 0.220 | 0.220 | | 0.220 | REFDLY at visited site |
| $u_{b,TOT}$ | 0.519 | 0.533 | 0.404 | 0.508 | |
| Link of the reference system to UTC(OP) | | | | | |
| $u_{b,31}$ | 0.220 | 0.220 | | 0.220 | REFDLY at OP |
| Link of the visited system to its local time scale | | | | | |
| $u_{b,32}$ | 0.220 | 0.220 | | 0.220 | REFDLY at visited site |
| Antenna cable delays | | | | | |
| $u_{b,41}$ | 0.000 | 0.000 | | 0.000 | CABDLY at OP |
| $u_{b,42}$ | 0.000 | 0.000 | | 0.000 | CABDLY at visited site |
| Type B uncertainties | | | | | |
| $u_{b,SYS}$ | 0.606 | 0.618 | | 0.596 | Quadratic sum of $u_b$ |
| Combined uncertainties | | | | | |
| $u_{CAL0}$ | 0.608 | 0.620 | | 0.611 | Composed of $u_a$ and $u_{b,SYS}$ |

Table 10: **ES09** uncertainty budget for **GPS** calibrated delays (all values in ns)

| Uncertainty type | P1 | P2 | P1-P2 | P3 | Description |
|---|---|---|---|---|---|
| $u_a$(Reference) | 0.030 | 0.042 | 0.051 | 0.107 | Largest TDEV(1 d) sigma between the start and the end of OP72 or OP74 against OP73 |
| $u_a$(ES09) | 0.047 | 0.083 | 0.096 | 0.093 | Largest TDEV(1 d) sigma of offset between visited station and OP72 or OP74 |
| Type A uncertainties | | | | | |
| $u_a$ | 0.056 | 0.094 | 0.109 | 0.142 | Visited against reference |
| Misclosure | | | | | |
| $u_{b,1}$ | 0.110 | 0.163 | 0.054 | 0.027 | Actual misclosure offset |
| Systematic components related to RAWDIF | | | | | |
| $u_{b,11}$ | 0.200 | 0.200 | 0.200 | 0.200 | Position error at OP |
| $u_{b,12}$ | 0.200 | 0.200 | 0.200 | 0.200 | Position error at visited site |
| $u_{b,13}$ | 0.200 | 0.200 | 0.200 | 0.200 | Multipaths at OP |
| $u_{b,14}$ | 0.200 | 0.200 | 0.200 | 0.200 | Multipaths at visited site |
| Link of the traveling system to local time scale | | | | | |
| $u_{b,21}$ | 0.220 | 0.220 | | 0.220 | REFDLY at OP |
| $u_{b,22}$ | 0.220 | 0.220 | | 0.220 | REFDLY at visited site |
| $u_{b,TOT}$ | 0.519 | 0.533 | 0.404 | 0.508 | |
| Link of the reference system to UTC(OP) | | | | | |
| $u_{b,31}$ | 0.220 | 0.220 | | 0.220 | REFDLY at OP |
| Link of the visited system to its local time scale | | | | | |
| $u_{b,32}$ | 0.220 | 0.220 | | 0.220 | REFDLY at visited site |
| Antenna cable delays | | | | | |
| $u_{b,41}$ | 0.000 | 0.000 | | 0.000 | CABDLY at OP |
| $u_{b,42}$ | 0.000 | 0.000 | | 0.000 | CABDLY at visited site |
| Type B uncertainties | | | | | |
| $u_{b,SYS}$ | 0.606 | 0.618 | | 0.596 | Quadratic sum of $u_b$ |
| Combined uncertainties | | | | | |
| $u_{CAL0}$ | 0.609 | 0.626 | | 0.613 | Composed of $u_a$ and $u_{b,SYS}$ |

Table 11: **TR01** uncertainty budget for **GPS** calibrated delays (all values in ns)

| Uncertainty type | P1 | P2 | P1-P2 | P3 | Description |
|---|---|---|---|---|---|
| $u_a$(Reference) | 0.030 | 0.042 | 0.051 | 0.107 | Largest TDEV(1 d) sigma between the start and the end of OP72 or OP74 against OP73 |
| $u_a$(TR01) | 0.031 | 0.075 | 0.082 | 0.138 | Largest TDEV(1 d) sigma of offset between visited station and OP72 or OP74 |
| Type A uncertainties | | | | | |
| $u_a$ | 0.044 | 0.086 | 0.097 | 0.175 | Visited against reference |
| Misclosure | | | | | |
| $u_{b,1}$ | 0.110 | 0.163 | 0.054 | 0.027 | Actual misclosure offset |
| Systematic components related to RAWDIF | | | | | |
| $u_{b,11}$ | 0.200 | 0.200 | 0.200 | 0.200 | Position error at OP |
| $u_{b,12}$ | 0.200 | 0.200 | 0.200 | 0.200 | Position error at visited site |
| $u_{b,13}$ | 0.200 | 0.200 | 0.200 | 0.200 | Multipaths at OP |
| $u_{b,14}$ | 0.200 | 0.200 | 0.200 | 0.200 | Multipaths at visited site |
| Link of the traveling system to local time scale | | | | | |
| $u_{b,21}$ | 0.220 | 0.220 | | 0.220 | REFDLY at OP |
| $u_{b,22}$ | 0.220 | 0.220 | | 0.220 | REFDLY at visited site |
| $u_{b,TOT}$ | 0.519 | 0.533 | 0.404 | 0.508 | |
| Link of the reference system to UTC(OP) | | | | | |
| $u_{b,31}$ | 0.220 | 0.220 | | 0.220 | REFDLY at OP |
| Link of the visited system to its local time scale | | | | | |
| $u_{b,32}$ | 0.220 | 0.220 | | 0.220 | REFDLY at visited site |
| Antenna cable delays | | | | | |
| $u_{b,41}$ | 0.000 | 0.000 | | 0.000 | CABDLY at OP |
| $u_{b,42}$ | 0.000 | 0.000 | | 0.000 | CABDLY at visited site |
| Type B uncertainties | | | | | |
| $u_{b,SYS}$ | 0.606 | 0.618 | | 0.596 | Quadratic sum of $u_b$ |
| Combined uncertainties | | | | | |
| $u_{CAL0}$ | 0.608 | 0.624 | | 0.622 | Composed of $u_a$ and $u_{b,SYS}$ |

Table 12: **NPL1** uncertainty budget for **GPS** calibrated delays (all values in ns)

| Uncertainty type | P1 | P2 | P1-P2 | P3 | Description |
|---|---|---|---|---|---|
| $u_a$(Reference) | 0.030 | 0.042 | 0.051 | 0.107 | Largest TDEV(1 d) sigma between the start and the end of OP72 or OP74 against OP73 |
| $u_a$(NPL1) | 0.033 | 0.043 | 0.055 | 0.125 | Largest TDEV(1 d) sigma of offset between visited station and OP72 or OP74 |
| Type A uncertainties | | | | | |
| $u_a$ | 0.045 | 0.061 | 0.076 | 0.165 | Visited against reference |
| Misclosure | | | | | |
| $u_{b,1}$ | 0.110 | 0.163 | 0.054 | 0.027 | Actual misclosure offset |
| Systematic components related to RAWDIF | | | | | |
| $u_{b,11}$ | 0.200 | 0.200 | 0.200 | 0.200 | Position error at OP |
| $u_{b,12}$ | 0.200 | 0.200 | 0.200 | 0.200 | Position error at visited site |
| $u_{b,13}$ | 0.200 | 0.200 | 0.200 | 0.200 | Multipaths at OP |
| $u_{b,14}$ | 0.200 | 0.200 | 0.200 | 0.200 | Multipaths at visited site |
| Link of the traveling system to local time scale | | | | | |
| $u_{b,21}$ | 0.220 | 0.220 | | 0.220 | REFDLY at OP |
| $u_{b,22}$ | 0.220 | 0.220 | | 0.220 | REFDLY at visited site |
| $u_{b,TOT}$ | 0.519 | 0.533 | 0.404 | 0.508 | |
| Link of the reference system to UTC(OP) | | | | | |
| $u_{b,31}$ | 0.220 | 0.220 | | 0.220 | REFDLY at OP |
| Link of the visited system to its local time scale | | | | | |
| $u_{b,32}$ | 0.220 | 0.220 | | 0.220 | REFDLY at visited site |
| Antenna cable delays | | | | | |
| $u_{b,41}$ | 0.000 | 0.000 | | 0.000 | CABDLY at OP |
| $u_{b,42}$ | 0.000 | 0.000 | | 0.000 | CABDLY at visited site |
| Type B uncertainties | | | | | |
| $u_{b,SYS}$ | 0.606 | 0.618 | | 0.596 | Quadratic sum of $u_b$ |
| Combined uncertainties | | | | | |
| $u_{CAL0}$ | 0.608 | 0.622 | | 0.619 | Composed of $u_a$ and $u_{b,SYS}$ |

Table 13: **NPL3** uncertainty budget for **GPS** calibrated delays (all values in ns)

| Uncertainty type | P1 | P2 | P1-P2 | P3 | Description |
|---|---|---|---|---|---|
| $u_a$(Reference) | 0.030 | 0.042 | 0.051 | 0.107 | Largest TDEV(1 d) sigma between the start and the end of OP72 or OP74 against OP73 |
| $u_a$(NPL3) | 0.067 | 0.059 | 0.090 | 0.163 | Largest TDEV(1 d) sigma of offset between visited station and OP72 or OP74 |
| Type A uncertainties | | | | | |
| $u_a$ | 0.074 | 0.073 | 0.104 | 0.195 | Visited against reference |
| Misclosure | | | | | |
| $u_{b,1}$ | 0.110 | 0.163 | 0.054 | 0.027 | Actual misclosure offset |
| Systematic components related to RAWDIF | | | | | |
| $u_{b,11}$ | 0.200 | 0.200 | 0.200 | 0.200 | Position error at OP |
| $u_{b,12}$ | 0.200 | 0.200 | 0.200 | 0.200 | Position error at visited site |
| $u_{b,13}$ | 0.200 | 0.200 | 0.200 | 0.200 | Multipaths at OP |
| $u_{b,14}$ | 0.200 | 0.200 | 0.200 | 0.200 | Multipaths at visited site |
| Link of the traveling system to local time scale | | | | | |
| $u_{b,21}$ | 0.220 | 0.220 | | 0.220 | REFDLY at OP |
| $u_{b,22}$ | 0.220 | 0.220 | | 0.220 | REFDLY at visited site |
| $u_{b,TOT}$ | 0.519 | 0.533 | 0.404 | 0.508 | |
| Link of the reference system to UTC(OP) | | | | | |
| $u_{b,31}$ | 0.220 | 0.220 | | 0.220 | REFDLY at OP |
| Link of the visited system to its local time scale | | | | | |
| $u_{b,32}$ | 0.220 | 0.220 | | 0.220 | REFDLY at visited site |
| Antenna cable delays | | | | | |
| $u_{b,41}$ | 0.000 | 0.000 | | 0.000 | CABDLY at OP |
| $u_{b,42}$ | 0.000 | 0.000 | | 0.000 | CABDLY at visited site |
| Type B uncertainties | | | | | |
| $u_{b,SYS}$ | 0.606 | 0.618 | | 0.596 | Quadratic sum of $u_b$ |
| Combined uncertainties | | | | | |
| $u_{CAL0}$ | 0.611 | 0.623 | | 0.628 | Composed of $u_a$ and $u_{b,SYS}$ |

Table 14: **NPL4** uncertainty budget for **GPS** calibrated delays (all values in ns)

| Uncertainty type | P1 | P2 | P1-P2 | P3 | Description |
|---|---|---|---|---|---|
| $u_a$(Reference) | 0.030 | 0.042 | 0.051 | 0.107 | Largest TDEV(1 d) sigma between the start and the end of OP72 or OP74 against OP73 |
| $u_a$(NPL4) | 0.037 | 0.076 | 0.085 | 0.107 | Largest TDEV(1 d) sigma of offset between visited station and OP72 or OP74 |
| Type A uncertainties | | | | | |
| $u_a$ | 0.048 | 0.087 | 0.100 | 0.152 | Visited against reference |
| Misclosure | | | | | |
| $u_{b,1}$ | 0.110 | 0.163 | 0.054 | 0.027 | Actual misclosure offset |
| Systematic components related to RAWDIF | | | | | |
| $u_{b,11}$ | 0.200 | 0.200 | 0.200 | 0.200 | Position error at OP |
| $u_{b,12}$ | 0.200 | 0.200 | 0.200 | 0.200 | Position error at visited site |
| $u_{b,13}$ | 0.200 | 0.200 | 0.200 | 0.200 | Multipaths at OP |
| $u_{b,14}$ | 0.200 | 0.200 | 0.200 | 0.200 | Multipaths at visited site |
| Link of the traveling system to local time scale | | | | | |
| $u_{b,21}$ | 0.220 | 0.220 | | 0.220 | REFDLY at OP |
| $u_{b,22}$ | 0.220 | 0.220 | | 0.220 | REFDLY at visited site |
| $u_{b,TOT}$ | 0.519 | 0.533 | 0.404 | 0.508 | |
| Link of the reference system to UTC(OP) | | | | | |
| $u_{b,31}$ | 0.220 | 0.220 | | 0.220 | REFDLY at OP |
| Link of the visited system to its local time scale | | | | | |
| $u_{b,32}$ | 0.220 | 0.220 | | 0.220 | REFDLY at visited site |
| Antenna cable delays | | | | | |
| $u_{b,41}$ | 0.000 | 0.000 | | 0.000 | CABDLY at OP |
| $u_{b,42}$ | 0.000 | 0.000 | | 0.000 | CABDLY at visited site |
| Type B uncertainties | | | | | |
| $u_{b,SYS}$ | 0.606 | 0.618 | | 0.596 | Quadratic sum of $u_b$ |
| Combined uncertainties | | | | | |
| $u_{CAL0}$ | 0.608 | 0.625 | | 0.616 | Composed of $u_a$ and $u_{b,SYS}$ |

Table 15: **NPL5** uncertainty budget for **GPS** calibrated delays (all values in ns)

| Uncertainty type | P1 | P2 | P1-P2 | P3 | Description |
|---|---|---|---|---|---|
| $u_a$(Reference) | 0.030 | 0.042 | 0.051 | 0.107 | Largest TDEV(1 d) sigma between the start and the end of OP72 or OP74 against OP73 |
| $u_a$(NPL5) | 0.070 | 0.116 | 0.136 | 0.095 | Largest TDEV(1 d) sigma of offset between visited station and OP72 or OP74 |
| Type A uncertainties | | | | | |
| $u_a$ | 0.077 | 0.124 | 0.146 | 0.144 | Visited against reference |
| Misclosure | | | | | |
| $u_{b,1}$ | 0.110 | 0.163 | 0.054 | 0.027 | Actual misclosure offset |
| Systematic components related to RAWDIF | | | | | |
| $u_{b,11}$ | 0.200 | 0.200 | 0.200 | 0.200 | Position error at OP |
| $u_{b,12}$ | 0.200 | 0.200 | 0.200 | 0.200 | Position error at visited site |
| $u_{b,13}$ | 0.200 | 0.200 | 0.200 | 0.200 | Multipaths at OP |
| $u_{b,14}$ | 0.200 | 0.200 | 0.200 | 0.200 | Multipaths at visited site |
| Link of the traveling system to local time scale | | | | | |
| $u_{b,21}$ | 0.220 | 0.220 | | 0.220 | REFDLY at OP |
| $u_{b,22}$ | 0.220 | 0.220 | | 0.220 | REFDLY at visited site |
| $u_{b,TOT}$ | 0.519 | 0.533 | 0.404 | 0.508 | |
| Link of the reference system to UTC(OP) | | | | | |
| $u_{b,31}$ | 0.220 | 0.220 | | 0.220 | REFDLY at OP |
| Link of the visited system to its local time scale | | | | | |
| $u_{b,32}$ | 0.220 | 0.220 | | 0.220 | REFDLY at visited site |
| Antenna cable delays | | | | | |
| $u_{b,41}$ | 0.000 | 0.000 | | 0.000 | CABDLY at OP |
| $u_{b,42}$ | 0.000 | 0.000 | | 0.000 | CABDLY at visited site |
| Type B uncertainties | | | | | |
| $u_{b,SYS}$ | 0.606 | 0.618 | | 0.596 | Quadratic sum of $u_b$ |
| Combined uncertainties | | | | | |
| $u_{CAL0}$ | 0.611 | 0.631 | | 0.614 | Composed of $u_a$ and $u_{b,SYS}$ |

Table 16: **ES07** uncertainty budget for **Galileo** calibrated delays (all values in ns)

| Uncertainty type | E1 | E5a | E1-E5a | E3 | Description |
|---|---|---|---|---|---|
| $u_a$(Reference) | 0.036 | 0.047 | 0.059 | 0.077 | Largest TDEV(1 d) sigma between the start and the end of OP72 or OP74 against OP73 |
| $u_a$(ES07) | 0.036 | 0.044 | 0.057 | 0.097 | Largest TDEV(1 d) sigma of offset between visited station and OP72 or OP74 |
| Type A uncertainties | | | | | |
| $u_a$ | 0.051 | 0.065 | 0.083 | 0.124 | Visited against reference |
| Misclosure | | | | | |
| $u_{b,1}$ | 0.084 | 0.028 | 0.111 | 0.223 | Actual misclosure offset |
| Systematic components related to RAWDIF | | | | | |
| $u_{b,11}$ | 0.200 | 0.200 | 0.200 | 0.200 | Position error at OP |
| $u_{b,12}$ | 0.200 | 0.200 | 0.200 | 0.200 | Position error at visited site |
| $u_{b,13}$ | 0.200 | 0.200 | 0.200 | 0.200 | Multipaths at OP |
| $u_{b,14}$ | 0.200 | 0.200 | 0.200 | 0.200 | Multipaths at visited site |
| Link of the traveling system to local time scale | | | | | |
| $u_{b,21}$ | 0.220 | 0.220 | | 0.220 | REFDLY at OP |
| $u_{b,22}$ | 0.220 | 0.220 | | 0.220 | REFDLY at visited site |
| $u_{b,TOT}$ | 0.514 | 0.508 | 0.416 | 0.554 | |
| Link of the reference system to UTC(OP) | | | | | |
| $u_{b,31}$ | 0.220 | 0.220 | | 0.220 | REFDLY at OP |
| Link of the visited system to its local time scale | | | | | |
| $u_{b,32}$ | 0.220 | 0.220 | | 0.220 | REFDLY at visited site |
| Antenna cable delays | | | | | |
| $u_{b,41}$ | 0.000 | 0.000 | | 0.000 | CABDLY at OP |
| $u_{b,42}$ | 0.000 | 0.000 | | 0.000 | CABDLY at visited site |
| Type B uncertainties | | | | | |
| $u_{b,SYS}$ | 0.601 | 0.596 | | 0.636 | Quadratic sum of $u_b$ |
| Combined uncertainties | | | | | |
| $u_{CAL0}$ | 0.604 | 0.600 | | 0.648 | Composed of $u_a$ and $u_{b,SYS}$ |

Table 17: **ES08** uncertainty budget for **Galileo** calibrated delays (all values in ns)

| Uncertainty type | E1 | E5a | E1-E5a | E3 | Description |
|---|---|---|---|---|---|
| $u_a$(Reference) | 0.036 | 0.047 | 0.059 | 0.077 | Largest TDEV(1 d) sigma between the start and the end of OP72 or OP74 against OP73 |
| $u_a$(ES08) | 0.025 | 0.041 | 0.049 | 0.047 | Largest TDEV(1 d) sigma of offset between visited station and OP72 or OP74 |
| Type A uncertainties | | | | | |
| $u_a$ | 0.044 | 0.063 | 0.077 | 0.091 | Visited against reference |
| Misclosure | | | | | |
| $u_{b,1}$ | 0.084 | 0.028 | 0.111 | 0.223 | Actual misclosure offset |
| Systematic components related to RAWDIF | | | | | |
| $u_{b,11}$ | 0.200 | 0.200 | 0.200 | 0.200 | Position error at OP |
| $u_{b,12}$ | 0.200 | 0.200 | 0.200 | 0.200 | Position error at visited site |
| $u_{b,13}$ | 0.200 | 0.200 | 0.200 | 0.200 | Multipaths at OP |
| $u_{b,14}$ | 0.200 | 0.200 | 0.200 | 0.200 | Multipaths at visited site |
| Link of the traveling system to local time scale | | | | | |
| $u_{b,21}$ | 0.220 | 0.220 | | 0.220 | REFDLY at OP |
| $u_{b,22}$ | 0.220 | 0.220 | | 0.220 | REFDLY at visited site |
| $u_{b,TOT}$ | 0.514 | 0.508 | 0.416 | 0.554 | |
| Link of the reference system to UTC(OP) | | | | | |
| $u_{b,31}$ | 0.220 | 0.220 | | 0.220 | REFDLY at OP |
| Link of the visited system to its local time scale | | | | | |
| $u_{b,32}$ | 0.220 | 0.220 | | 0.220 | REFDLY at visited site |
| Antenna cable delays | | | | | |
| $u_{b,41}$ | 0.000 | 0.000 | | 0.000 | CABDLY at OP |
| $u_{b,42}$ | 0.000 | 0.000 | | 0.000 | CABDLY at visited site |
| Type B uncertainties | | | | | |
| $u_{b,SYS}$ | 0.601 | 0.596 | | 0.636 | Quadratic sum of $u_b$ |
| Combined uncertainties | | | | | |
| $u_{CAL0}$ | 0.603 | 0.600 | | 0.643 | Composed of $u_a$ and $u_{b,SYS}$ |

Table 18: **ES09** uncertainty budget for **Galileo** calibrated delays (all values in ns)

| Uncertainty type | E1 | E5a | E1-E5a | E3 | Description |
|---|---|---|---|---|---|
| $u_a$(Reference) | 0.036 | 0.047 | 0.059 | 0.077 | Largest TDEV(1 d) sigma between the start and the end of OP72 or OP74 against OP73 |
| $u_a$(ES09) | 0.065 | 0.100 | 0.120 | 0.076 | Largest TDEV(1 d) sigma of offset between visited station and OP72 or OP74 |
| Type A uncertainties | | | | | |
| $u_a$ | 0.075 | 0.111 | 0.134 | 0.109 | Visited against reference |
| Misclosure | | | | | |
| $u_{b,1}$ | 0.084 | 0.028 | 0.111 | 0.223 | Actual misclosure offset |
| Systematic components related to RAWDIF | | | | | |
| $u_{b,11}$ | 0.200 | 0.200 | 0.200 | 0.200 | Position error at OP |
| $u_{b,12}$ | 0.200 | 0.200 | 0.200 | 0.200 | Position error at visited site |
| $u_{b,13}$ | 0.200 | 0.200 | 0.200 | 0.200 | Multipaths at OP |
| $u_{b,14}$ | 0.200 | 0.200 | 0.200 | 0.200 | Multipaths at visited site |
| Link of the traveling system to local time scale | | | | | |
| $u_{b,21}$ | 0.220 | 0.220 | | 0.220 | REFDLY at OP |
| $u_{b,22}$ | 0.220 | 0.220 | | 0.220 | REFDLY at visited site |
| $u_{b,TOT}$ | 0.514 | 0.508 | 0.416 | 0.554 | |
| Link of the reference system to UTC(OP) | | | | | |
| $u_{b,31}$ | 0.220 | 0.220 | | 0.220 | REFDLY at OP |
| Link of the visited system to its local time scale | | | | | |
| $u_{b,32}$ | 0.220 | 0.220 | | 0.220 | REFDLY at visited site |
| Antenna cable delays | | | | | |
| $u_{b,41}$ | 0.000 | 0.000 | | 0.000 | CABDLY at OP |
| $u_{b,42}$ | 0.000 | 0.000 | | 0.000 | CABDLY at visited site |
| Type B uncertainties | | | | | |
| $u_{b,SYS}$ | 0.601 | 0.596 | | 0.636 | Quadratic sum of $u_b$ |
| Combined uncertainties | | | | | |
| $u_{CAL0}$ | 0.606 | 0.607 | | 0.646 | Composed of $u_a$ and $u_{b,SYS}$ |

Table 19: **TR01** uncertainty budget for **Galileo** calibrated delays (all values in ns)

| Uncertainty type | E1 | E5a | E1-E5a | E3 | Description |
|---|---|---|---|---|---|
| $u_a$(Reference) | 0.036 | 0.047 | 0.059 | 0.077 | Largest TDEV(1 d) sigma between the start and the end of OP72 or OP74 against OP73 |
| $u_a$(TR01) | 0.031 | 0.044 | 0.054 | 0.080 | Largest TDEV(1 d) sigma of offset between visited station and OP72 or OP74 |
| Type A uncertainties | | | | | |
| $u_a$ | 0.048 | 0.065 | 0.080 | 0.112 | Visited against reference |
| Misclosure | | | | | |
| $u_{b,1}$ | 0.084 | 0.028 | 0.111 | 0.223 | Actual misclosure offset |
| Systematic components related to RAWDIF | | | | | |
| $u_{b,11}$ | 0.200 | 0.200 | 0.200 | 0.200 | Position error at OP |
| $u_{b,12}$ | 0.200 | 0.200 | 0.200 | 0.200 | Position error at visited site |
| $u_{b,13}$ | 0.200 | 0.200 | 0.200 | 0.200 | Multipaths at OP |
| $u_{b,14}$ | 0.200 | 0.200 | 0.200 | 0.200 | Multipaths at visited site |
| Link of the traveling system to local time scale | | | | | |
| $u_{b,21}$ | 0.220 | 0.220 | | 0.220 | REFDLY at OP |
| $u_{b,22}$ | 0.220 | 0.220 | | 0.220 | REFDLY at visited site |
| $u_{b,TOT}$ | 0.514 | 0.508 | 0.416 | 0.554 | |
| Link of the reference system to UTC(OP) | | | | | |
| $u_{b,31}$ | 0.220 | 0.220 | | 0.220 | REFDLY at OP |
| Link of the visited system to its local time scale | | | | | |
| $u_{b,32}$ | 0.220 | 0.220 | | 0.220 | REFDLY at visited site |
| Antenna cable delays | | | | | |
| $u_{b,41}$ | 0.000 | 0.000 | | 0.000 | CABDLY at OP |
| $u_{b,42}$ | 0.000 | 0.000 | | 0.000 | CABDLY at visited site |
| Type B uncertainties | | | | | |
| $u_{b,SYS}$ | 0.601 | 0.596 | | 0.636 | Quadratic sum of $u_b$ |
| Combined uncertainties | | | | | |
| $u_{CAL0}$ | 0.603 | 0.600 | | 0.646 | Composed of $u_a$ and $u_{b,SYS}$ |

Table 20: **NPL3** uncertainty budget for **Galileo** calibrated delays (all values in ns)

| Uncertainty type | E1 | E5a | E1-E5a | E3 | Description |
|---|---|---|---|---|---|
| $u_a$(Reference) | 0.036 | 0.047 | 0.059 | 0.077 | Largest TDEV(1 d) sigma between the start and the end of OP72 or OP74 against OP73 |
| $u_a$(NPL3) | 0.056 | 0.108 | 0.122 | 0.116 | Largest TDEV(1 d) sigma of offset between visited station and OP72 or OP74 |
| Type A uncertainties | | | | | |
| $u_a$ | 0.067 | 0.118 | 0.136 | 0.140 | Visited against reference |
| Misclosure | | | | | |
| $u_{b,1}$ | 0.084 | 0.028 | 0.111 | 0.223 | Actual misclosure offset |
| Systematic components related to RAWDIF | | | | | |
| $u_{b,11}$ | 0.200 | 0.200 | 0.200 | 0.200 | Position error at OP |
| $u_{b,12}$ | 0.200 | 0.200 | 0.200 | 0.200 | Position error at visited site |
| $u_{b,13}$ | 0.200 | 0.200 | 0.200 | 0.200 | Multipaths at OP |
| $u_{b,14}$ | 0.200 | 0.200 | 0.200 | 0.200 | Multipaths at visited site |
| Link of the traveling system to local time scale | | | | | |
| $u_{b,21}$ | 0.220 | 0.220 | | 0.220 | REFDLY at OP |
| $u_{b,22}$ | 0.220 | 0.220 | | 0.220 | REFDLY at visited site |
| $u_{b,TOT}$ | 0.514 | 0.508 | 0.416 | 0.554 | |
| Link of the reference system to UTC(OP) | | | | | |
| $u_{b,31}$ | 0.220 | 0.220 | | 0.220 | REFDLY at OP |
| Link of the visited system to its local time scale | | | | | |
| $u_{b,32}$ | 0.220 | 0.220 | | 0.220 | REFDLY at visited site |
| Antenna cable delays | | | | | |
| $u_{b,41}$ | 0.000 | 0.000 | | 0.000 | CABDLY at OP |
| $u_{b,42}$ | 0.000 | 0.000 | | 0.000 | CABDLY at visited site |
| Type B uncertainties | | | | | |
| $u_{b,SYS}$ | 0.601 | 0.596 | | 0.636 | Quadratic sum of $u_b$ |
| Combined uncertainties | | | | | |
| $u_{CAL0}$ | 0.605 | 0.608 | | 0.652 | Composed of $u_a$ and $u_{b,SYS}$ |

Table 21: **NPL4** uncertainty budget for **Galileo** calibrated delays (all values in ns)

| Uncertainty type | E1 | E5a | E1-E5a | E3 | Description |
|---|---|---|---|---|---|
| $u_a$(Reference) | 0.036 | 0.047 | 0.059 | 0.077 | Largest TDEV(1 d) sigma between the start and the end of OP72 or OP74 against OP73 |
| $u_a$(NPL4) | 0.054 | 0.059 | 0.080 | 0.139 | Largest TDEV(1 d) sigma of offset between visited station and OP72 or OP74 |
| Type A uncertainties | | | | | |
| $u_a$ | 0.065 | 0.076 | 0.100 | 0.159 | Visited against reference |
| Misclosure | | | | | |
| $u_{b,1}$ | 0.084 | 0.028 | 0.111 | 0.223 | Actual misclosure offset |
| Systematic components related to RAWDIF | | | | | |
| $u_{b,11}$ | 0.200 | 0.200 | 0.200 | 0.200 | Position error at OP |
| $u_{b,12}$ | 0.200 | 0.200 | 0.200 | 0.200 | Position error at visited site |
| $u_{b,13}$ | 0.200 | 0.200 | 0.200 | 0.200 | Multipaths at OP |
| $u_{b,14}$ | 0.200 | 0.200 | 0.200 | 0.200 | Multipaths at visited site |
| Link of the traveling system to local time scale | | | | | |
| $u_{b,21}$ | 0.220 | 0.220 | | 0.220 | REFDLY at OP |
| $u_{b,22}$ | 0.220 | 0.220 | | 0.220 | REFDLY at visited site |
| $u_{b,TOT}$ | 0.514 | 0.508 | 0.416 | 0.554 | |
| Link of the reference system to UTC(OP) | | | | | |
| $u_{b,31}$ | 0.220 | 0.220 | | 0.220 | REFDLY at OP |
| Link of the visited system to its local time scale | | | | | |
| $u_{b,32}$ | 0.220 | 0.220 | | 0.220 | REFDLY at visited site |
| Antenna cable delays | | | | | |
| $u_{b,41}$ | 0.000 | 0.000 | | 0.000 | CABDLY at OP |
| $u_{b,42}$ | 0.000 | 0.000 | | 0.000 | CABDLY at visited site |
| Type B uncertainties | | | | | |
| $u_{b,SYS}$ | 0.601 | 0.596 | | 0.636 | Quadratic sum of $u_b$ |
| Combined uncertainties | | | | | |
| $u_{CAL0}$ | 0.605 | 0.601 | | 0.656 | Composed of $u_a$ and $u_{b,SYS}$ |

Table 22: **NPL5** uncertainty budget for **Galileo** calibrated delays (all values in ns)

| Uncertainty type | E1 | E5a | E1-E5a | E3 | Description |
|---|---|---|---|---|---|
| $u_a$(Reference) | 0.036 | 0.047 | 0.059 | 0.077 | Largest TDEV(1 d) sigma between the start and the end of OP72 or OP74 against OP73 |
| $u_a$(NPL5) | 0.076 | 0.133 | 0.154 | 0.098 | Largest TDEV(1 d) sigma of offset between visited station and OP72 or OP74 |
| Type A uncertainties | | | | | |
| $u_a$ | 0.085 | 0.142 | 0.165 | 0.125 | Visited against reference |
| Misclosure | | | | | |
| $u_{b,1}$ | 0.084 | 0.028 | 0.111 | 0.223 | Actual misclosure offset |
| Systematic components related to RAWDIF | | | | | |
| $u_{b,11}$ | 0.200 | 0.200 | 0.200 | 0.200 | Position error at OP |
| $u_{b,12}$ | 0.200 | 0.200 | 0.200 | 0.200 | Position error at visited site |
| $u_{b,13}$ | 0.200 | 0.200 | 0.200 | 0.200 | Multipaths at OP |
| $u_{b,14}$ | 0.200 | 0.200 | 0.200 | 0.200 | Multipaths at visited site |
| Link of the traveling system to local time scale | | | | | |
| $u_{b,21}$ | 0.220 | 0.220 | | 0.220 | REFDLY at OP |
| $u_{b,22}$ | 0.220 | 0.220 | | 0.220 | REFDLY at visited site |
| $u_{b,TOT}$ | 0.514 | 0.508 | 0.416 | 0.554 | |
| Link of the reference system to UTC(OP) | | | | | |
| $u_{b,31}$ | 0.220 | 0.220 | | 0.220 | REFDLY at OP |
| Link of the visited system to its local time scale | | | | | |
| $u_{b,32}$ | 0.220 | 0.220 | | 0.220 | REFDLY at visited site |
| Antenna cable delays | | | | | |
| $u_{b,41}$ | 0.000 | 0.000 | | 0.000 | CABDLY at OP |
| $u_{b,42}$ | 0.000 | 0.000 | | 0.000 | CABDLY at visited site |
| Type B uncertainties | | | | | |
| $u_{b,SYS}$ | 0.601 | 0.596 | | 0.636 | Quadratic sum of $u_b$ |
| Combined uncertainties | | | | | |
| $u_{CAL0}$ | 0.607 | 0.613 | | 0.649 | Composed of $u_a$ and $u_{b,SYS}$ |

Table 23: **ES07** uncertainty budget for **Beidou** calibrated delays (all values in ns)

| Uncertainty type | B1C | B2a | B1C-B2a | B3 | Description |
|---|---|---|---|---|---|
| $u_a$(Reference) | 0.040 | 0.035 | 0.053 | 0.081 | Largest TDEV(1 d) sigma between the start and the end of OP72 or OP74 against OP73 |
| $u_a$(ES07) | 0.030 | 0.040 | 0.050 | 0.094 | Largest TDEV(1 d) sigma of offset between visited station and OP72 or OP74 |
| Type A uncertainties | | | | | |
| $u_a$ | 0.050 | 0.054 | 0.073 | 0.125 | Visited against reference |
| Misclosure | | | | | |
| $u_{b,1}$ | 0.083 | 0.013 | 0.096 | 0.202 | Actual misclosure offset |
| Systematic components related to RAWDIF | | | | | |
| $u_{b,11}$ | 0.200 | 0.200 | 0.200 | 0.200 | Position error at OP |
| $u_{b,12}$ | 0.200 | 0.200 | 0.200 | 0.200 | Position error at visited site |
| $u_{b,13}$ | 0.200 | 0.200 | 0.200 | 0.200 | Multipaths at OP |
| $u_{b,14}$ | 0.200 | 0.200 | 0.200 | 0.200 | Multipaths at visited site |
| Link of the traveling system to local time scale | | | | | |
| $u_{b,21}$ | 0.220 | 0.220 | | 0.220 | REFDLY at OP |
| $u_{b,22}$ | 0.220 | 0.220 | | 0.220 | REFDLY at visited site |
| $u_{b,TOT}$ | 0.514 | 0.507 | 0.412 | 0.546 | |
| Link of the reference system to UTC(OP) | | | | | |
| $u_{b,31}$ | 0.220 | 0.220 | | 0.220 | REFDLY at OP |
| Link of the visited system to its local time scale | | | | | |
| $u_{b,32}$ | 0.220 | 0.220 | | 0.220 | REFDLY at visited site |
| Antenna cable delays | | | | | |
| $u_{b,41}$ | 0.000 | 0.000 | | 0.000 | CABDLY at OP |
| $u_{b,42}$ | 0.000 | 0.000 | | 0.000 | CABDLY at visited site |
| Type B uncertainties | | | | | |
| $u_{b,SYS}$ | 0.601 | 0.595 | | 0.629 | Quadratic sum of $u_b$ |
| Combined uncertainties | | | | | |
| $u_{CAL0}$ | 0.604 | 0.598 | | 0.642 | Composed of $u_a$ and $u_{b,SYS}$ |

Table 24: **ES08** uncertainty budget for **Beidou** calibrated delays (all values in ns)

| Uncertainty type | B1C | B2a | B1C-B2a | B3 | Description |
|---|---|---|---|---|---|
| $u_a$(Reference) | 0.040 | 0.035 | 0.053 | 0.081 | Largest TDEV(1 d) sigma between the start and the end of OP72 or OP74 against OP73 |
| $u_a$(ES08) | 0.028 | 0.034 | 0.045 | 0.075 | Largest TDEV(1 d) sigma of offset between visited station and OP72 or OP74 |
| Type A uncertainties | | | | | |
| $u_a$ | 0.049 | 0.049 | 0.070 | 0.111 | Visited against reference |
| Misclosure | | | | | |
| $u_{b,1}$ | 0.083 | 0.013 | 0.096 | 0.202 | Actual misclosure offset |
| Systematic components related to RAWDIF | | | | | |
| $u_{b,11}$ | 0.200 | 0.200 | 0.200 | 0.200 | Position error at OP |
| $u_{b,12}$ | 0.200 | 0.200 | 0.200 | 0.200 | Position error at visited site |
| $u_{b,13}$ | 0.200 | 0.200 | 0.200 | 0.200 | Multipaths at OP |
| $u_{b,14}$ | 0.200 | 0.200 | 0.200 | 0.200 | Multipaths at visited site |
| Link of the traveling system to local time scale | | | | | |
| $u_{b,21}$ | 0.220 | 0.220 | | 0.220 | REFDLY at OP |
| $u_{b,22}$ | 0.220 | 0.220 | | 0.220 | REFDLY at visited site |
| $u_{b,TOT}$ | 0.514 | 0.507 | 0.412 | 0.546 | |
| Link of the reference system to UTC(OP) | | | | | |
| $u_{b,31}$ | 0.220 | 0.220 | | 0.220 | REFDLY at OP |
| Link of the visited system to its local time scale | | | | | |
| $u_{b,32}$ | 0.220 | 0.220 | | 0.220 | REFDLY at visited site |
| Antenna cable delays | | | | | |
| $u_{b,41}$ | 0.000 | 0.000 | | 0.000 | CABDLY at OP |
| $u_{b,42}$ | 0.000 | 0.000 | | 0.000 | CABDLY at visited site |
| Type B uncertainties | | | | | |
| $u_{b,SYS}$ | 0.601 | 0.595 | | 0.629 | Quadratic sum of $u_b$ |
| Combined uncertainties | | | | | |
| $u_{CAL0}$ | 0.603 | 0.598 | | 0.639 | Composed of $u_a$ and $u_{b,SYS}$ |

Table 25: **ES09** uncertainty budget for **Beidou** calibrated delays (all values in ns)

| Uncertainty type | B1C | B2a | B1C-B2a | B3 | Description |
|---|---|---|---|---|---|
| $u_a$(Reference) | 0.040 | 0.035 | 0.053 | 0.081 | Largest TDEV(1 d) sigma between the start and the end of OP72 or OP74 against OP73 |
| $u_a$(ES09) | 0.076 | 0.098 | 0.125 | 0.201 | Largest TDEV(1 d) sigma of offset between visited station and OP72 or OP74 |
| Type A uncertainties | | | | | |
| $u_a$ | 0.086 | 0.105 | 0.136 | 0.217 | Visited against reference |
| Misclosure | | | | | |
| $u_{b,1}$ | 0.083 | 0.013 | 0.096 | 0.202 | Actual misclosure offset |
| Systematic components related to RAWDIF | | | | | |
| $u_{b,11}$ | 0.200 | 0.200 | 0.200 | 0.200 | Position error at OP |
| $u_{b,12}$ | 0.200 | 0.200 | 0.200 | 0.200 | Position error at visited site |
| $u_{b,13}$ | 0.200 | 0.200 | 0.200 | 0.200 | Multipaths at OP |
| $u_{b,14}$ | 0.200 | 0.200 | 0.200 | 0.200 | Multipaths at visited site |
| Link of the traveling system to local time scale | | | | | |
| $u_{b,21}$ | 0.220 | 0.220 | | 0.220 | REFDLY at OP |
| $u_{b,22}$ | 0.220 | 0.220 | | 0.220 | REFDLY at visited site |
| $u_{b,TOT}$ | 0.514 | 0.507 | 0.412 | 0.546 | |
| Link of the reference system to UTC(OP) | | | | | |
| $u_{b,31}$ | 0.220 | 0.220 | | 0.220 | REFDLY at OP |
| Link of the visited system to its local time scale | | | | | |
| $u_{b,32}$ | 0.220 | 0.220 | | 0.220 | REFDLY at visited site |
| Antenna cable delays | | | | | |
| $u_{b,41}$ | 0.000 | 0.000 | | 0.000 | CABDLY at OP |
| $u_{b,42}$ | 0.000 | 0.000 | | 0.000 | CABDLY at visited site |
| Type B uncertainties | | | | | |
| $u_{b,SYS}$ | 0.601 | 0.595 | | 0.629 | Quadratic sum of $u_b$ |
| Combined uncertainties | | | | | |
| $u_{CAL0}$ | 0.608 | 0.605 | | 0.666 | Composed of $u_a$ and $u_{b,SYS}$ |

Table 26: **TR01** uncertainty budget for **Beidou** calibrated delays (all values in ns)

| Uncertainty type | B1C | B2a | B1C-B2a | B3 | Description |
|---|---|---|---|---|---|
| $u_a$(Reference) | 0.040 | 0.035 | 0.053 | 0.081 | Largest TDEV(1 d) sigma between the start and the end of OP72 or OP74 against OP73 |
| $u_a$(TR01) | 0.026 | 0.066 | 0.071 | 0.094 | Largest TDEV(1 d) sigma of offset between visited station and OP72 or OP74 |
| Type A uncertainties | | | | | |
| $u_a$ | 0.048 | 0.075 | 0.089 | 0.125 | Visited against reference |
| Misclosure | | | | | |
| $u_{b,1}$ | 0.083 | 0.013 | 0.096 | 0.202 | Actual misclosure offset |
| Systematic components related to RAWDIF | | | | | |
| $u_{b,11}$ | 0.200 | 0.200 | 0.200 | 0.200 | Position error at OP |
| $u_{b,12}$ | 0.200 | 0.200 | 0.200 | 0.200 | Position error at visited site |
| $u_{b,13}$ | 0.200 | 0.200 | 0.200 | 0.200 | Multipaths at OP |
| $u_{b,14}$ | 0.200 | 0.200 | 0.200 | 0.200 | Multipaths at visited site |
| Link of the traveling system to local time scale | | | | | |
| $u_{b,21}$ | 0.220 | 0.220 | | 0.220 | REFDLY at OP |
| $u_{b,22}$ | 0.220 | 0.220 | | 0.220 | REFDLY at visited site |
| $u_{b,TOT}$ | 0.514 | 0.507 | 0.412 | 0.546 | |
| Link of the reference system to UTC(OP) | | | | | |
| $u_{b,31}$ | 0.220 | 0.220 | | 0.220 | REFDLY at OP |
| Link of the visited system to its local time scale | | | | | |
| $u_{b,32}$ | 0.220 | 0.220 | | 0.220 | REFDLY at visited site |
| Antenna cable delays | | | | | |
| $u_{b,41}$ | 0.000 | 0.000 | | 0.000 | CABDLY at OP |
| $u_{b,42}$ | 0.000 | 0.000 | | 0.000 | CABDLY at visited site |
| Type B uncertainties | | | | | |
| $u_{b,SYS}$ | 0.601 | 0.595 | | 0.629 | Quadratic sum of $u_b$ |
| Combined uncertainties | | | | | |
| $u_{CAL0}$ | 0.603 | 0.600 | | 0.642 | Composed of $u_a$ and $u_{b,SYS}$ |

Table 27: **NPL3** uncertainty budget for **Beidou** calibrated delays (all values in ns)

| Uncertainty type | B1C | B2a | B1C-B2a | B3 | Description |
|---|---|---|---|---|---|
| $u_a$(Reference) | 0.040 | 0.035 | 0.053 | 0.081 | Largest TDEV(1 d) sigma between the start and the end of OP72 or OP74 against OP73 |
| $u_a$(NPL3) | 0.063 | 0.096 | 0.115 | 0.121 | Largest TDEV(1 d) sigma of offset between visited station and OP72 or OP74 |
| Type A uncertainties | | | | | |
| $u_a$ | 0.075 | 0.103 | 0.127 | 0.146 | Visited against reference |
| Misclosure | | | | | |
| $u_{b,1}$ | 0.083 | 0.013 | 0.096 | 0.202 | Actual misclosure offset |
| Systematic components related to RAWDIF | | | | | |
| $u_{b,11}$ | 0.200 | 0.200 | 0.200 | 0.200 | Position error at OP |
| $u_{b,12}$ | 0.200 | 0.200 | 0.200 | 0.200 | Position error at visited site |
| $u_{b,13}$ | 0.200 | 0.200 | 0.200 | 0.200 | Multipaths at OP |
| $u_{b,14}$ | 0.200 | 0.200 | 0.200 | 0.200 | Multipaths at visited site |
| Link of the traveling system to local time scale | | | | | |
| $u_{b,21}$ | 0.220 | 0.220 | | 0.220 | REFDLY at OP |
| $u_{b,22}$ | 0.220 | 0.220 | | 0.220 | REFDLY at visited site |
| $u_{b,TOT}$ | 0.514 | 0.507 | 0.412 | 0.546 | |
| Link of the reference system to UTC(OP) | | | | | |
| $u_{b,31}$ | 0.220 | 0.220 | | 0.220 | REFDLY at OP |
| Link of the visited system to its local time scale | | | | | |
| $u_{b,32}$ | 0.220 | 0.220 | | 0.220 | REFDLY at visited site |
| Antenna cable delays | | | | | |
| $u_{b,41}$ | 0.000 | 0.000 | | 0.000 | CABDLY at OP |
| $u_{b,42}$ | 0.000 | 0.000 | | 0.000 | CABDLY at visited site |
| Type B uncertainties | | | | | |
| $u_{b,SYS}$ | 0.601 | 0.595 | | 0.629 | Quadratic sum of $u_b$ |
| Combined uncertainties | | | | | |
| $u_{CAL0}$ | 0.606 | 0.604 | | 0.646 | Composed of $u_a$ and $u_{b,SYS}$ |

Table 28: **NPL5** uncertainty budget for **Beidou** calibrated delays (all values in ns)

| Uncertainty type | B1C | B2a | B1C-B2a | B3 | Description |
|---|---|---|---|---|---|
| $u_a$(Reference) | 0.040 | 0.035 | 0.053 | 0.081 | Largest TDEV(1 d) sigma between the start and the end of OP72 or OP74 against OP73 |
| $u_a$(NPL5) | 0.114 | 0.146 | 0.186 | 0.190 | Largest TDEV(1 d) sigma of offset between visited station and OP72 or OP74 |
| Type A uncertainties | | | | | |
| $u_a$ | 0.121 | 0.151 | 0.194 | 0.207 | Visited against reference |
| Misclosure | | | | | |
| $u_{b,1}$ | 0.083 | 0.013 | 0.096 | 0.202 | Actual misclosure offset |
| Systematic components related to RAWDIF | | | | | |
| $u_{b,11}$ | 0.200 | 0.200 | 0.200 | 0.200 | Position error at OP |
| $u_{b,12}$ | 0.200 | 0.200 | 0.200 | 0.200 | Position error at visited site |
| $u_{b,13}$ | 0.200 | 0.200 | 0.200 | 0.200 | Multipaths at OP |
| $u_{b,14}$ | 0.200 | 0.200 | 0.200 | 0.200 | Multipaths at visited site |
| Link of the traveling system to local time scale | | | | | |
| $u_{b,21}$ | 0.220 | 0.220 | | 0.220 | REFDLY at OP |
| $u_{b,22}$ | 0.220 | 0.220 | | 0.220 | REFDLY at visited site |
| $u_{b,TOT}$ | 0.514 | 0.507 | 0.412 | 0.546 | |
| Link of the reference system to UTC(OP) | | | | | |
| $u_{b,31}$ | 0.220 | 0.220 | | 0.220 | REFDLY at OP |
| Link of the visited system to its local time scale | | | | | |
| $u_{b,32}$ | 0.220 | 0.220 | | 0.220 | REFDLY at visited site |
| Antenna cable delays | | | | | |
| $u_{b,41}$ | 0.000 | 0.000 | | 0.000 | CABDLY at OP |
| $u_{b,42}$ | 0.000 | 0.000 | | 0.000 | CABDLY at visited site |
| Type B uncertainties | | | | | |
| $u_{b,SYS}$ | 0.601 | 0.595 | | 0.629 | Quadratic sum of $u_b$ |
| Combined uncertainties | | | | | |
| $u_{CAL0}$ | 0.614 | 0.614 | | 0.663 | Composed of $u_a$ and $u_{b,SYS}$ |

# 7 Validation of the result.

## 7.1 Stability of the reference station.

The reference station in OP was based on a Septentrio PolaRx5TR receiver called OP73. Figure 1 is showing a plot which demonstrate the stability of this GNSS station during the calibration campaign. The plot is the daily averaged offset between the TWSDRR technique (Two-Way Satellite Time and Frequency Transfer, with Satre modem emision and Software Defined Radio reception) between OP and PTB, and the GNSS Common View (CV) time transfer using P3 GPS or E3 Galileo data between OP and PTB, based on OP73 in OP side and on PTBB in PTB side. In both laboratories, the signal source is a UTC(k) time scale: UTC(OP) and UTC(PTB). In this computation, the time scales being cancelled, what remains is only the offset between the two time transfer techniques.

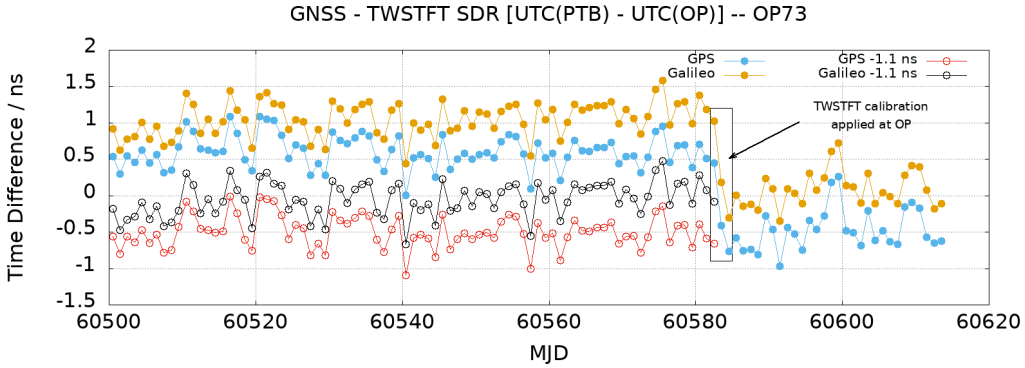


Figure 1: Daily averaged offset between TWSDRR and GPS P3 or Galileo E3 CV on the link OP-PTB during the calibration campaign.

The time step of -1.1 ns at MJD 60584 is due to the application updated calibration values in both TWSTFT stations (Cal ID # 0624-2024). If we correct the technique comparison results from this time step, the standard deviation estimated over the overall 60500 – 60613 period is 237 ps for GPS and 243 ps for Galileo. In addition, the mean offsets over the period 60586 – 60613, after the implementation of the updated TWSTFT calibration, is about -0.5 ns for GPS and 0.1 ns for Galileo.
This access the excellent stability of OP73 reference station and the consistency of the TAI network. We estimate that any potential effect of OP73 on this calibration campaign can be disregarded with respect to the final uncertainty of the calibration.

## 7.2 Offset between the two traveling receivers.

Figure 2, Figure 3 and Figure 4 are showing the offset between the two traveling receivers during the whole calibration campaign, based on CV between CGGTTS P3 (GPS), E3 (Galileo) and B3 (Beidou) data, by using for OP72 and OP74 the average delays computed against OP73 between the start and the closure of the campaign. The average offsets between the receivers before, during and after the trip, are lower than 200 ps, with a standard deviation below 100 ps. The traveling equipment remained very stable during the calibration campaign. We can consider that the effect of these offsets on the calibration results have a limitted impact.

Table 29: Average offsets between OP72 and OP74 during the calibration (all values in ns)

| **Institute** | ΔP3 | Uncertainty | ΔE3 | Uncertainty | ΔB3 | Uncertainty |
|---|---|---|---|---|---|---|
| OP (Start) | -0.001 | 0.089 | -0.003 | 0.053 | 0.001 | 0.050 |
| ESTEC | -0.029 | 0.089 | -0.031 | 0.050 | -0.032 | 0.048 |
| NPL | -0.139 | 0.088 | -0.199 | 0.055 | -0.199 | 0.053 |
| OP (Closure) | 0.000 | 0.087 | 0.002 | 0.050 | 0.001 | 0.050 |

Figure 2: Offset between OP72 and OP74 during the calibration, based on CGGTTS P3 CV data

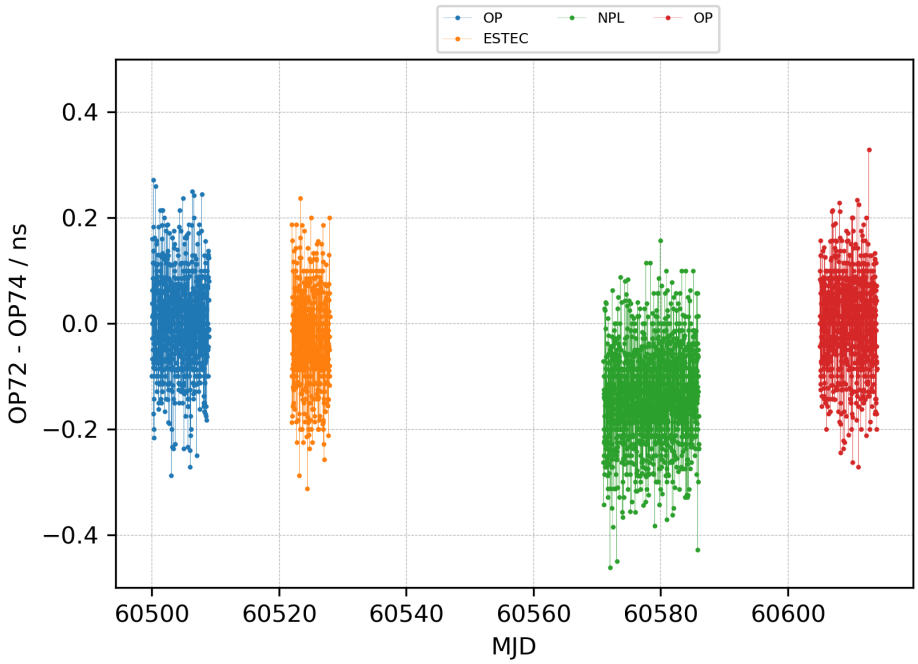


Figure 3: Offset between OP72 and OP74 during the calibration, based on CGGTTS E3 CV data

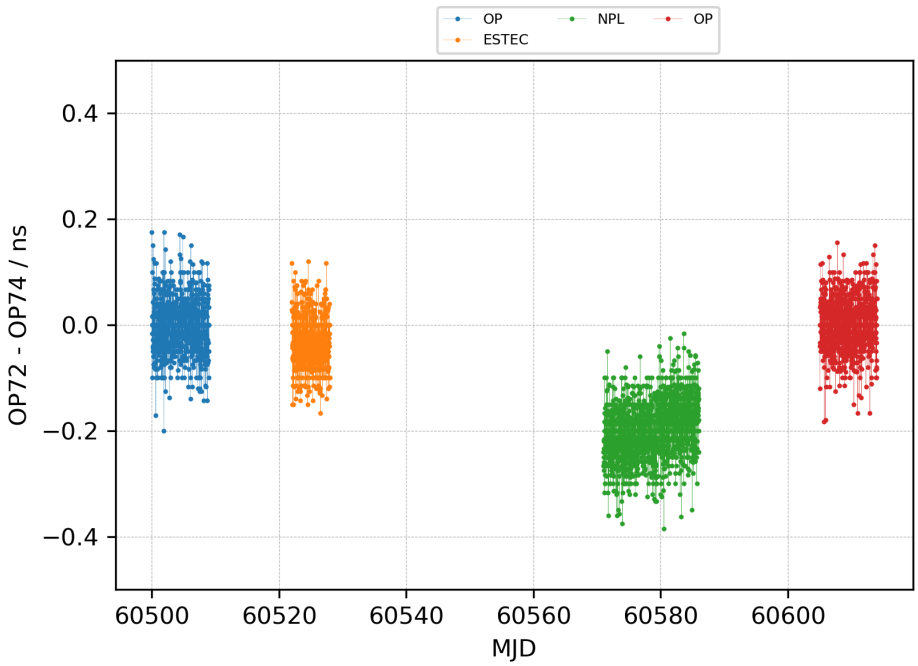

Figure 4: Offset between OP72 and OP74 during the calibration, based on CGGTTS B3 CV data

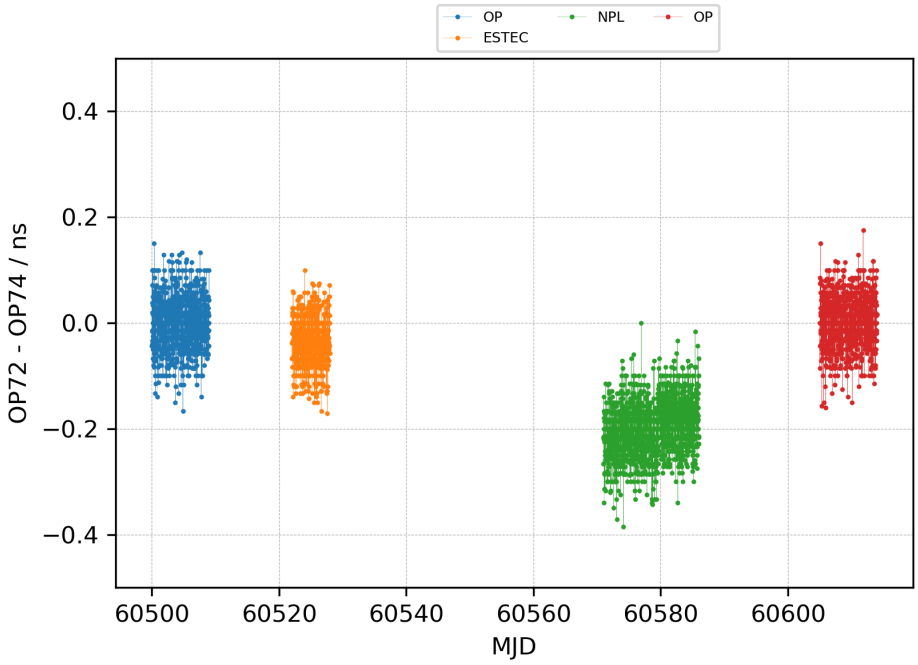

# A Annex A: BIPM information sheet.

## A.1 Implementation in OP.

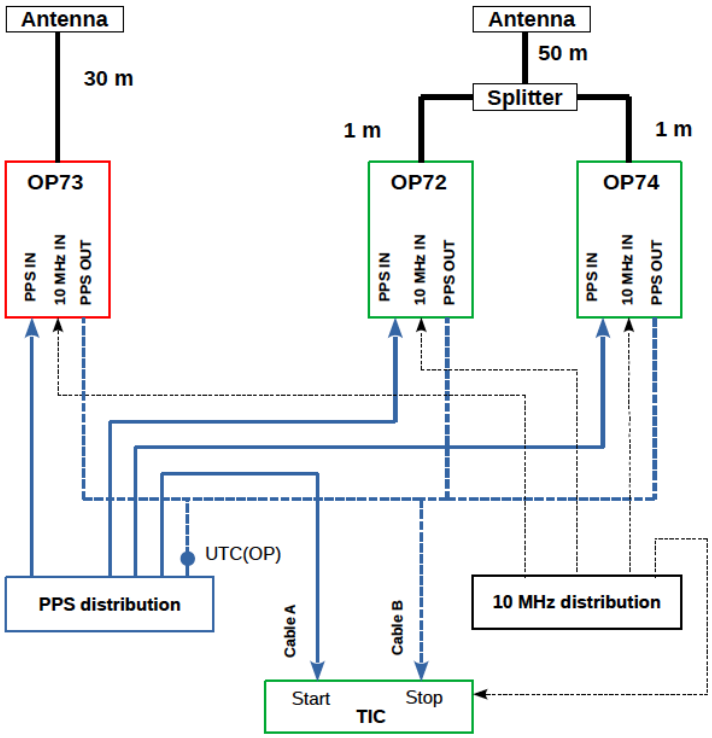


Figure 5: Implementation of OP traveling equipment in OP

## A.2 Implementation in ESTEC.

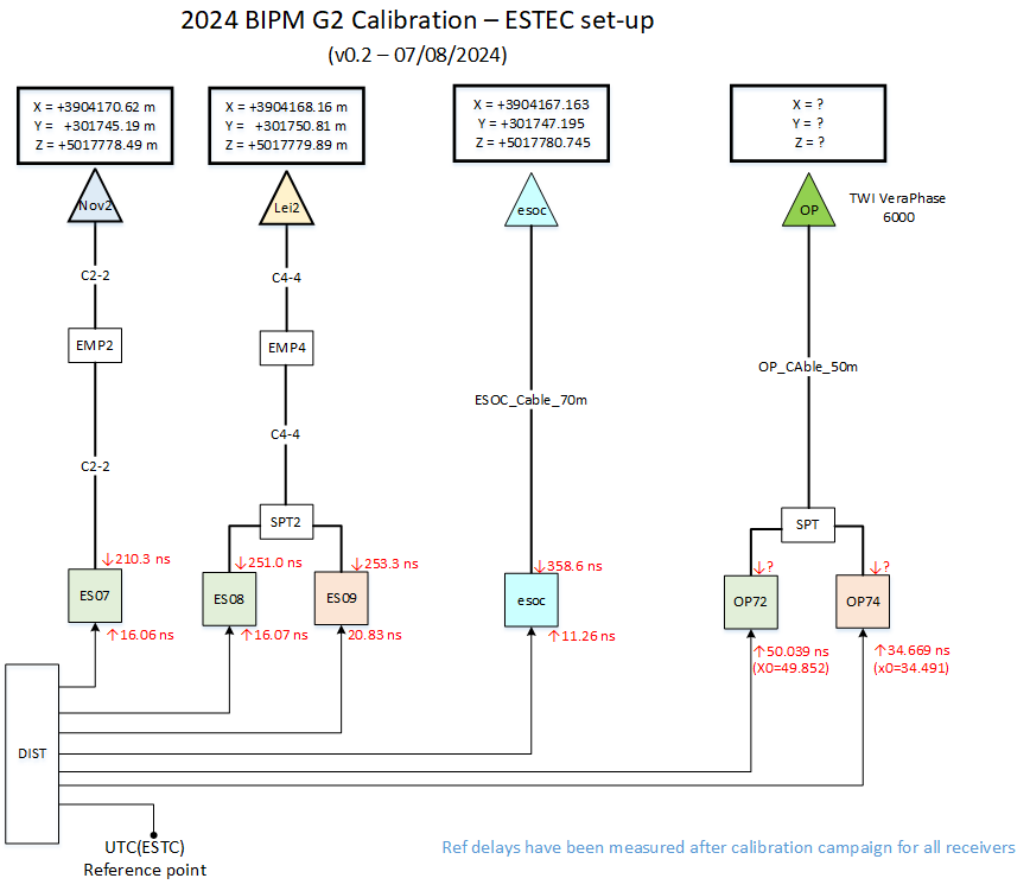


Figure 6: Implementation of ESTEC equipment

## A.3 Implementation in NPL.

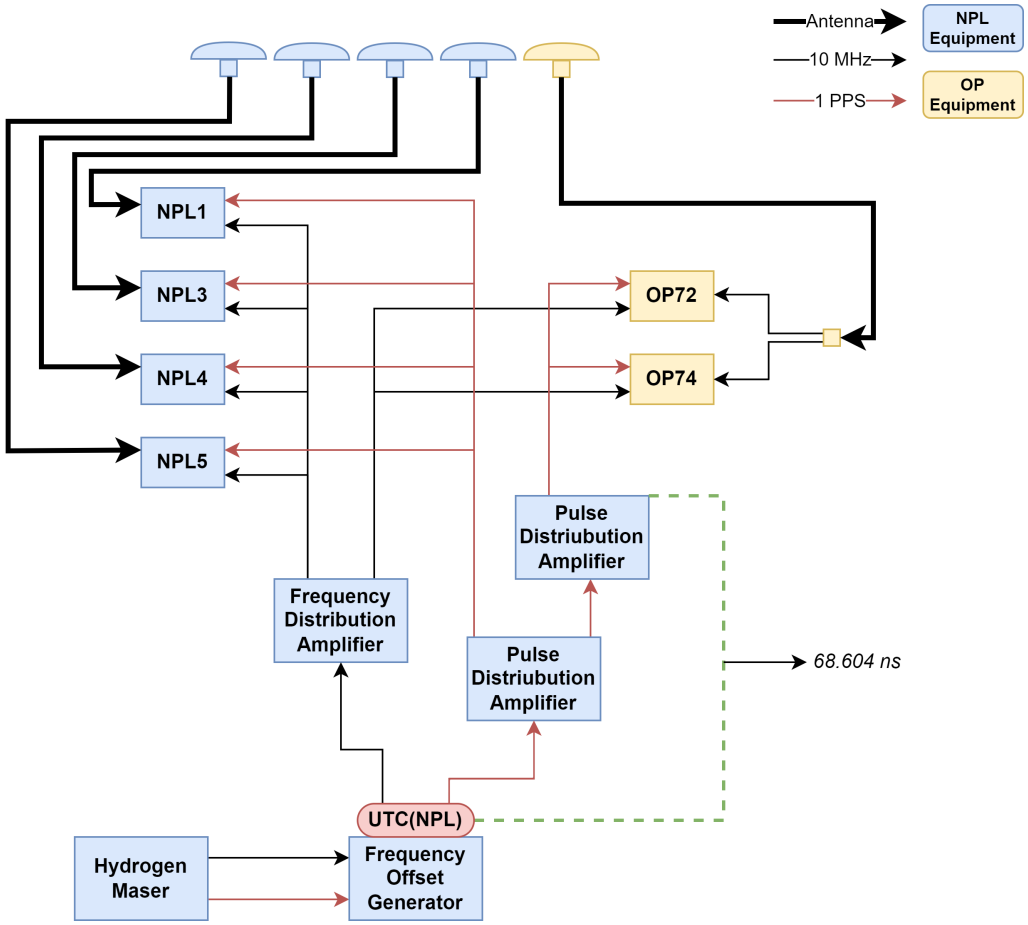


Figure 7: Implementation of NPL equipment

Cal Id: 1017-2024 Version / Date: 25/11/2024

**BIPM Information sheet**

| | |
|---|---|
| Laboratory | OP (Open) |
| Date and hour beginning of measurements | 09/07/2024 00:00:00 |
| Date and hour end measurements | 17/07/2024 23:59:59 |

| **Information on the system** | | | |
|---|---|---|---|
| | **Local** | **Traveling** | |
| 4-Character BIPM code | OP73 | OP72 | OP74 |
| Receiver maker and type | PolaRx5TR | PolaRx5TR | PolaRx5TR |
| Receiver serial number | 3069470 | 3069829 | 3069591 |
| 1 PPS triger level / V | 1 | 1 | 1 |
| Antenna cable marker and type | | HY 400 UF | HY 400 UF |
| Phase stabilized cable (Y/N) | N | N | N |
| Cable length outside building / m | 20 | 20 | 20 |
| Antenna maker and type | SEPCHOKE_B3E6 | TWIVP6000 | TWIVP6000 |
| Antenna serial number | 5769 | 33-685000-01-01 | 33-685000-01-01 |
| Temperature if stabilized / °C | | | |

| **Mesured delays / ns** | | | |
|---|---|---|---|
| | **Local** | **Traveling** | |
| Delay from local UTC(k) to receiver 1 PPS_IN | | | |
| Delay from 1 PPS_IN to internal reference (see Annex 1) | Compensation disabled | Compensation disabled | Compensation disabled |
| Antenna cable delay | | | |
| Splitter delay | | | |
| Additional cable delay | | | |

| **Data used for the generation of CGGTTS files** | | | |
|---|---|---|---|
| | **Local** | **Traveling** | |
| INT DLY (GPS) / ns | P1: 29.55 P2: 26.02 | P1: 224.238 P2: 222.135 | P1: 224.913 P2: 222.872 |
| INT DLY (Galileo) / ns | E1: 31.78 E5a: 31.52 | E1: 226.595 E5a: 225.976 | E1: 227.412 E5a: 226.730 |
| INT DLY (Beidou) / ns | B1c: 31.63 B2a: 30.93 | B1c: 226.375 B2a: 225.409 | B1c: 227.283 B2a: 226.165 |
| CAB DLY / ns | 129.6 | 0.0 | 0.0 |
| REF DLY / ns | 85.2 | 93.3 | 111.3 |
| Coordinate reference frame | ITRF | ITRF | ITRF |
| Latitude or X / m | 4202777.071 | 4202781.362 | 4202781.362 |
| Longitude or Y / m | 171367.028 | 171369.370 | 171369.370 |
| Height or Z / m | 4778661.392 | 4778659.038 | 4778659.038 |

| **General Information** | |
|---|---|
| Rise time of local UTC pulse | 500 ps |
| Air conditioning (Y/N) | Y |
| Set temperature value and uncertainty | 22+/-1°C |
| Set humidity value and uncertainty | NA |

Cal Id: 1017-2024 Version / Date: 25/11/2024

**BIPM Information sheet**

| | |
|---|---|
| Laboratory | OP (Close) |
| Date and hour beginning of measurements | 22/10/2024 00:00:00 |
| Date and hour end measurements | 30/10/2024 23:59:59 |

| **Information on the system** | | | |
|---|---|---|---|
| | **Local** | **Traveling** | |
| 4-Character BIPM code | OP73 | OP72 | OP74 |
| Receiver maker and type | PolaRx5TR | PolaRx5TR | PolaRx5TR |
| Receiver serial number | 3069470 | 3069829 | 3069591 |
| 1 PPS triger level / V | 1 | 1 | 1 |
| Antenna cable marker and type | | HY 400 UF | HY 400 UF |
| Phase stabilized cable (Y/N) | N | N | N |
| Cable length outside building / m | 20 | 20 | 20 |
| Antenna maker and type | SEPCHOKE_B3E6 | TWIVP6000 | TWIVP6000 |
| Antenna serial number | 5769 | 33-685000-01-01 | 33-685000-01-01 |
| Temperature if stabilized / °C | | | |

| **Mesured delays / ns** | | | |
|---|---|---|---|
| | **Local** | **Traveling** | |
| Delay from local UTC(k) to receiver 1 PPS_IN | | | |
| Delay from 1 PPS_IN to internal reference (see Annex 1) | Compensation disabled | Compensation disabled | Compensation disabled |
| Antenna cable delay | | | |
| Splitter delay | | | |
| Additional cable delay | | | |

| **Data used for the generation of CGGTTS files** | | | |
|---|---|---|---|
| | **Local** | **Traveling** | |
| INT DLY (GPS) / ns | P1: 29.55 P2: 26.02 | P1: 224.145 P2: 221.990 | P1: 224.789 P2: 222.693 |
| INT DLY (Galileo) / ns | E1: 31.78 E5a: 31.52 | E1: 226.528 E5a: 226.017 | E1: 227.313 E5a: 226.744 |
| INT DLY (Beidou) / ns | B1c: 31.63 B2a: 30.93 | B1c: 226.308 B2a: 225.436 | B1c: 227.186 B2a: 226.164 |
| CAB DLY / ns | 129.6 | 0.0 | 0.0 |
| REF DLY / ns | 85.2 | 93.4 | 111.4 |
| Coordinate reference frame | ITRF | ITRF | ITRF |
| Latitude or X / m | 4202777.071 | 4202781.393 | 4202781.393 |
| Longitude or Y / m | 171367.028 | 171369.415 | 171369.415 |
| Height or Z / m | 4778661.392 | 4778659.066 | 4778659.066 |

| **General Information** | |
|---|---|
| Rise time of local UTC pulse | 500 ps |
| Air conditioning (Y/N) | Y |
| Set temperature value and uncertainty | 22+/-1°C |
| Set humidity value and uncertainty | NA |

Cal Id: 1017-2024 Version / Date: 25/11/2024

**BIPM Information sheet**

| | |
|---|---|
| Laboratory | ESA ESTEC UTC Laboratory |
| Date and hour beginning of measurements | 31.07.2024 00:00 |
| Date and hour end measurements | 05.08.2024 23:59 |

| **Information on the system** | | | |
|---|---|---|---|
| | **Local** | **Traveling** | |
| 4-Character BIPM code | ES07 | OP72 | OP74 |
| Receiver maker and type | SEPT POLARX5TR | PolaRx5TR | PolaRx5TR |
| Receiver serial number | 3018491 | 3069829 | 3069591 |
| 1 PPS triger level / V | 1 | 1 | 1 |
| Antenna cable marker and type | H+S SUCOFEED 1/2 | HY 400 UF | HY 400 UF |
| Phase stabilized cable (Y/N) | N | N | N |
| Cable length outside building / m | 30 | 30 | 30 |
| Antenna maker and type | NOV750.R4 | TWIVP6000 | TWIVP6000 |
| Antenna serial number | SN1018874 | 33-685000-01-01 | 33-685000-01-01 |
| Temperature if stabilized / °C | 22.4 | 22.4 | 22.4 |

| **Mesured delays / ns** | | | |
|---|---|---|---|
| | **Local** | **Traveling** | |
| Delay from local UTC(k) to receiver 1 PPS_IN | 16.06 | | |
| Delay from 1 PPS_IN to internal reference (see Annex 1) | 0 (Compensation enabled) | Compensation disabled | Compensation disabled |
| Antenna cable delay | 210.3 | N/A | N/A |
| Splitter delay | N/A | N/A | N/A |
| Additional cable delay | N/A | N/A | N/A |

| **Data used for the generation of CGGTTS files** | | | |
|---|---|---|---|
| | **Local** | **Traveling** | |
| INT DLY (GPS) / ns | P1: 28.062 P2: 24.720 | P1: 224.191 P2: 224.191 | P1: 224.851 P2: 222.782 |
| INT DLY (Galileo) / ns | E1: 30.410 E5a: 30.098 | E1: 226.561 E5a: 225.997 | E1: 227.363 E5a: 226.737 |
| INT DLY (Beidou) / ns | B1c: 30.214 B2a: 29.528 | B1c: 226.341 B2a: 225.422 | B1c: 227.235 B2a: 226.164 |
| CAB DLY / ns | 210.3 | 0.0 | 0.0 |
| REF DLY / ns | 16.06 | 50.056 | 34.668 |
| Coordinate reference frame | ITRF | ITRF | ITRF |
| Latitude or X / m | +3904170.571 | +3904165.842 | +3904165.842 |
| Longitude or Y / m | +301745.265 | +301748.046 | +301748.046 |
| Height or Z / m | +5017778.558 | +5017781.907 | +5017781.907 |

| **General Information** | |
|---|---|
| Rise time of local UTC pulse | 560 ps (TPDIS1)500 ps |
| Air conditioning (Y/N) | Y |
| Set temperature value and uncertainty | μ = 22.0 °C, σ = 0.5 °C |
| Set humidity value and uncertainty | μ = 50 %, σ = 5 % |

Cal Id: 1017-2024 Version / Date: 25/11/2024

**BIPM Information sheet**

| | |
|---|---|
| Laboratory | ESA ESTEC UTC Laboratory |
| Date and hour beginning of measurements | 31.07.2024 00:00 |
| Date and hour end measurements | 05.08.2024 23:59 |

| Information on the system | | | |
|---|---|---|---|
| | **Local** | **Traveling** | |
| 4-Character BIPM code | ES08 | OP72 | OP74 |
| Receiver maker and type | SEPT POLARX5TR | PolaRx5TR | PolaRx5TR |
| Receiver serial number | 3022405 | 3069829 | 3069591 |
| 1 PPS triger level / V | 1 | 1 | 1 |
| Antenna cable marker and type | H+S SUCOFEED 1/2 | HY 400 UF | HY 400 UF |
| Phase stabilized cable (Y/N) | N | N | N |
| Cable length outside building / m | 30 | 30 | 30 |
| Antenna maker and type | LEIAR20 | TWIVP6000 | TWIVP6000 |
| Antenna serial number | 21102015 | 33-685000-01-01 | 33-685000-01-01 |
| Temperature if stabilized / °C | 22.4 | 22.4 | 22.4 |

| Mesured delays / ns | | | |
|---|---|---|---|
| | **Local** | **Traveling** | |
| Delay from local UTC(k) to receiver 1 PPS_IN | 16.07 | | |
| Delay from 1 PPS_IN to internal reference (see Annex 1) | 0 (Compensation enabled) | Compensation disabled | Compensation disabled |
| Antenna cable delay | 251.0 | N/A | N/A |
| Splitter delay | Inc. in ant. cab. delay | N/A | N/A |
| Additional cable delay | N/A | N/A | N/A |

| Data used for the generation of CGGTTS files | | | |
|---|---|---|---|
| | **Local** | **Traveling** | |
| INT DLY (GPS) / ns | P1: 29.464 P2: 27.655 | P1: 224.191 P2: 222.062 | P1: 224.851 P2: 222.782 |
| INT DLY (Galileo) / ns | E1: 32.078 E5a: 34.705 | E1: 226.561 E5a: 225.997 | E1: 227.363 E5a: 226.737 |
| INT DLY (Beidou) / ns | B1c: 31.912 B2a: 34.126 | B1c: 226.341 B2a: 225.422 | B1c: 227.235 B2a: 226.164 |
| CAB DLY / ns | 251.0 | 0.0 | 0.0 |
| REF DLY / ns | 16.07 | 50.056 | 34.668 |
| Coordinate reference frame | ITRF | ITRF | ITRF |
| Latitude or X / m | +3904168.114 | +3904165.842 | +3904165.842 |
| Longitude or Y / m | +301750.882 | +301748.046 | +301748.046 |
| Height or Z / m | +5017779.948 | +5017781.907 | +5017781.907 |

| General Information | |
|---|---|
| Rise time of local UTC pulse | 560 ps |
| Air conditioning (Y/N) | Y |
| Set temperature value and uncertainty | μ = 22.0 °C, σ = 0.5 °C |
| Set humidity value and uncertainty | μ = 50 %, σ = 5 % |

Cal Id: 1017-2024 Version / Date: 25/11/2024

**BIPM Information sheet**

| | |
|---|---|
| Laboratory | ESA ESTEC UTC Laboratory |
| Date and hour beginning of measurements | 31.07.2024 00:00 |
| Date and hour end measurements | 05.08.2024 23:59 |

| Information on the system | | | |
|---|---|---|---|
| | **Local** | **Traveling** | |
| 4-Character BIPM code | ES09 | OP72 | OP74 |
| Receiver maker and type | MESIT GTR55 | PolaRx5TR | PolaRx5TR |
| Receiver serial number | 1808067 | 3069829 | 3069591 |
| 1 PPS triger level / V | 1 V | 1 | 1 |
| Antenna cable marker and type | H+S SUCOFEED 1/2 | HY 400 UF | HY 400 UF |
| Phase stabilized cable (Y/N) | N | N | N |
| Cable length outside building / m | 30 | 30 | 30 |
| Antenna maker and type | LEIAR20 | TWIVP6000 | TWIVP6000 |
| Antenna serial number | 21102015 | 33-685000-01-01 | 33-685000-01-01 |
| Temperature if stabilized / °C | 22.4 | 22.4 | 22.4 |

| Mesured delays / ns | | | |
|---|---|---|---|
| | **Local** | **Traveling** | |
| Delay from local UTC(k) to receiver 1 PPS_IN | 20.83 | | |
| Delay from 1 PPS_IN to internal reference (see Annex 1) | | Compensation disabled | Compensation disabled |
| Antenna cable delay | 253.3 | N/A | N/A |
| Splitter delay | Inc. in ant. cab. delay | N/A | N/A |
| Additional cable delay | N/A | N/A | N/A |

| Data used for the generation of CGGTTS files | | | |
|---|---|---|---|
| | **Local** | **Traveling** | |
| INT DLY (GPS) / ns | P1: 19.240 P2: 16.202 | P1: 224.191 P2: 222.062 | P1: 224.851 P2: 222.782 |
| INT DLY (Galileo) / ns | E1: 19.822 E5a: 22.875 | E1: 226.561 E5a: 225.997 | E1: 227.363 E5a: 226.737 |
| INT DLY (Beidou) / ns | B1c: 19.295 B2a: 21.952 | B1c: 226.341 B2a: 225.422 | B1c: 227.235 B2a: 226.164 |
| CAB DLY / ns | 253.3 | 0.0 | 0.0 |
| REF DLY / ns | 20.83 | 50.056 | 34.668 |
| Coordinate reference frame | ITRF | ITRF | ITRF |
| Latitude or X / m | +3904168.114 | +3904165.842 | +3904165.842 |
| Longitude or Y / m | +301750.882 | +301748.046 | +301748.046 |
| Height or Z / m | +5017779.948 | +5017781.907 | +5017781.907 |

| General Information | |
|---|---|
| Rise time of local UTC pulse | 560 ps |
| Air conditioning (Y/N) | Y |
| Set temperature value and uncertainty | μ = 22.0 °C, σ = 0.5 °C |
| Set humidity value and uncertainty | μ = 50 %, σ = 5 % |

Cal Id: 1017-2024 Version / Date: 25/11/2024

**BIPM Information sheet**

| | |
|---|---|
| Laboratory | ESA ESTEC UTC Laboratory |
| Date and hour beginning of measurements | 31.07.2024 00:00 |
| Date and hour end measurements | 05.08.2024 23:59 |

| Information on the system | | | |
|---|---|---|---|
| | **Local** | **Traveling** | |
| 4-Character BIPM code | TR01 | OP72 | OP74 |
| Receiver maker and type | SEPT POLARX5TR | PolaRx5TR | PolaRx5TR |
| Receiver serial number | 3088050 | 3069829 | 3069591 |
| 1 PPS triger level / V | 1 V | 1 | 1 |
| Antenna cable marker and type | N/A | HY 400 UF | HY 400 UF |
| Phase stabilized cable (Y/N) | N | N | N |
| Cable length outside building / m | 30 | 30 | 30 |
| Antenna maker and type | SEPCHOKE_B3E6 | TWIVP6000 | TWIVP6000 |
| Antenna serial number | N/A | 33-685000-01-01 | 33-685000-01-01 |
| Temperature if stabilized / °C | 22.4 | 22.4 | 22.4 |

| Mesured delays / ns | | | |
|---|---|---|---|
| | **Local** | **Traveling** | |
| Delay from local UTC(k) to receiver 1 PPS_IN | 11.26 | | |
| Delay from 1 PPS_IN to internal reference (see Annex 1) | 0 (Compensation enabled) | Compensation disabled | Compensation disabled |
| Antenna cable delay | 358.6 | N/A | N/A |
| Splitter delay | N/A | N/A | N/A |
| Additional cable delay | N/A | N/A | N/A |

| Data used for the generation of CGGTTS files | | | |
|---|---|---|---|
| | **Local** | **Traveling** | |
| INT DLY (GPS) / ns | P1: 24.739 P2: 22.036 | P1: 224.191 P2: 224.191 | P1: 224.851 P2: 222.782 |
| INT DLY (Galileo) / ns | E1: 27.149 E5a: 27.268 | E1: 226.561 E5a: 225.997 | E1: 227.363 E5a: 226.737 |
| INT DLY (Beidou) / ns | B1c: 26.844 B2a: 26.723 | B1c: 226.341 B2a: 225.422 | B1c: 227.235 B2a: 226.164 |
| CAB DLY / ns | 358.6 | 0.0 | 0.0 |
| REF DLY / ns | 11.26 | 50.056 | 34.668 |
| Coordinate reference frame | ITRF | ITRF | ITRF |
| Latitude or X / m | +3904167.239 | +3904165.842 | +3904165.842 |
| Longitude or Y / m | +301747.201 | +301748.046 | +301748.046 |
| Height or Z / m | +5017780.865 | +5017781.907 | +5017781.907 |

| General Information | |
|---|---|
| Rise time of local UTC pulse | 560 ps |
| Air conditioning (Y/N) | Y |
| Set temperature value and uncertainty | μ = 22.0 °C, σ = 0.5 °C |
| Set humidity value and uncertainty | μ = 50 %, σ = 5 % |

Cal Id: 1017-2024 Version / Date: 25/11/2024

**BIPM Information sheet**

| | |
|---|---|
| Laboratory | NPL |
| Date and hour beginning of measurements | 18/09/2024 00:00 UTC |
| Date and hour end measurements | 02/10/2024 23:59 UTC |

| **Information on the system** | | | |
|---|---|---|---|
| | **Local** | **Traveling** | |
| 4-Character BIPM code | NPL1 | OP72 | OP74 |
| Receiver maker and type | DICOM GTR-50 | PolaRx5TR | PolaRx5TR |
| Receiver serial number | 0807183 | 3069829 | 3069591 |
| 1 PPS triger level / V | 1 V | 1 | 1 |
| Antenna cable marker and type | Andrew Heliax FSJ1-50 | HY 400 UF | HY 400 UF |
| Phase stabilized cable (Y/N) | Y | N | N |
| Cable length outside building / m | Approx. 6m | Approx. 8m | Approx. 8m |
| Antenna maker and type | Novatel GPS-720 | TWIVP6000 | TWIVP6000 |
| Antenna serial number | NAE1230001 | 33-685000-01-01 | 33-685000-01-01 |
| Temperature if stabilized / °C | N/A | N/A | N/A |

| **Mesured delays / ns** | | | |
|---|---|---|---|
| | **Local** | **Traveling** | |
| Delay from local UTC(k) to receiver 1 PPS_IN | 68.397 | | |
| Delay from 1 PPS_IN to internal reference (see Annex 1) | N/A | Compensation disabled | Compensation disabled |
| Antenna cable delay | 251.5 | N/A | N/A |
| Splitter delay | N/A | N/A | N/A |
| Additional cable delay | N/A | N/A | N/A |

| **Data used for the generation of CGGTTS files** | | | |
|---|---|---|---|
| | **Local** | **Traveling** | |
| INT DLY (GPS) / ns | P1: -35.723 P2: -26.902 | P1: 224.191 P2: 224.191 | P1: 224.851 P2: 222.782 |
| INT DLY (Galileo) / ns | E1: E5a: | E1: 226.561 E5a: 225.997 | E1: 227.363 E5a: 226.737 |
| INT DLY (Beidou) / ns | B1c: B2a: | B1c: 226.341 B2a: 225.422 | B1c: 227.235 B2a: 226.164 |
| CAB DLY / ns | 251.5 | 0.0 | 0.0 |
| REF DLY / ns | 68.397 | 111.418 | 129.248 |
| Coordinate reference frame | ITRF20 | ITRF20 | ITRF20 |
| Latitude or X / m | +3985120.141 m | +3985110.174 m | +3985110.174 m |
| Longitude or Y / m | -23893.587 m | -23888.810 m | -23888.810 m |
| Height or Z / m | +4963240.484 m | +4963248.574 m | +4963248.574 m |

| **General Information** | |
|---|---|
| Rise time of local UTC pulse | |
| Air conditioning (Y/N) | Y |
| Set temperature value and uncertainty | 23 +/1 1°C |
| Set humidity value and uncertainty | N/A |

Cal Id: 1017-2024 Version / Date: 25/11/2024

**BIPM Information sheet**

| | |
|---|---|
| Laboratory | NPL |
| Date and hour beginning of measurements | 18/09/2024 00:00 UTC |
| Date and hour end measurements | 02/10/2024 23:59 UTC |

| Information on the system | | | |
|---|---|---|---|
| | **Local** | **Traveling** | |
| 4-Character BIPM code | NPL3 | OP72 | OP74 |
| Receiver maker and type | Septentrio PolaRx5TR | PolaRx5TR | PolaRx5TR |
| Receiver serial number | 4701299 | 3069829 | 3069591 |
| 1 PPS triger level / V | 1 V | 1 | 1 |
| Antenna cable marker and type | Times Microwave LMR-400 | HY 400 UF | HY 400 UF |
| Phase stabilized cable (Y/N) | Y | N | N |
| Cable length outside building / m | Approx. 4m | Approx. 8m | Approx. 8m |
| Antenna maker and type | AT1675-540S | TWIVP6000 | TWIVP6000 |
| Antenna serial number | 14255 | 33-685000-01-01 | 33-685000-01-01 |
| Temperature if stabilized / °C | N/A | N/A | N/A |

| Mesured delays / ns | | | |
|---|---|---|---|
| | **Local** | **Traveling** | |
| Delay from local UTC(k) to receiver 1 PPS_IN | 73.310 ns | | |
| Delay from 1 PPS_IN to internal reference (see Annex 1) | 0 (Compensation enabled) | Compensation disabled | Compensation disabled |
| Antenna cable delay | 294.7 ns | N/A | N/A |
| Splitter delay | N/A | N/A | N/A |
| Additional cable delay | N/A | N/A | N/A |

| Data used for the generation of CGGTTS files | | | |
|---|---|---|---|
| | **Local** | **Traveling** | |
| INT DLY (GPS) / ns | P1: 21.622 P2: 21.596 | P1: 224.191 P2: 224.191 | P1: 224.851 P2: 222.782 |
| INT DLY (Galileo) / ns | E1: 24.319 E5a: 26.184 | E1: 226.561 E5a: 225.997 | E1: 227.363 E5a: 226.737 |
| INT DLY (Beidou) / ns | B1c: 23.961 B2a: 25.604 | B1c: 226.341 B2a: 225.422 | B1c: 227.235 B2a: 226.164 |
| CAB DLY / ns | 294.7 | 0.0 | 0.0 |
| REF DLY / ns | 73.310 | 111.418 | 129.248 |
| Coordinate reference frame | ITRF20 | ITRF20 | ITRF20 |
| Latitude or X / m | 3985114.226 m | +3985110.174 m | +3985110.174 m |
| Longitude or Y / m | -23890.768 m | -23888.810 m | -23888.810 m |
| Height or Z / m | 4963245.184 m | +4963248.574 m | +4963248.574 m |

| General Information | |
|---|---|
| Rise time of local UTC pulse | |
| Air conditioning (Y/N) | Y |
| Set temperature value and uncertainty | 23 +/1 1°C |
| Set humidity value and uncertainty | N/A |

Cal Id: 1017-2024 Version / Date: 25/11/2024

**BIPM Information sheet**

| | |
|---|---|
| Laboratory | NPL |
| Date and hour beginning of measurements | 18/09/2024 00:00 UTC |
| Date and hour end measurements | 02/10/2024 23:59 UTC |

| Information on the system | | | |
|---|---|---|---|
| | **Local** | **Traveling** | |
| 4-Character BIPM code | NPL4 | OP72 | OP74 |
| Receiver maker and type | MESIT GTR-51 | PolaRx5TR | PolaRx5TR |
| Receiver serial number | 41611078 | 3069829 | 3069591 |
| 1 PPS triger level / V | 1 V | 1 | 1 |
| Antenna cable marker and type | ndrew Helia FSJ1-50A | HY 400 UF | HY 400 UF |
| Phase stabilized cable (Y/N) | Y | N | N |
| Cable length outside building / m | Approx. 4m | Approx. 8m | Approx. 8m |
| Antenna maker and type | Novatel GPS-703-GGG | TWIVP6000 | TWIVP6000 |
| Antenna serial number | NEG17070065 | 33-685000-01-01 | 33-685000-01-01 |
| Temperature if stabilized / °C | N/A | N/A | N/A |

| Mesured delays / ns | | | |
|---|---|---|---|
| | **Local** | **Traveling** | |
| Delay from local UTC(k) to receiver 1 PPS_IN | 63.452 | | |
| Delay from 1 PPS_IN to internal reference (see Annex 1) | N/A | Compensation disabled | Compensation disabled |
| Antenna cable delay | 336.2 | N/A | N/A |
| Splitter delay | N/A | N/A | N/A |
| Additional cable delay | N/A | N/A | N/A |

| Data used for the generation of CGGTTS files | | | |
|---|---|---|---|
| | **Local** | **Traveling** | |
| INT DLY (GPS) / ns | P1: 27.235 P2: 27.920 | P1: 224.191 P2: 224.191 | P1: 224.851 P2: 222.782 |
| INT DLY (Galileo) / ns | E1: 30.618 E5a: 29.275 | E1: 226.561 E5a: 225.997 | E1: 227.363 E5a: 226.737 |
| INT DLY (Beidou) / ns | B1c: B2a: | B1c: 226.341 B2a: 225.422 | B1c: 227.235 B2a: 226.164 |
| CAB DLY / ns | 336.2 | 0.0 | 0.0 |
| REF DLY / ns | 63.452 | 111.418 | 129.248 |
| Coordinate reference frame | ITRF20 | ITRF20 | ITRF20 |
| Latitude or X / m | +3985112.192 m | +3985110.174 m | +3985110.174 m |
| Longitude or Y / m | -23889.790 m | -23888.810 m | -23888.810 m |
| Height or Z / m | +4963246.844 m | +4963248.574 m | +4963248.574 m |

| General Information | |
|---|---|
| Rise time of local UTC pulse | |
| Air conditioning (Y/N) | Y |
| Set temperature value and uncertainty | 23 +/1 1°C |
| Set humidity value and uncertainty | N/A |

Cal Id: 1017-2024 Version / Date: 25/11/2024

**BIPM Information sheet**

| | |
|---|---|
| Laboratory | NPL |
| Date and hour beginning of measurements | 18/09/2024 00:00 UTC |
| Date and hour end measurements | 02/10/2024 23:59 UTC |

| Information on the system | | | |
|---|---|---|---|
| | **Local** | **Traveling** | |
| 4-Character BIPM code | NPL5 | OP72 | OP74 |
| Receiver maker and type | MESIT GTR-55 | PolaRx5TR | PolaRx5TR |
| Receiver serial number | 2010008 | 3069829 | 3069591 |
| 1 PPS triger level / V | 1 V | 1 | 1 |
| Antenna cable marker and type | ndrew Helia FSJ1-50A | HY 400 UF | HY 400 UF |
| Phase stabilized cable (Y/N) | Y | N | N |
| Cable length outside building / m | Approx. 4m | Approx. 8m | Approx. 8m |
| Antenna maker and type | Novatel GNSS-850 | TWIVP6000 | TWIVP6000 |
| Antenna serial number | NMLK20310022H | 33-685000-01-01 | 33-685000-01-01 |
| Temperature if stabilized / °C | N/A | N/A | N/A |

| Mesured delays / ns | | | |
|---|---|---|---|
| | **Local** | **Traveling** | |
| Delay from local UTC(k) to receiver 1 PPS_IN | 65.404 | | |
| Delay from 1 PPS_IN to internal reference (see Annex 1) | N/A | Compensation disabled | Compensation disabled |
| Antenna cable delay | 261.2 | N/A | N/A |
| Splitter delay | N/A | N/A | N/A |
| Additional cable delay | N/A | N/A | N/A |

| Data used for the generation of CGGTTS files | | | |
|---|---|---|---|
| | **Local** | **Traveling** | |
| INT DLY (GPS) / ns | P1: 11.806 P2: 10.714 | P1: 224.191 P2: 224.191 | P1: 224.851 P2: 222.782 |
| INT DLY (Galileo) / ns | E1: 12.648 E5a: 11.890 | E1: 226.561 E5a: 225.997 | E1: 227.363 E5a: 226.737 |
| INT DLY (Beidou) / ns | B1c: 11.542 B2a: 10.874 | B1c: 226.341 B2a: 225.422 | B1c: 227.235 B2a: 226.164 |
| CAB DLY / ns | 261.2 | 0.0 | 0.0 |
| REF DLY / ns | 65.404 | 111.418 | 129.248 |
| Coordinate reference frame | ITRF20 | ITRF20 | ITRF20 |
| Latitude or X / m | +3985118.136 m | +3985110.174 m | +3985110.174 m |
| Longitude or Y / m | -23892.595 m | -23888.810 m | -23888.810 m |
| Height or Z / m | +4963242.176 m | +4963248.574 m | +4963248.574 m |

| General Information | |
|---|---|
| Rise time of local UTC pulse | |
| Air conditioning (Y/N) | Y |
| Set temperature value and uncertainty | 23 +/1 1°C |
| Set humidity value and uncertainty | N/A |

# B Annex B: Plots of raw data and TDEV analysis for GPS and Galileo.

## B.1 GPS calibration.

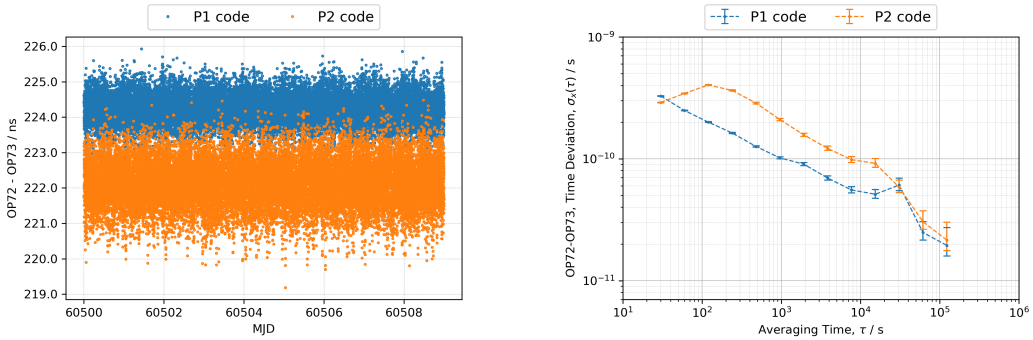


(a) P-code phase differences

(b) TDEV of P-code delays

Figure 8: Relative calibration of OP72 with respect to OP73

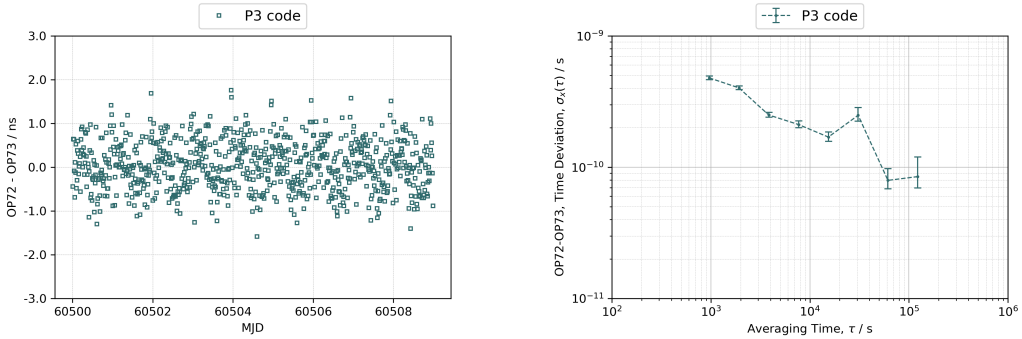


(a) P3 CV after calibration

(b) TDEV of P3 CV

Figure 9: P3 CV time difference OP72 with respect to OP73

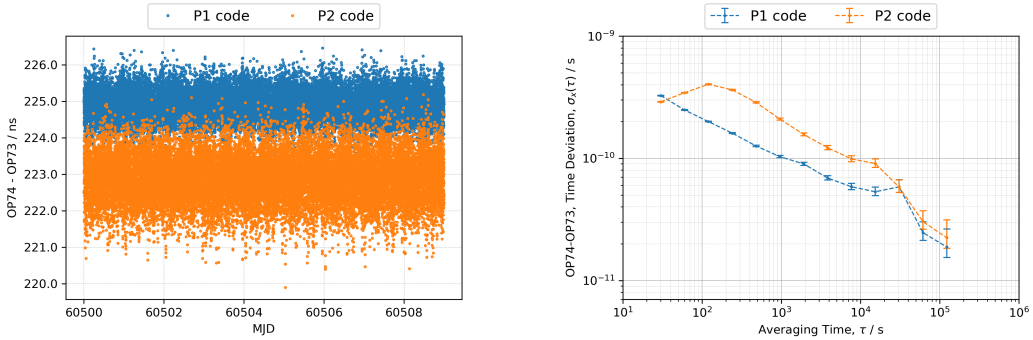


(a) P-code phase differences

(b) TDEV of P-code delays

Figure 10: Relative calibration of OP74 with respect to OP73


(a) P3 CV after calibration

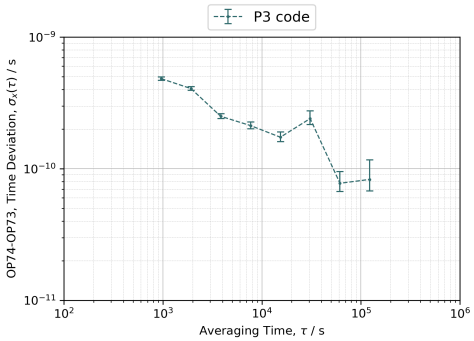


(b) TDEV of P3 CV

Figure 11: P3 CV time difference OP74 with respect to OP73

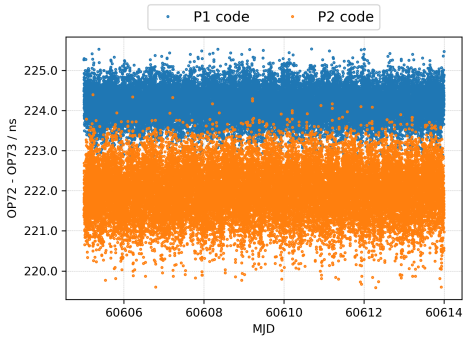


(a) P-code phase differences

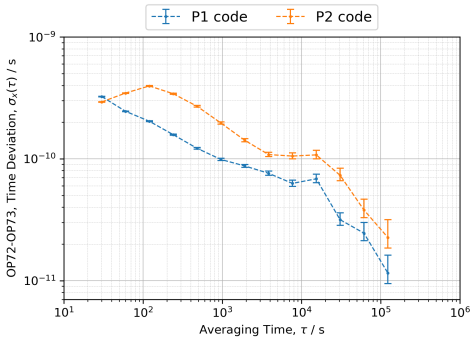


(b) TDEV of P-code delays

Figure 12: Relative calibration of OP72 with respect to OP73

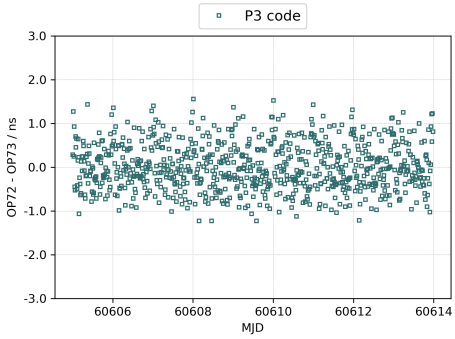


(a) P3 CV after calibration

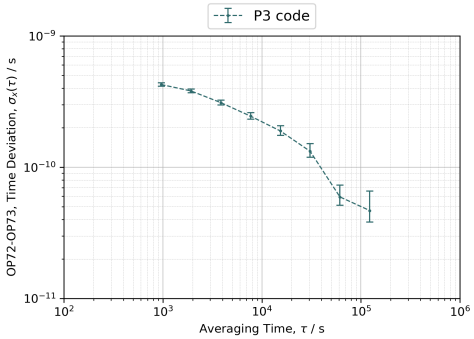


(b) TDEV of P3 CV

Figure 13: P3 CV time difference OP72 with respect to OP73

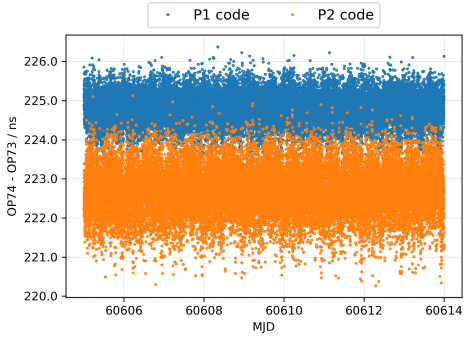


(a) P-code phase differences

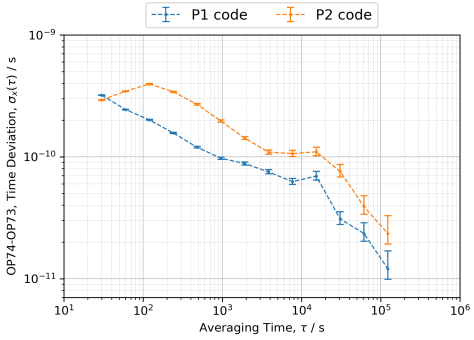


(b) TDEV of P-code delays

Figure 14: Relative calibration of OP74 with respect to OP73

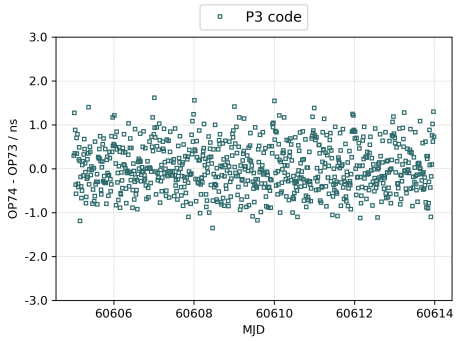


(a) P3 CV after calibration

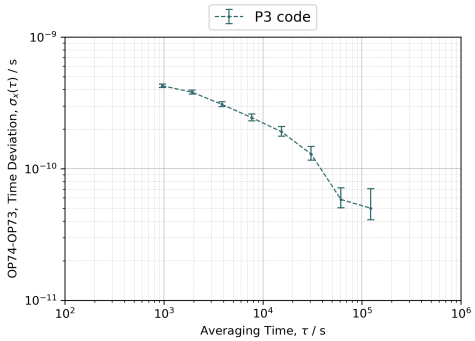


(b) TDEV of P3 CV

Figure 15: P3 CV time difference OP74 with respect to OP73


(a) P-code phase differences

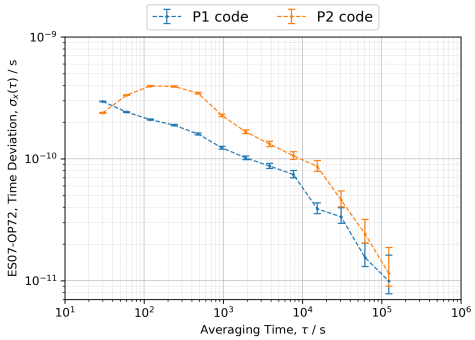


(b) TDEV of P-code delays

Figure 16: Relative calibration of ES07 with respect to OP72

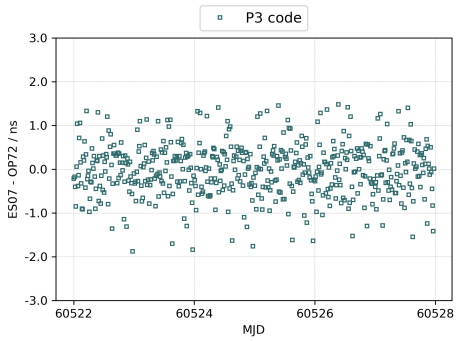


(a) P3 CV after calibration

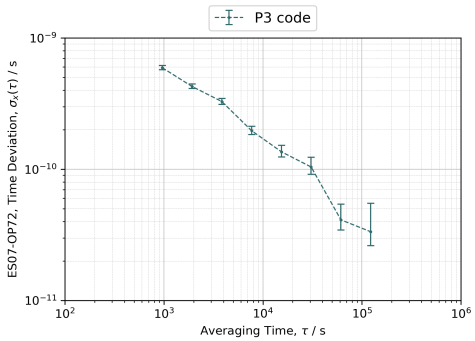


(b) TDEV of P3 CV

Figure 17: P3 CV time difference ES07 with respect to OP72

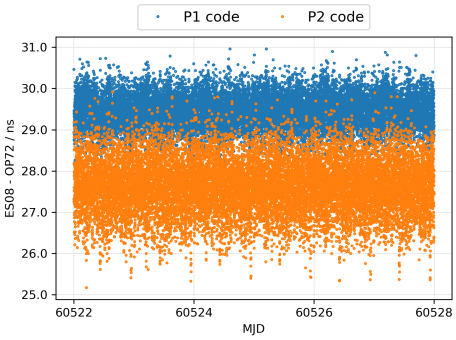


(a) P-code phase differences

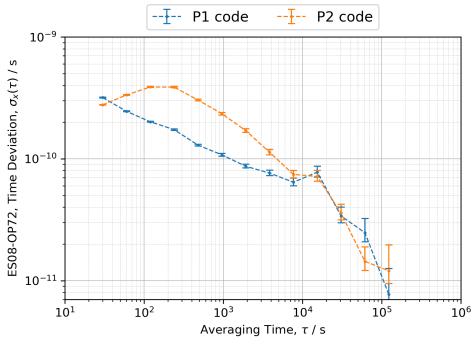


(b) TDEV of P-code delays

Figure 18: Relative calibration of ES08 with respect to OP72

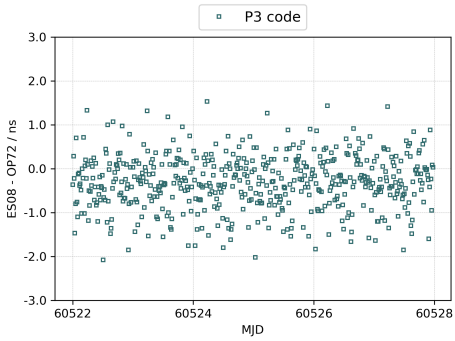


(a) P3 CV after calibration

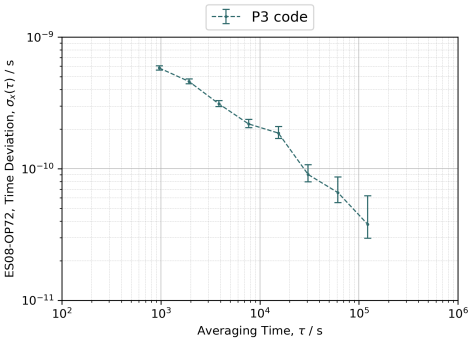


(b) TDEV of P3 CV

Figure 19: P3 CV time difference ES08 with respect to OP72


(a) P-code phase differences

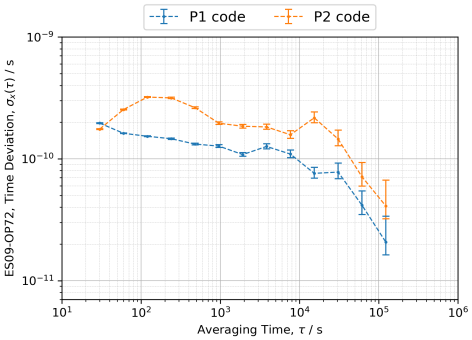


(b) TDEV of P-code delays

Figure 20: Relative calibration of ES09 with respect to OP72

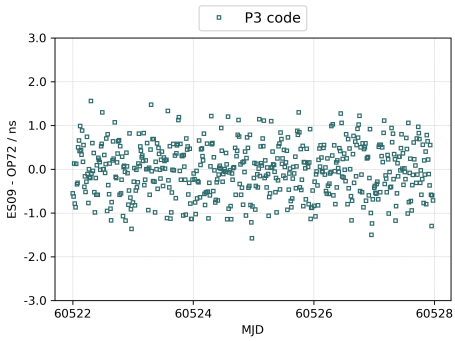


(a) P3 CV after calibration

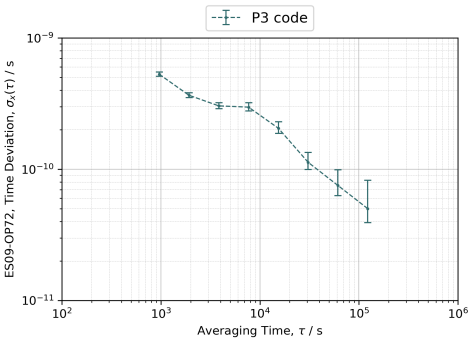


(b) TDEV of P3 CV

Figure 21: P3 CV time difference ES09 with respect to OP72

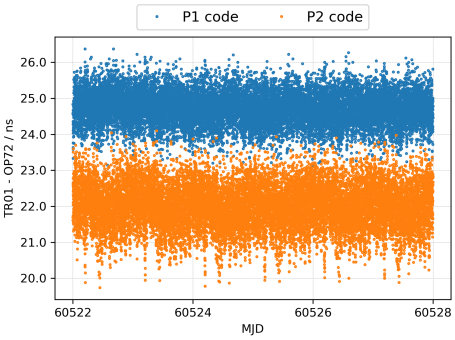


(a) P-code phase differences

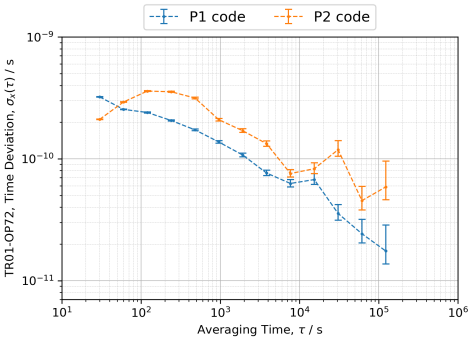


(b) TDEV of P-code delays

Figure 22: Relative calibration of TR01 with respect to OP72

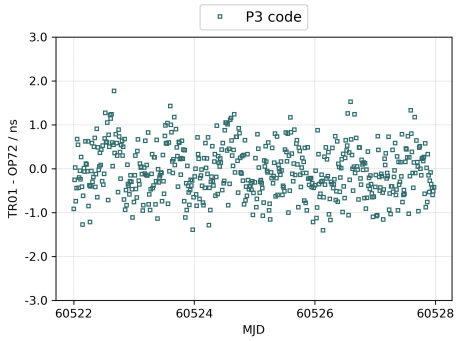


(a) P3 CV after calibration

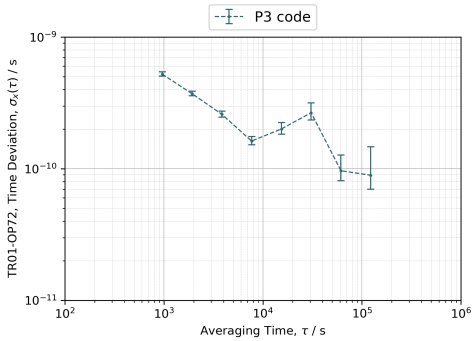


(b) TDEV of P3 CV

Figure 23: P3 CV time difference TR01 with respect to OP72


(a) P-code phase differences

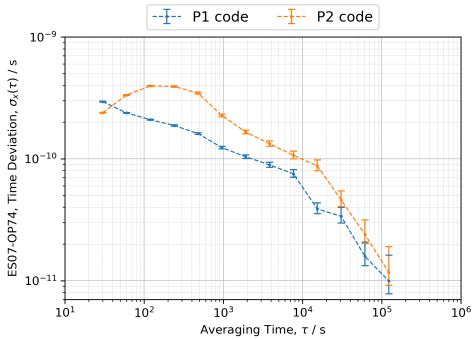


(b) TDEV of P-code delays

Figure 24: Relative calibration of ES07 with respect to OP74

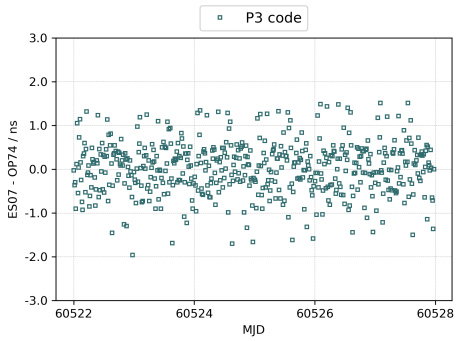


(a) P3 CV after calibration

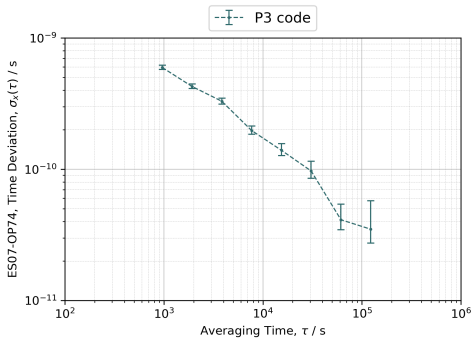


(b) TDEV of P3 CV

Figure 25: P3 CV time difference ES07 with respect to OP74

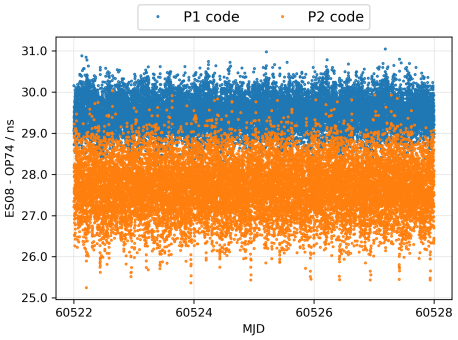


(a) P-code phase differences

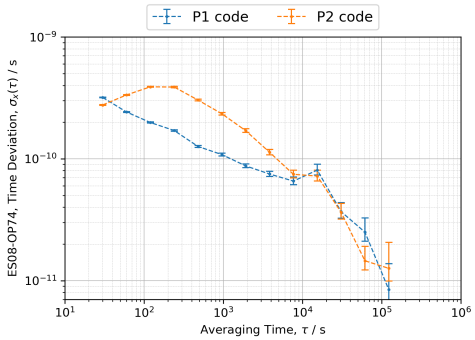


(b) TDEV of P-code delays

Figure 26: Relative calibration of ES08 with respect to OP74


(a) P3 CV after calibration

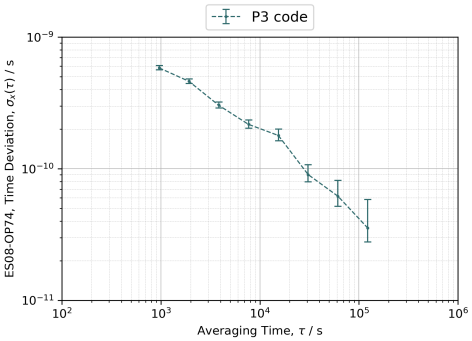


(b) TDEV of P3 CV

Figure 27: P3 CV time difference ES08 with respect to OP74


(a) P-code phase differences

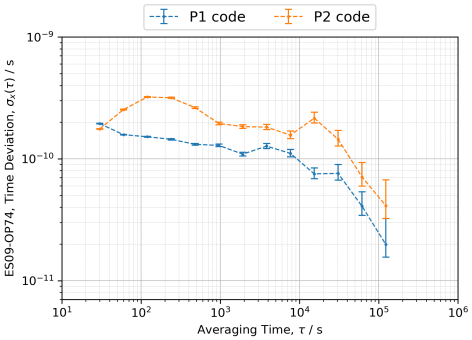


(b) TDEV of P-code delays

Figure 28: Relative calibration of ES09 with respect to OP74

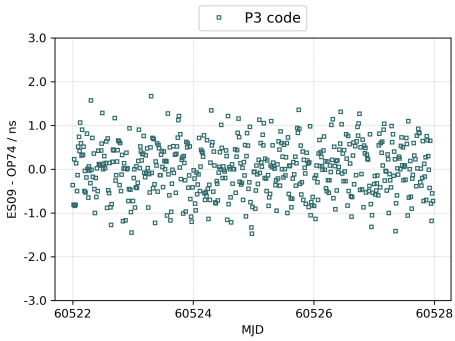


(a) P3 CV after calibration

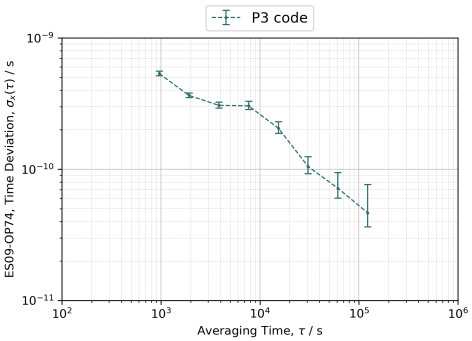


(b) TDEV of P3 CV

Figure 29: P3 CV time difference ES09 with respect to OP74


(a) P-code phase differences

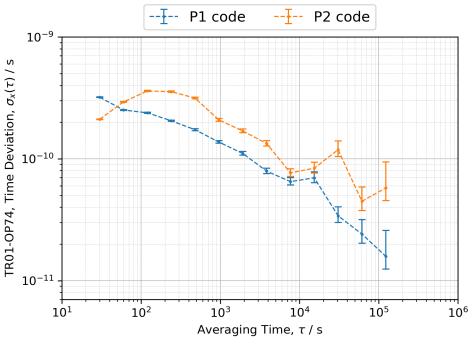


(b) TDEV of P-code delays

Figure 30: Relative calibration of TR01 with respect to OP74


(a) P3 CV after calibration

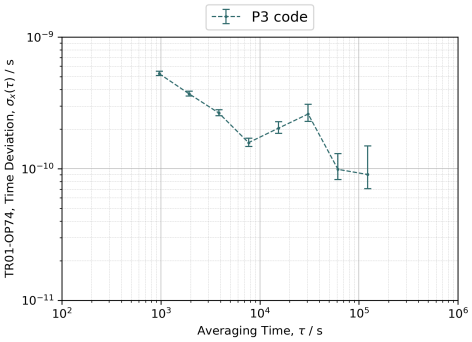


(b) TDEV of P3 CV

Figure 31: P3 CV time difference TR01 with respect to OP74


(a) P-code phase differences

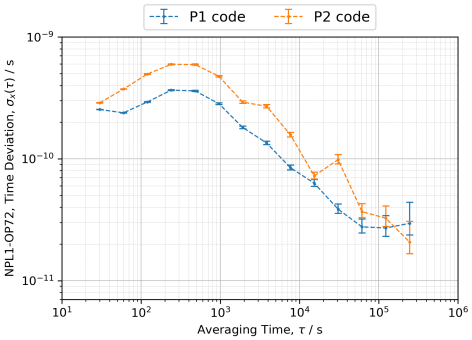


(b) TDEV of P-code delays

Figure 32: Relative calibration of NPL1 with respect to OP72

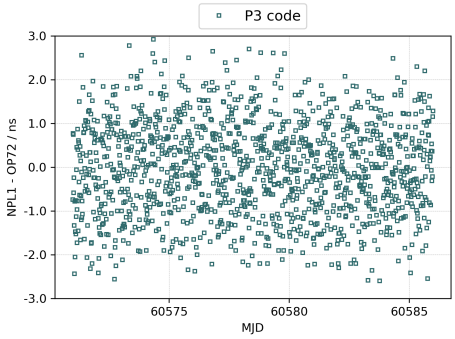


(a) P3 CV after calibration

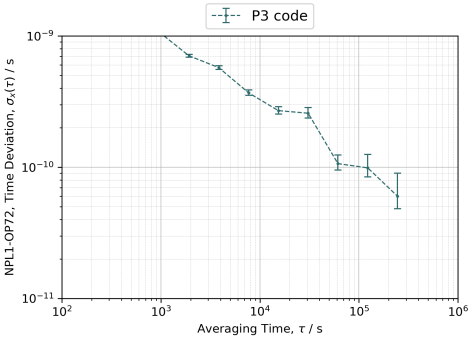


(b) TDEV of P3 CV

Figure 33: P3 CV time difference NPL1 with respect to OP72

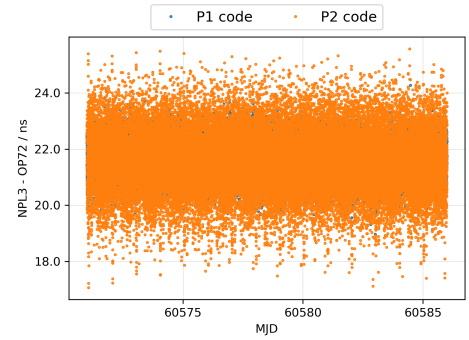


(a) P-code phase differences

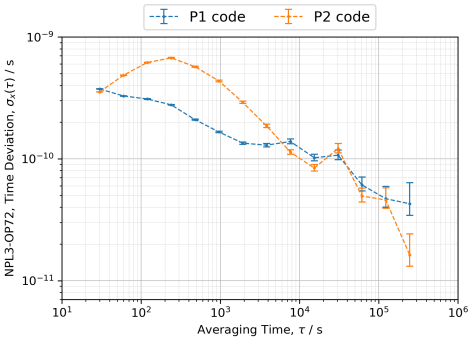


(b) TDEV of P-code delays

Figure 34: Relative calibration of NPL3 with respect to OP72

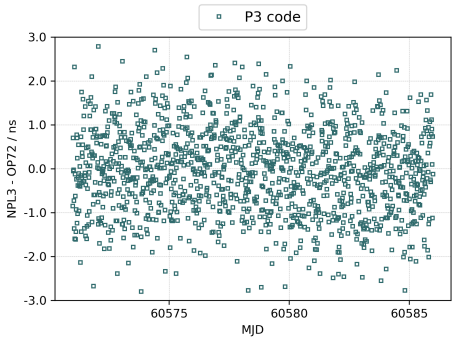


(a) P3 CV after calibration

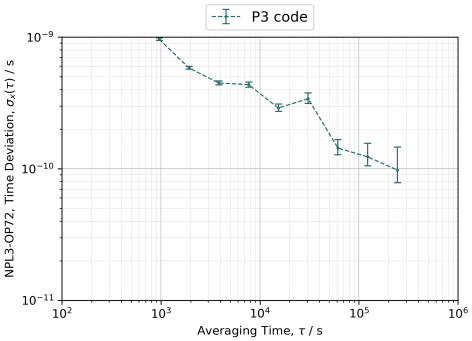


(b) TDEV of P3 CV

Figure 35: P3 CV time difference NPL3 with respect to OP72

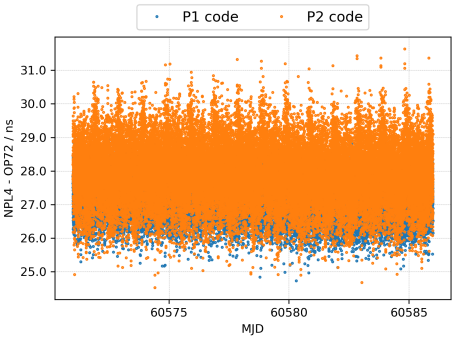


(a) P-code phase differences

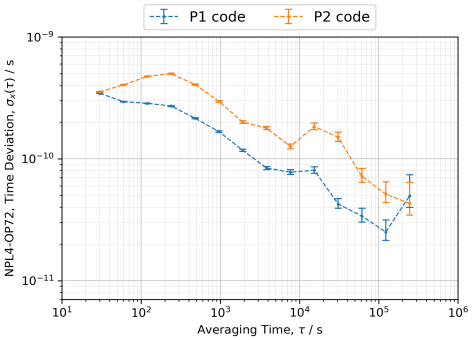


(b) TDEV of P-code delays

Figure 36: Relative calibration of NPL4 with respect to OP72


(a) P3 CV after calibration

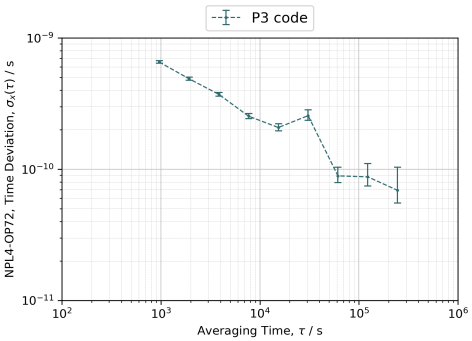


(b) TDEV of P3 CV

Figure 37: P3 CV time difference NPL4 with respect to OP72


(a) P-code phase differences

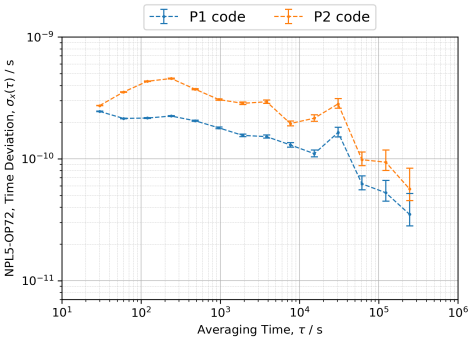


(b) TDEV of P-code delays

Figure 38: Relative calibration of NPL5 with respect to OP72


(a) P3 CV after calibration

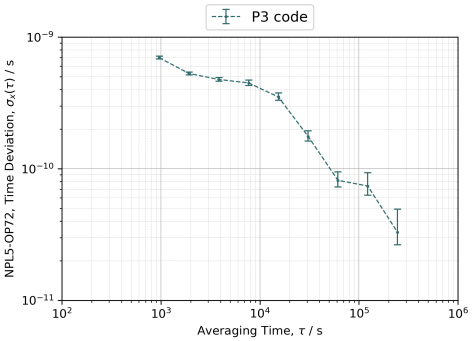


(b) TDEV of P3 CV

Figure 39: P3 CV time difference NPL5 with respect to OP72


(a) P-code phase differences

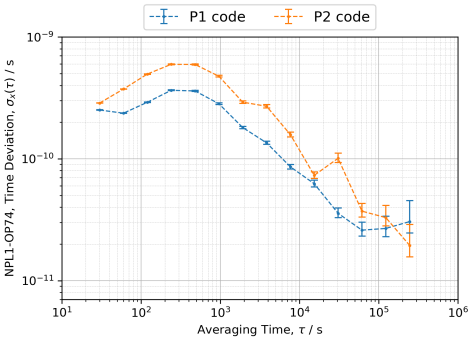


(b) TDEV of P-code delays

Figure 40: Relative calibration of NPL1 with respect to OP74

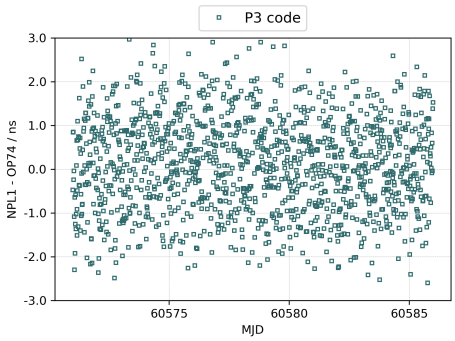


(a) P3 CV after calibration

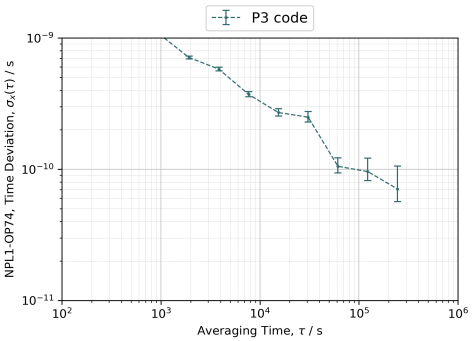


(b) TDEV of P3 CV

Figure 41: P3 CV time difference NPL1 with respect to OP74

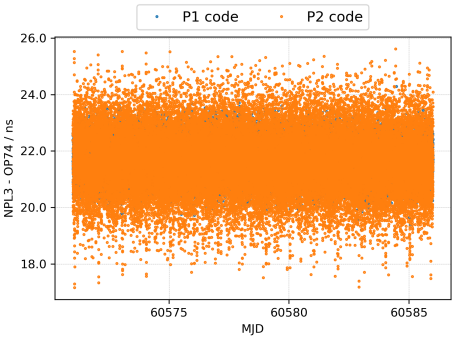


(a) P-code phase differences

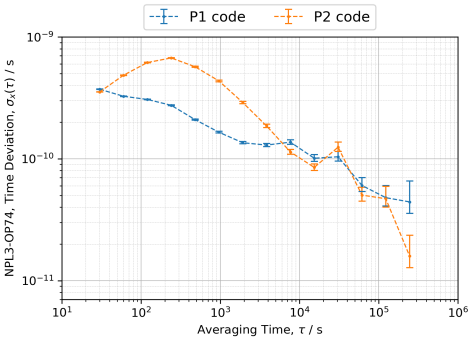


(b) TDEV of P-code delays

Figure 42: Relative calibration of NPL3 with respect to OP74

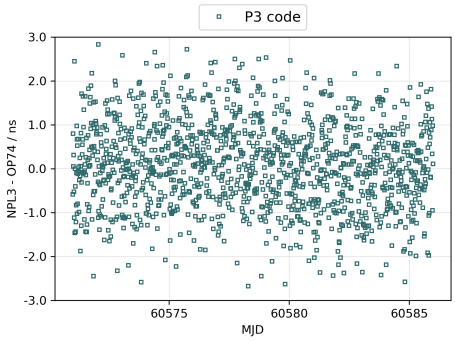


(a) P3 CV after calibration

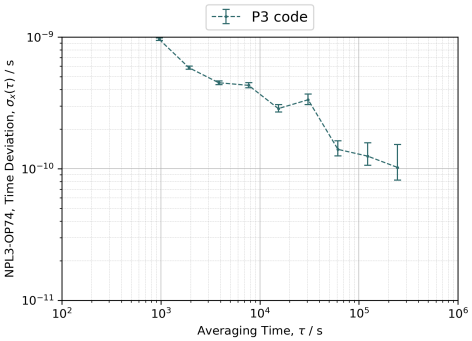


(b) TDEV of P3 CV

Figure 43: P3 CV time difference NPL3 with respect to OP74

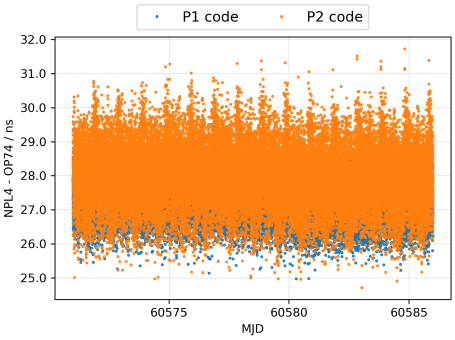


(a) P-code phase differences

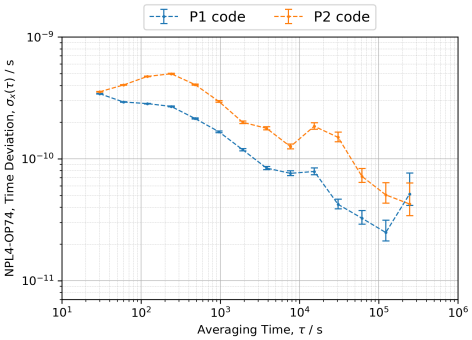


(b) TDEV of P-code delays

Figure 44: Relative calibration of NPL4 with respect to OP74


(a) P3 CV after calibration

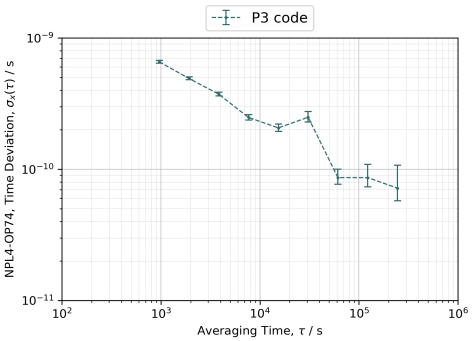


(b) TDEV of P3 CV

Figure 45: P3 CV time difference NPL4 with respect to OP74

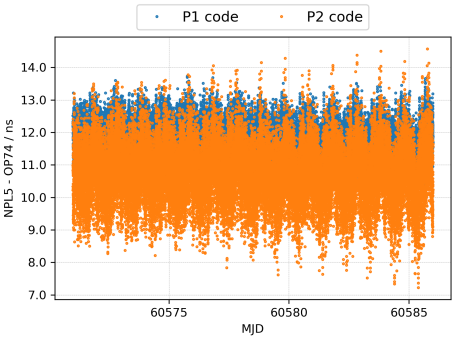


(a) P-code phase differences

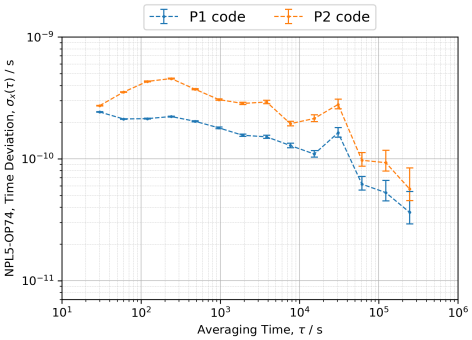


(b) TDEV of P-code delays

Figure 46: Relative calibration of NPL5 with respect to OP74

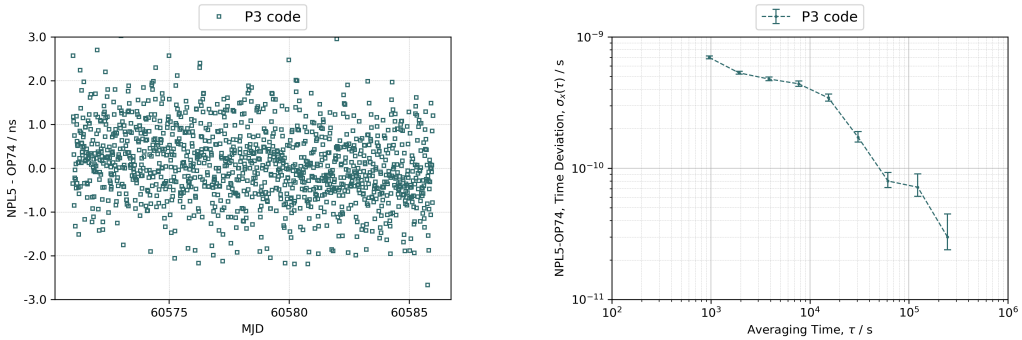


(a) P3 CV after calibration

(b) TDEV of P3 CV

Figure 47: P3 CV time difference NPL5 with respect to OP74

## B.2 Galileo calibration.

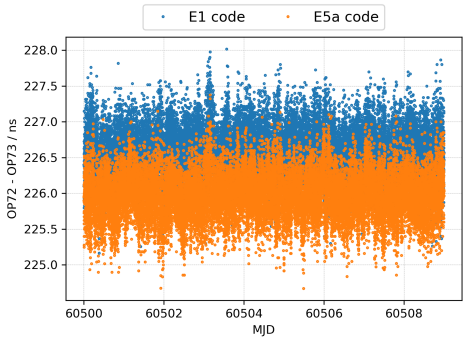


(a) E-code phase differences

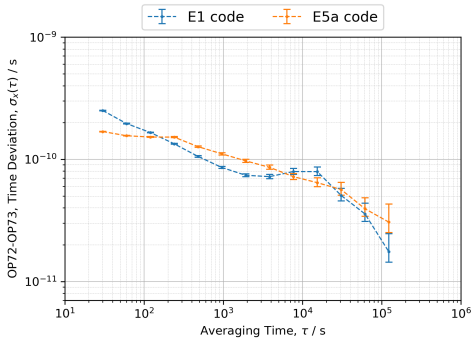


(b) TDEV of E-code delays

Figure 48: Relative calibration of OP72 with respect to OP73

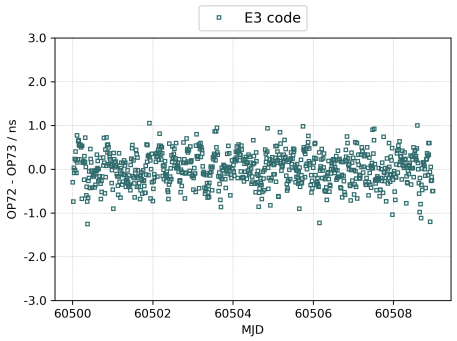


(a) E3 CV after calibration

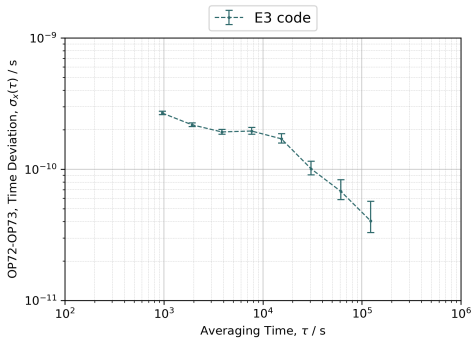


(b) TDEV of E3 CV

Figure 49: E3 CV time difference OP72 with respect to OP73

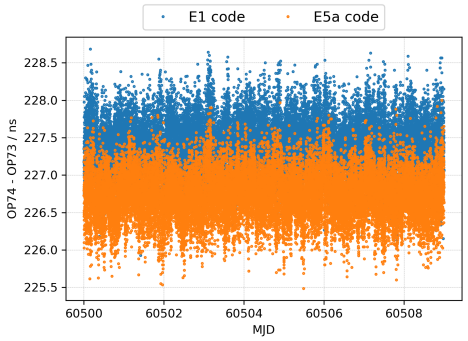


(a) E-code phase differences

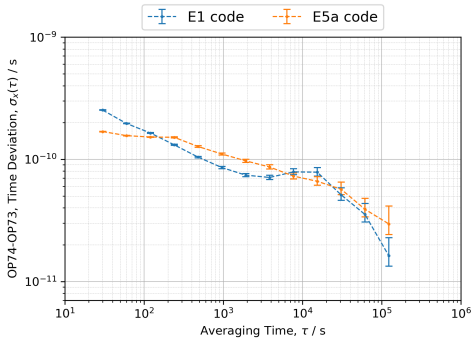


(b) TDEV of E-code delays

Figure 50: Relative calibration of OP74 with respect to OP73

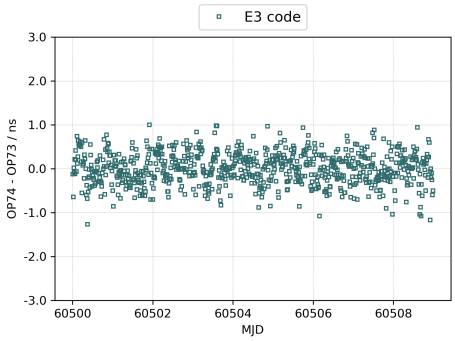


(a) E3 CV after calibration

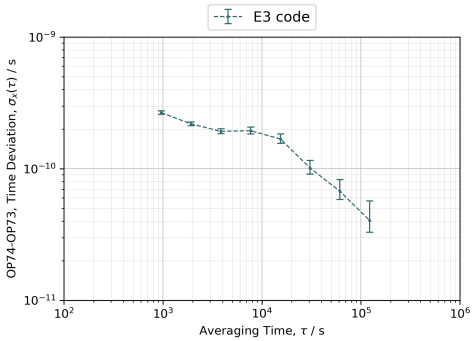


(b) TDEV of E3 CV

Figure 51: E3 CV time difference OP74 with respect to OP73

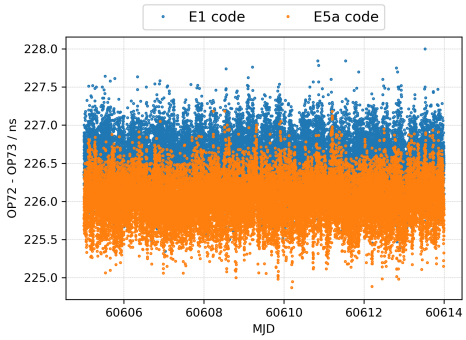


(a) E-code phase differences

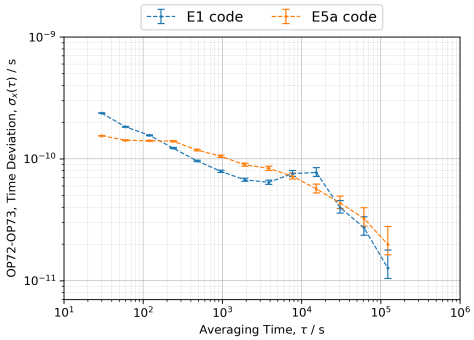


(b) TDEV of E-code delays

Figure 52: Relative calibration of OP72 with respect to OP73

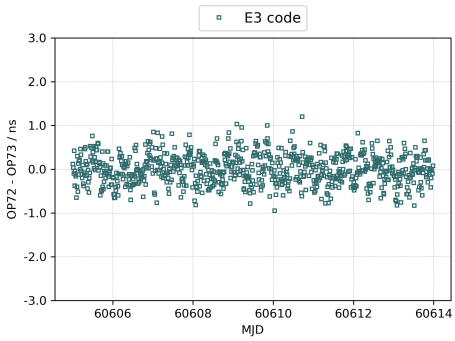


(a) E3 CV after calibration

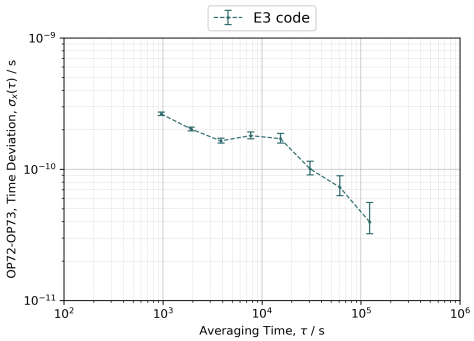


(b) TDEV of E3 CV

Figure 53: E3 CV time difference OP72 with respect to OP73

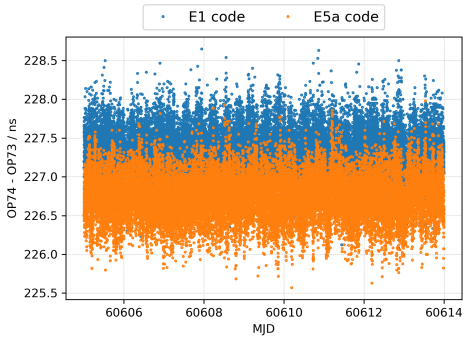


(a) E-code phase differences

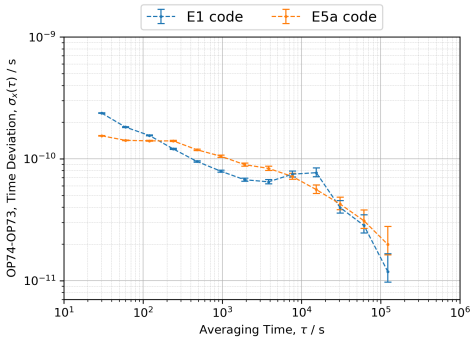


(b) TDEV of E-code delays

Figure 54: Relative calibration of OP74 with respect to OP73

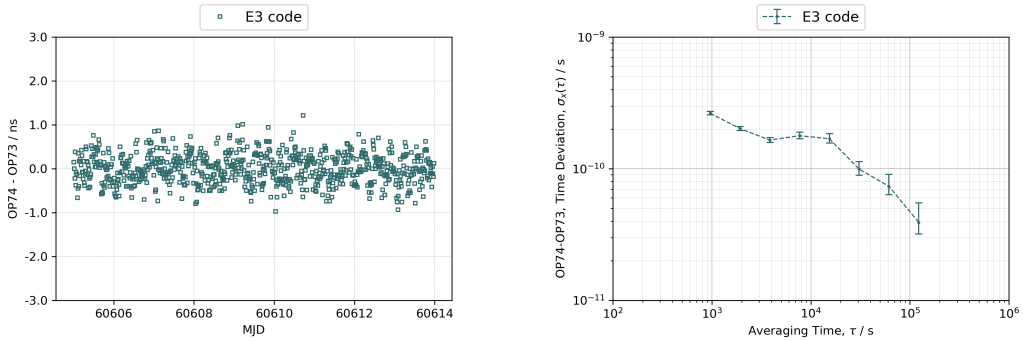


(a) E3 CV after calibration

(b) TDEV of E3 CV

Figure 55: E3 CV time difference OP74 with respect to OP73

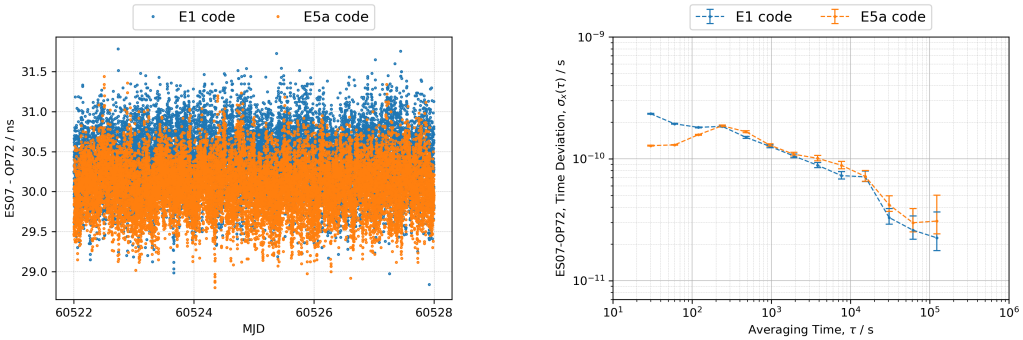


(a) E-code phase differences

(b) TDEV of E-code delays

Figure 56: Relative calibration of ES07 with respect to OP72

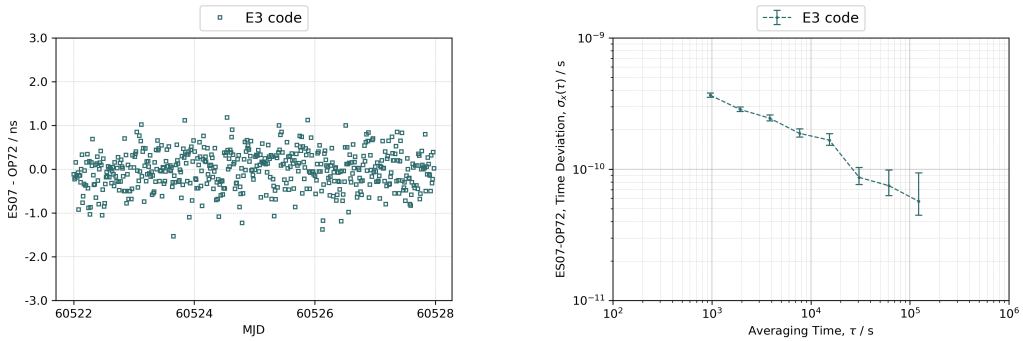


(a) E3 CV after calibration

(b) TDEV of E3 CV

Figure 57: E3 CV time difference ES07 with respect to OP72

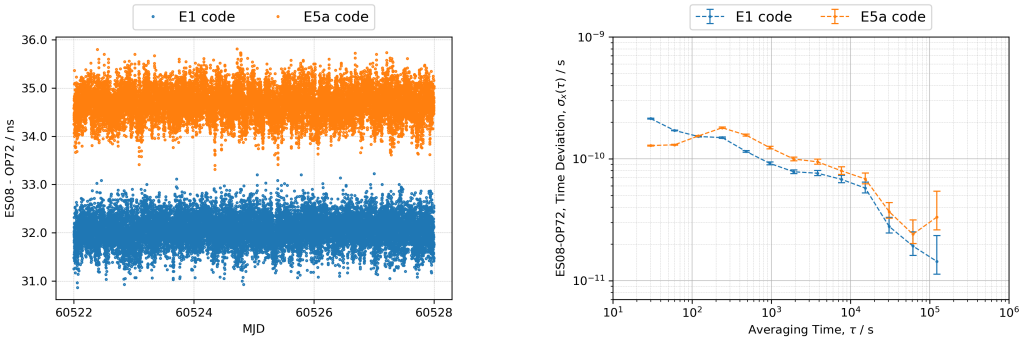


(a) E-code phase differences

(b) TDEV of E-code delays

Figure 58: Relative calibration of ES08 with respect to OP72

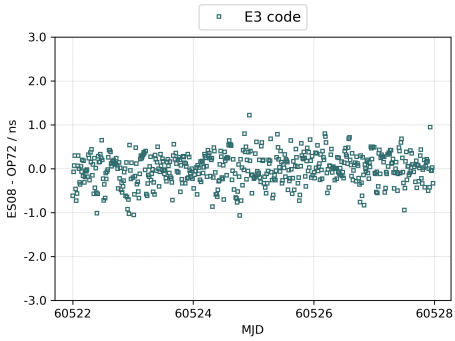


(a) E3 CV after calibration

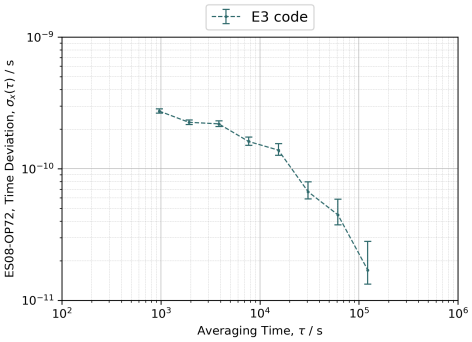


(b) TDEV of E3 CV

Figure 59: E3 CV time difference ES08 with respect to OP72

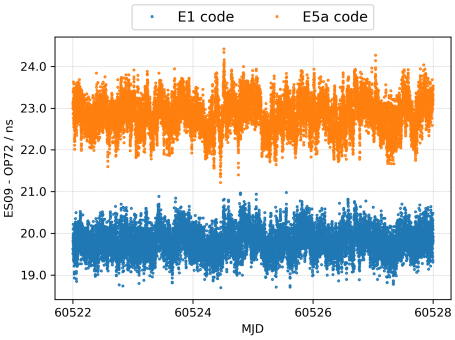


(a) E-code phase differences

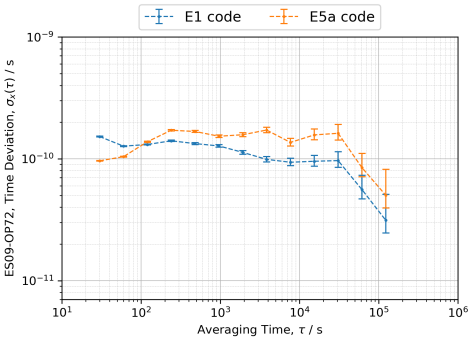


(b) TDEV of E-code delays

Figure 60: Relative calibration of ES09 with respect to OP72

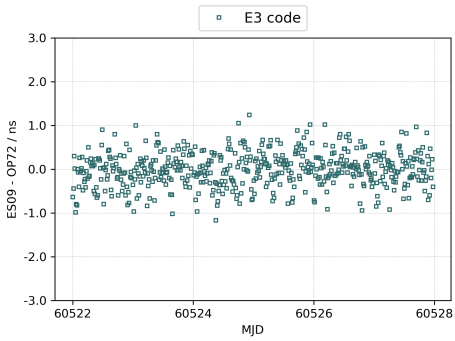


(a) E3 CV after calibration

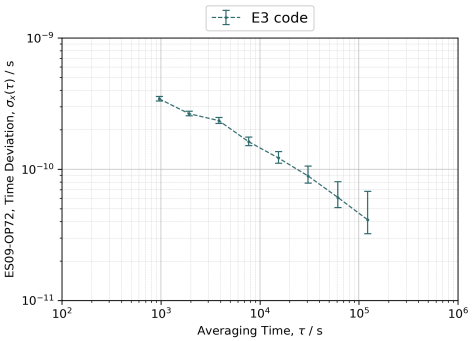


(b) TDEV of E3 CV

Figure 61: E3 CV time difference ES09 with respect to OP72

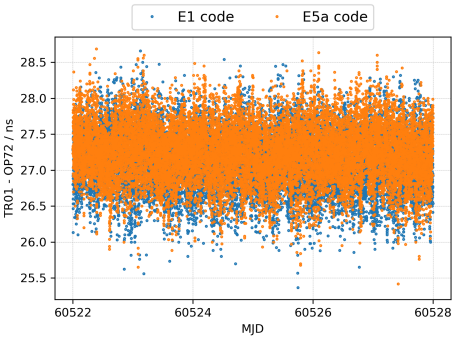


(a) E-code phase differences

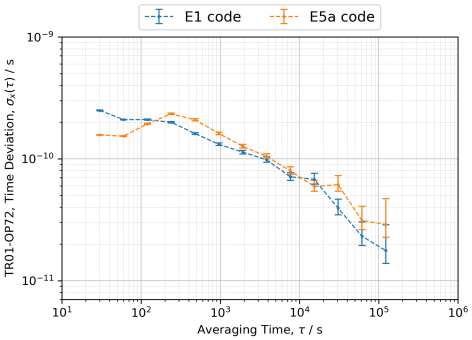


(b) TDEV of E-code delays

Figure 62: Relative calibration of TR01 with respect to OP72

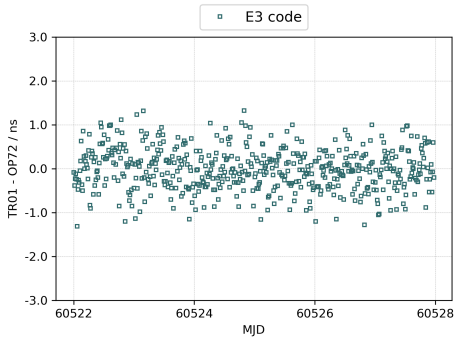


(a) E3 CV after calibration

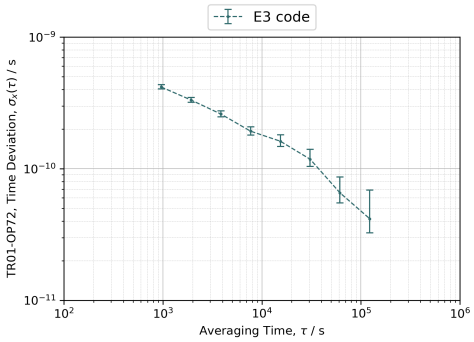


(b) TDEV of E3 CV

Figure 63: E3 CV time difference TR01 with respect to OP72

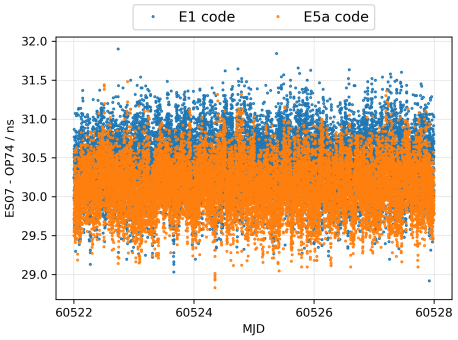


(a) E-code phase differences

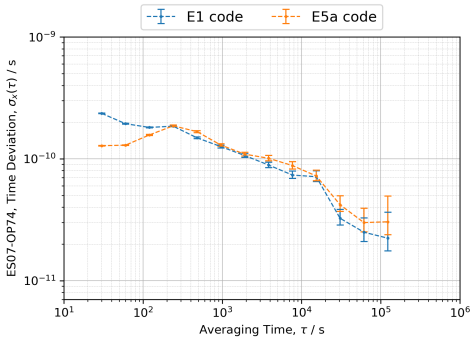


(b) TDEV of E-code delays

Figure 64: Relative calibration of ES07 with respect to OP74

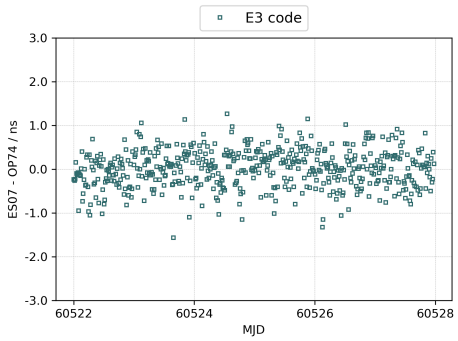


(a) E3 CV after calibration

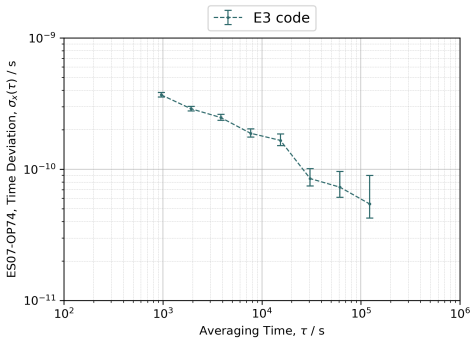


(b) TDEV of E3 CV

Figure 65: E3 CV time difference ES07 with respect to OP74

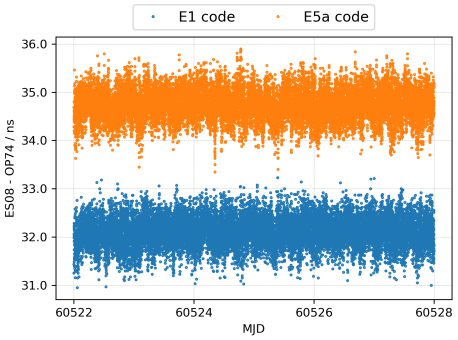


(a) E-code phase differences

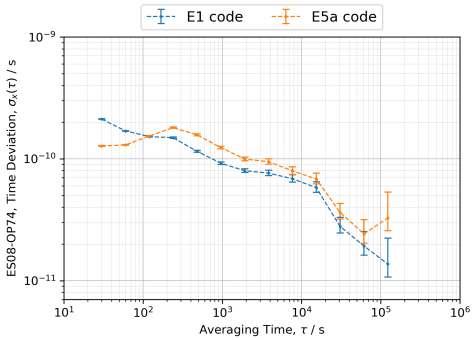


(b) TDEV of E-code delays

Figure 66: Relative calibration of ES08 with respect to OP74

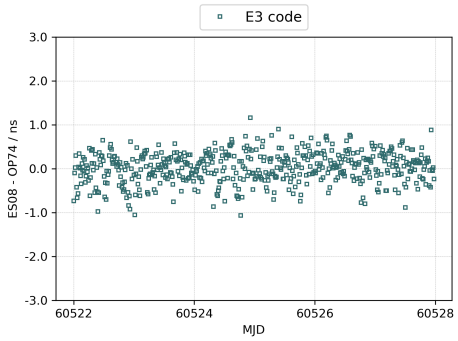


(a) E3 CV after calibration

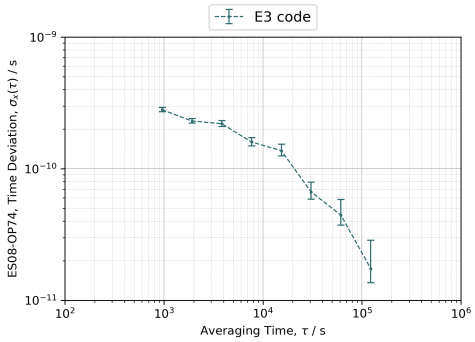


(b) TDEV of E3 CV

Figure 67: E3 CV time difference ES08 with respect to OP74

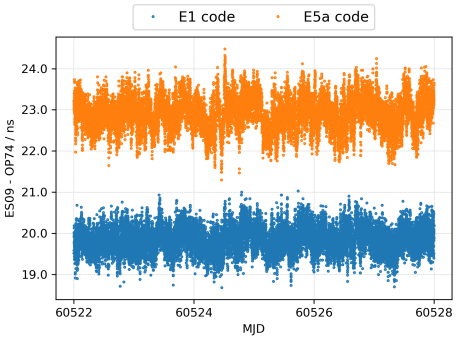


(a) E-code phase differences

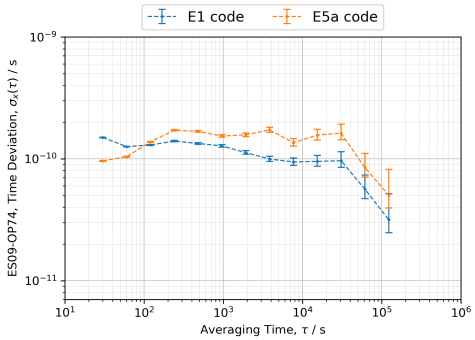


(b) TDEV of E-code delays

Figure 68: Relative calibration of ES09 with respect to OP74

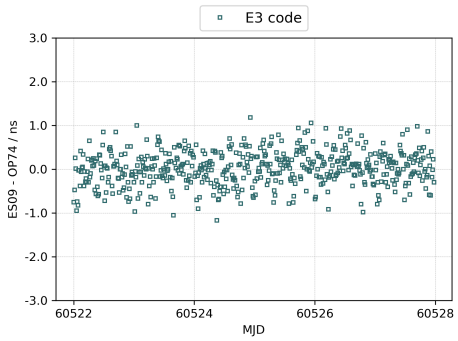


(a) E3 CV after calibration

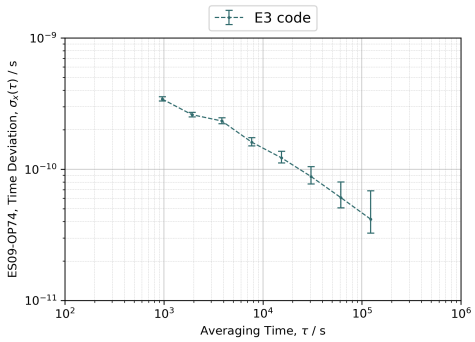


(b) TDEV of E3 CV

Figure 69: E3 CV time difference ES09 with respect to OP74

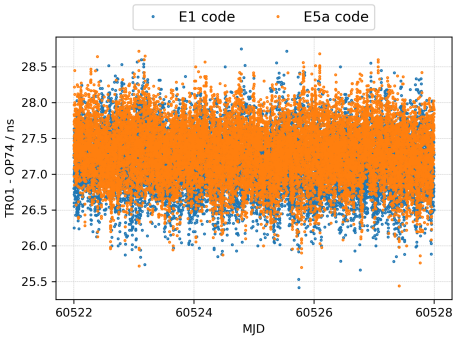


(a) E-code phase differences

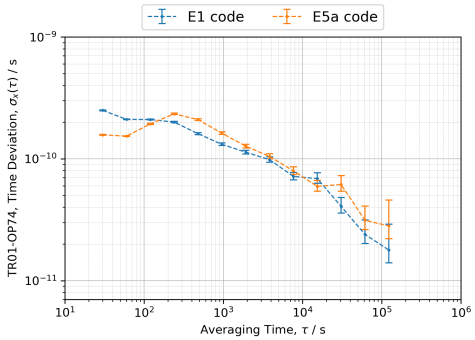


(b) TDEV of E-code delays

Figure 70: Relative calibration of TR01 with respect to OP74

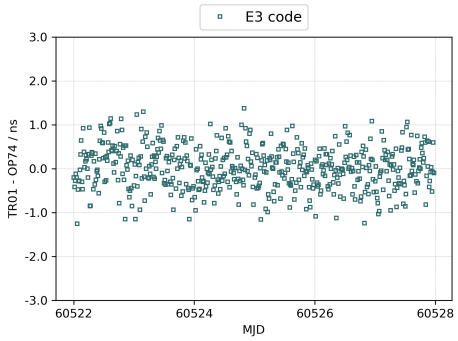


(a) E3 CV after calibration

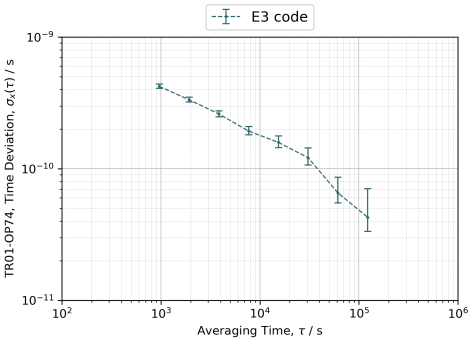


(b) TDEV of E3 CV

Figure 71: E3 CV time difference TR01 with respect to OP74

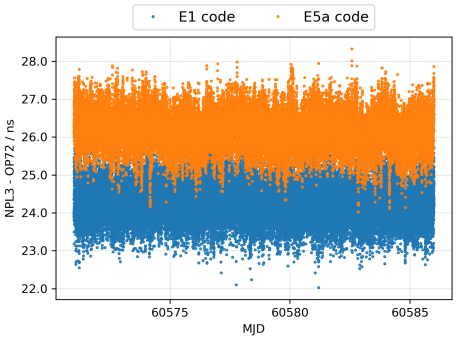


(a) E-code phase differences

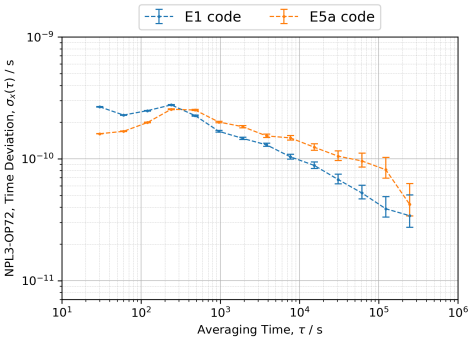


(b) TDEV of E-code delays

Figure 72: Relative calibration of NPL3 with respect to OP72

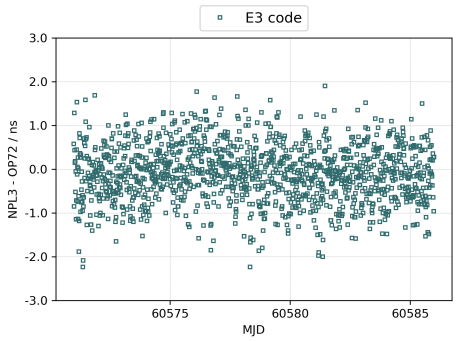


(a) E3 CV after calibration

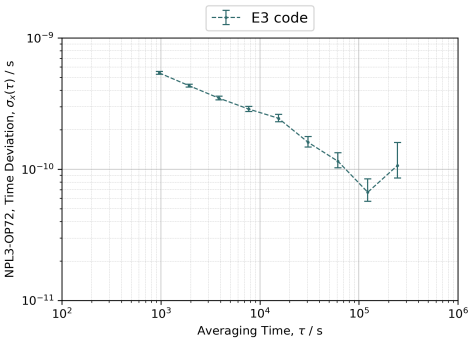


(b) TDEV of E3 CV

Figure 73: E3 CV time difference NPL3 with respect to OP72

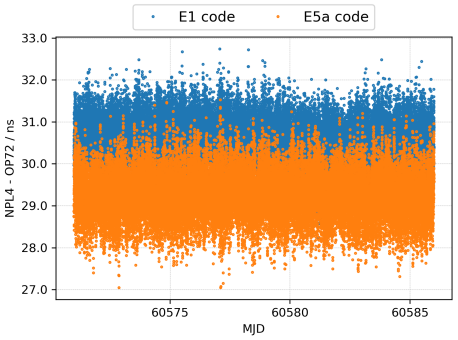


(a) E-code phase differences

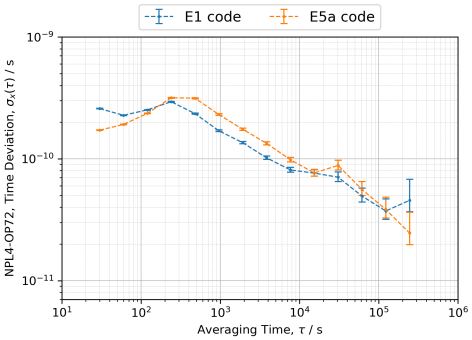


(b) TDEV of E-code delays

Figure 74: Relative calibration of NPL4 with respect to OP72

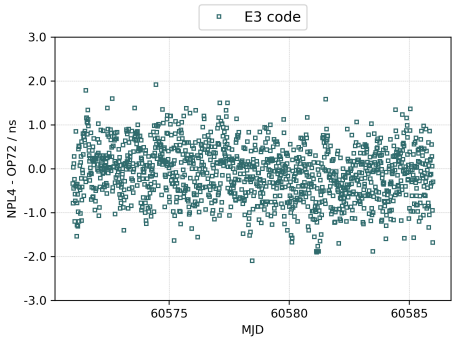


(a) E3 CV after calibration

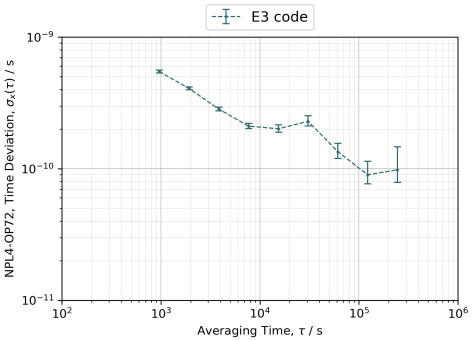


(b) TDEV of E3 CV

Figure 75: E3 CV time difference NPL4 with respect to OP72

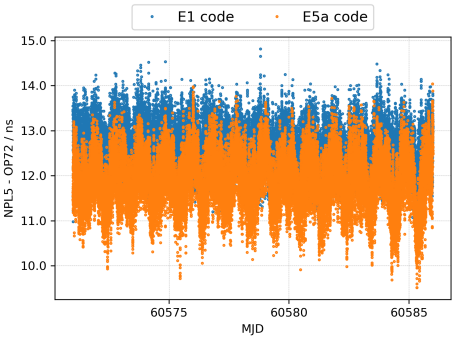


(a) E-code phase differences

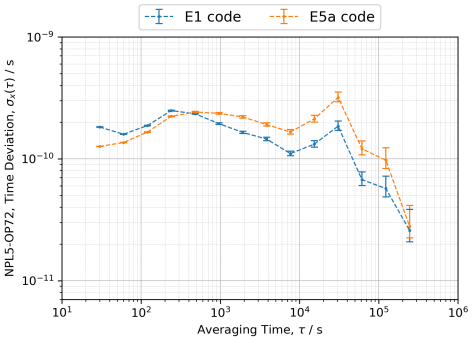


(b) TDEV of E-code delays

Figure 76: Relative calibration of NPL5 with respect to OP72

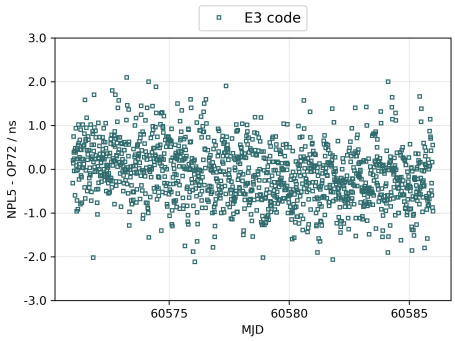


(a) E3 CV after calibration

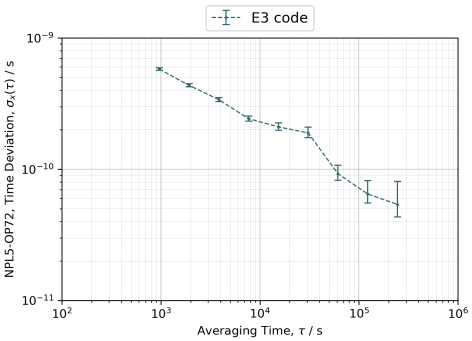


(b) TDEV of E3 CV

Figure 77: E3 CV time difference NPL5 with respect to OP72

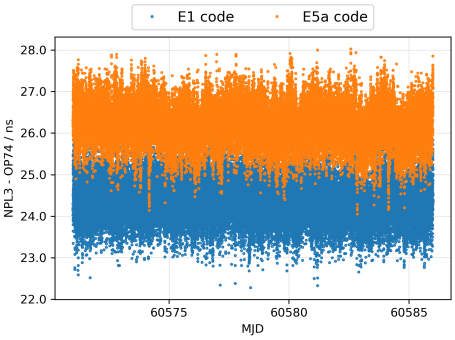


(a) E-code phase differences

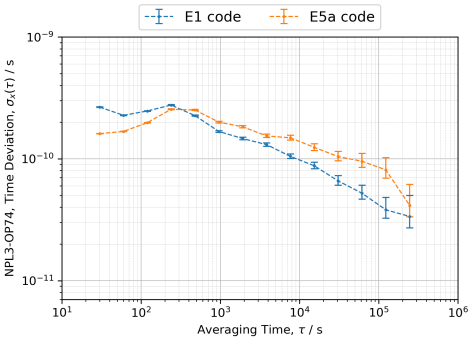


(b) TDEV of E-code delays

Figure 78: Relative calibration of NPL3 with respect to OP74

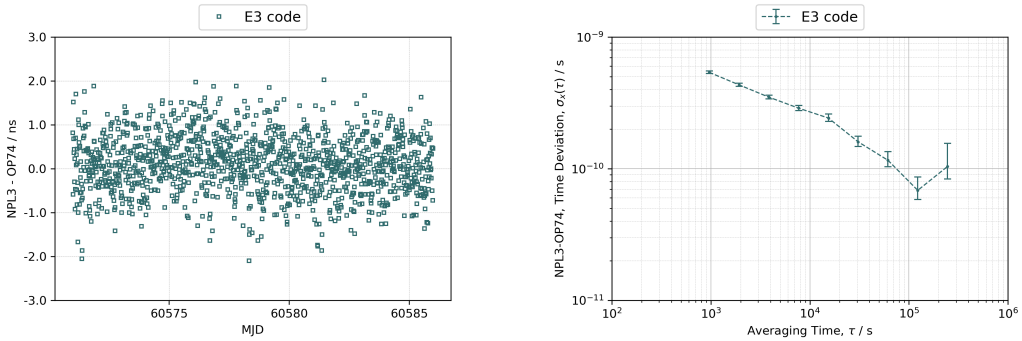


(a) E3 CV after calibration

(b) TDEV of E3 CV

Figure 79: E3 CV time difference NPL3 with respect to OP74

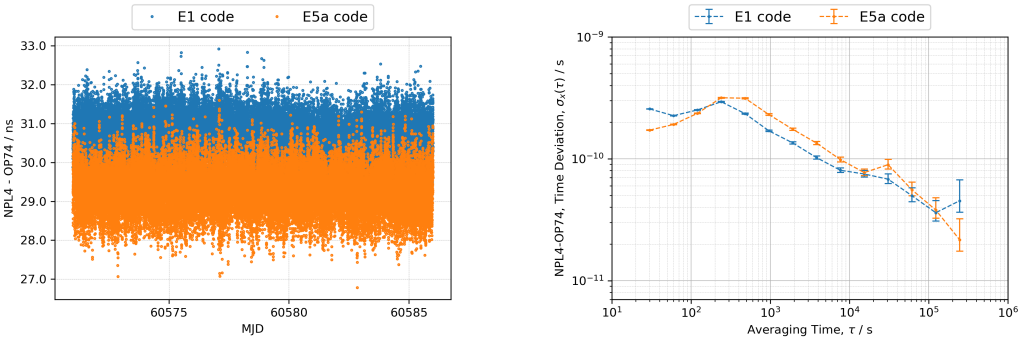


(a) E-code phase differences

(b) TDEV of E-code delays

Figure 80: Relative calibration of NPL4 with respect to OP74

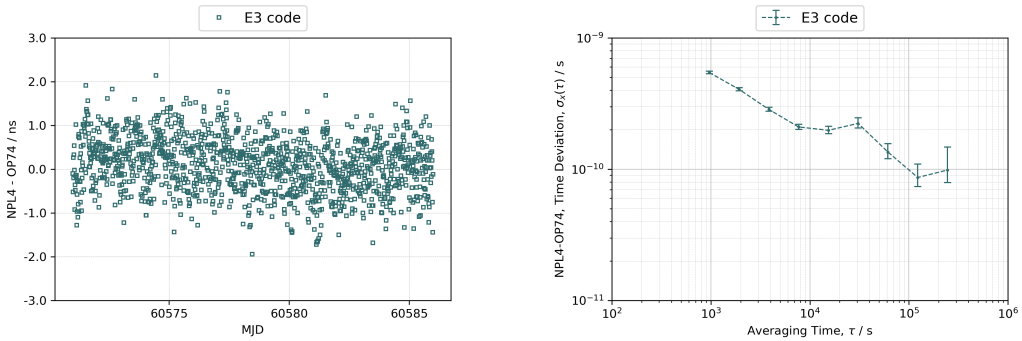


(a) E3 CV after calibration

(b) TDEV of E3 CV

Figure 81: E3 CV time difference NPL4 with respect to OP74

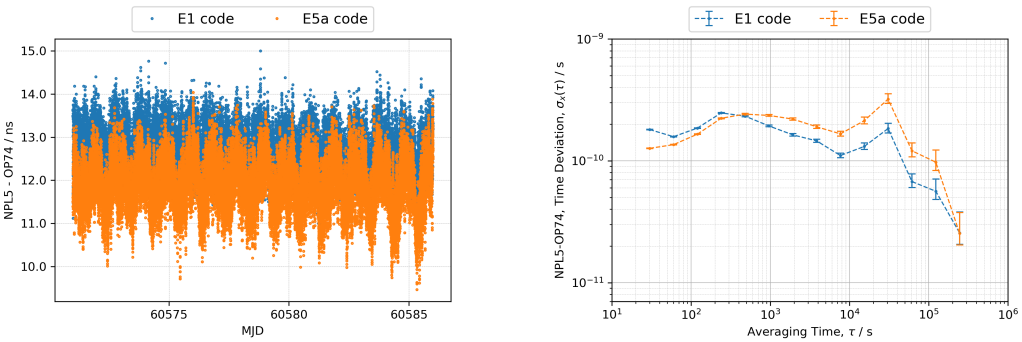


(a) E-code phase differences

(b) TDEV of E-code delays

Figure 82: Relative calibration of NPL5 with respect to OP74

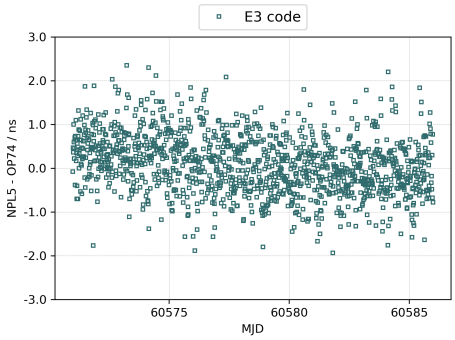


(a) E3 CV after calibration

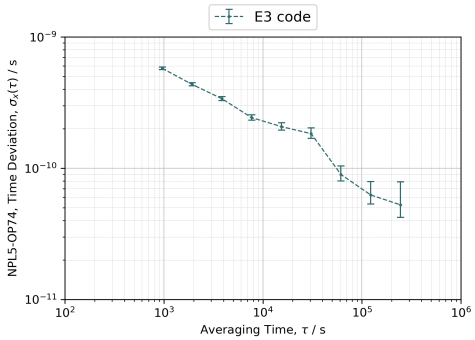


(b) TDEV of E3 CV

Figure 83: E3 CV time difference NPL5 with respect to OP74

## B.3 Beidou calibration.

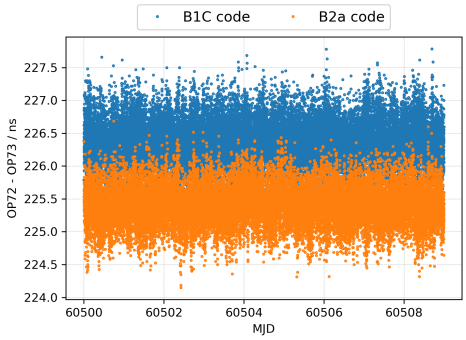


(a) B-code phase differences

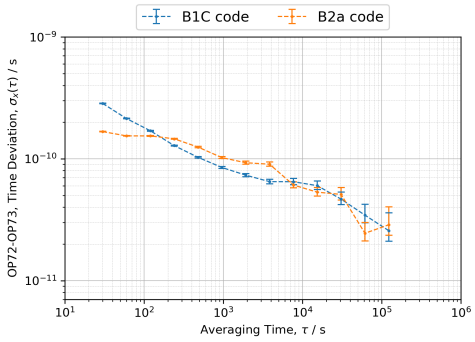


(b) TDEV of B-code delays

Figure 84: Relative calibration of OP72 with respect to OP73

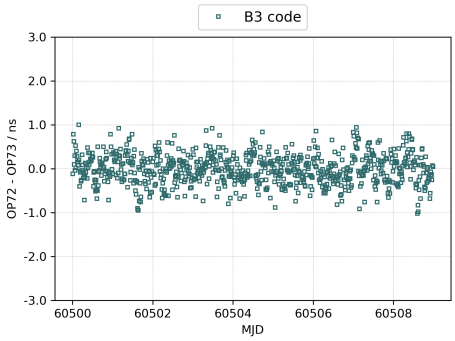


(a) B3 CV after calibration

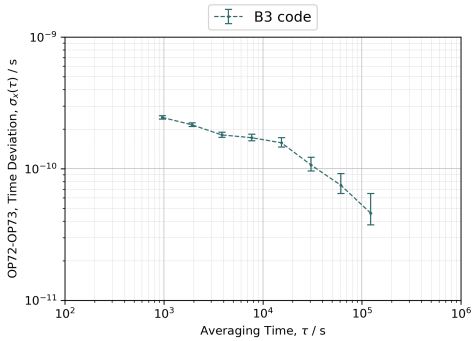


(b) TDEV of B3 CV

Figure 85: B3 CV time difference OP72 with respect to OP73

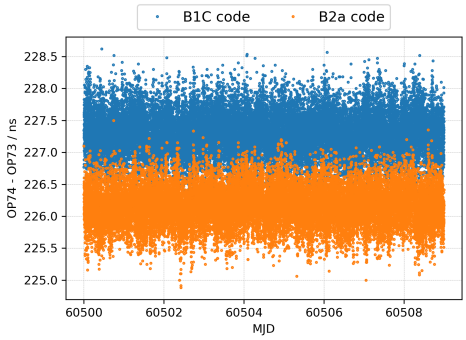


(a) B-code phase differences

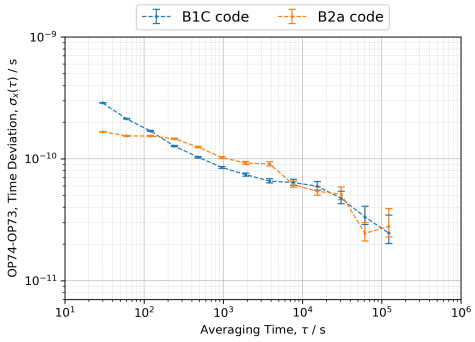


(b) TDEV of B-code delays

Figure 86: Relative calibration of OP74 with respect to OP73

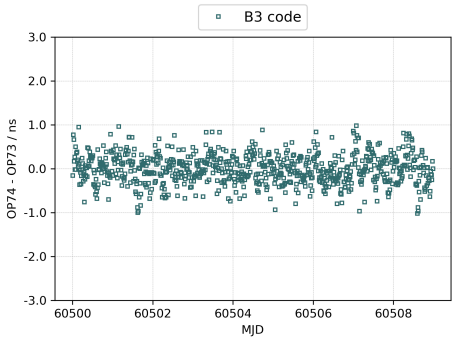


(a) B3 CV after calibration

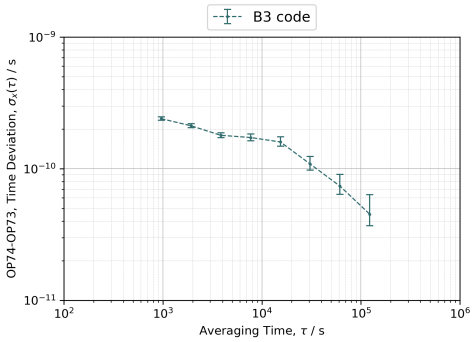


(b) TDEV of B3 CV

Figure 87: B3 CV time difference OP74 with respect to OP73

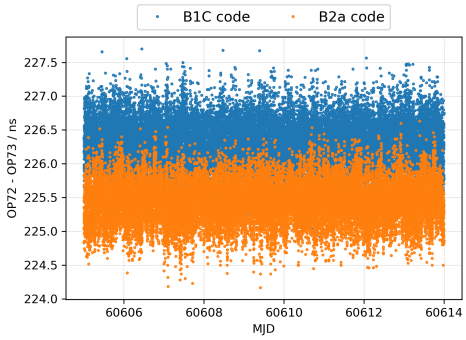


(a) B-code phase differences

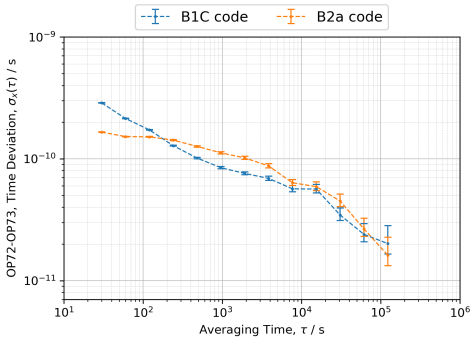


(b) TDEV of B-code delays

Figure 88: Relative calibration of OP72 with respect to OP73

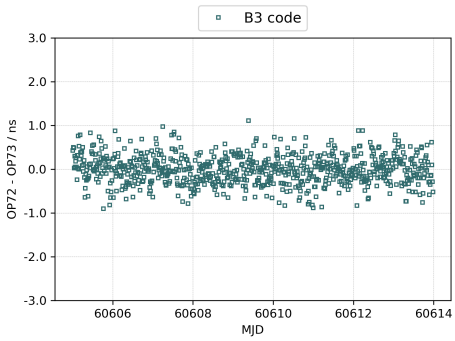


(a) B3 CV after calibration

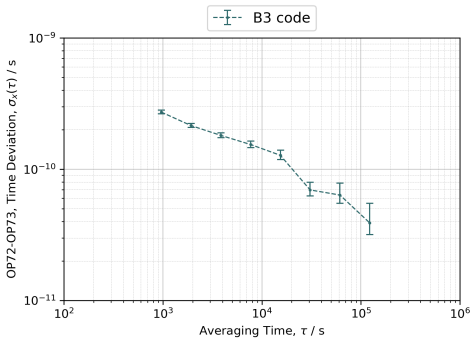


(b) TDEV of B3 CV

Figure 89: B3 CV time difference OP72 with respect to OP73


(a) B-code phase differences

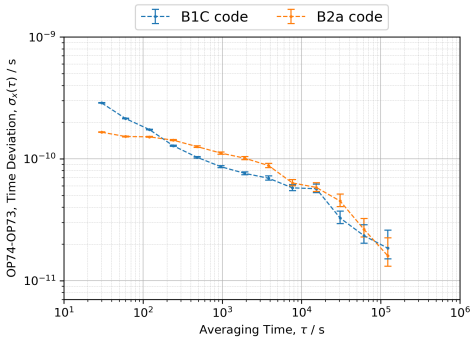


(b) TDEV of B-code delays

Figure 90: Relative calibration of OP74 with respect to OP73

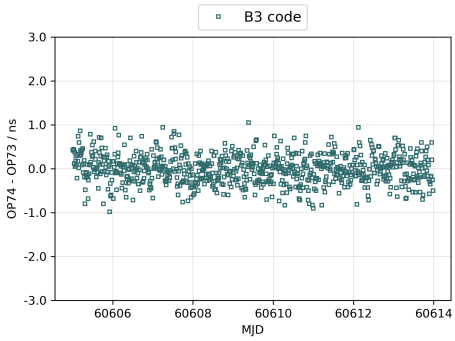


(a) B3 CV after calibration

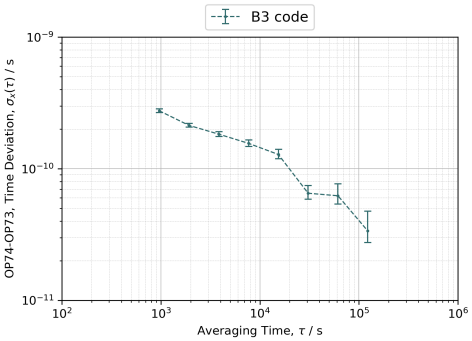


(b) TDEV of B3 CV

Figure 91: B3 CV time difference OP74 with respect to OP73

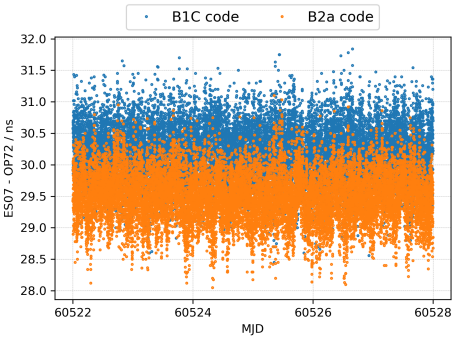


(a) B-code phase differences

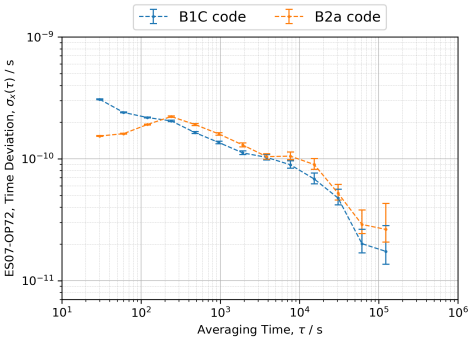


(b) TDEV of B-code delays

Figure 92: Relative calibration of ES07 with respect to OP72

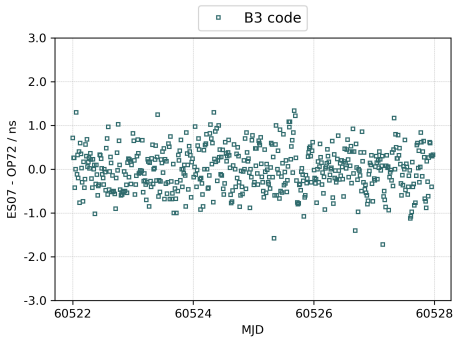


(a) B3 CV after calibration

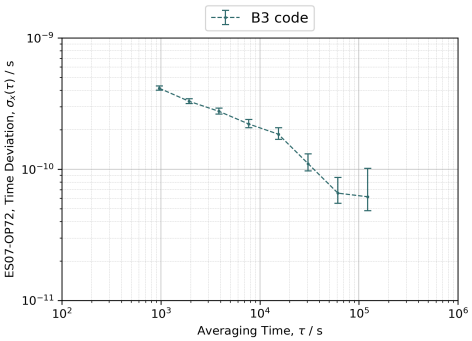


(b) TDEV of B3 CV

Figure 93: B3 CV time difference ES07 with respect to OP72

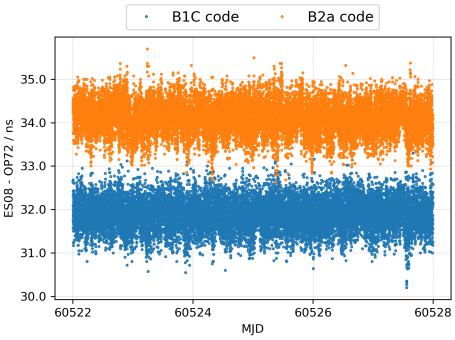


(a) B-code phase differences

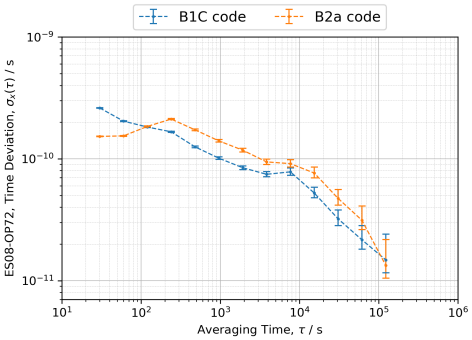


(b) TDEV of B-code delays

Figure 94: Relative calibration of ES08 with respect to OP72

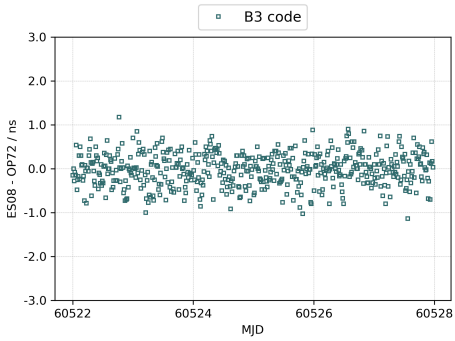


(a) B3 CV after calibration

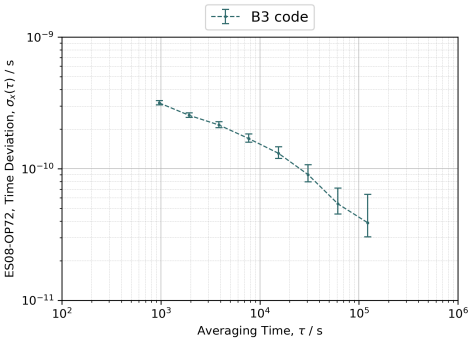


(b) TDEV of B3 CV

Figure 95: B3 CV time difference ES08 with respect to OP72

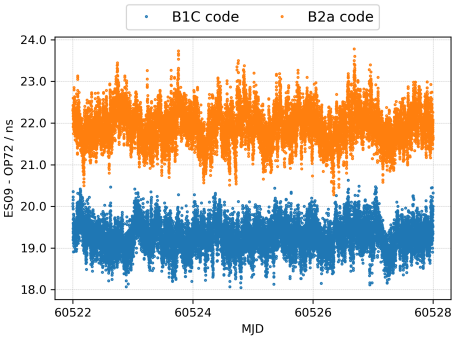


(a) B-code phase differences

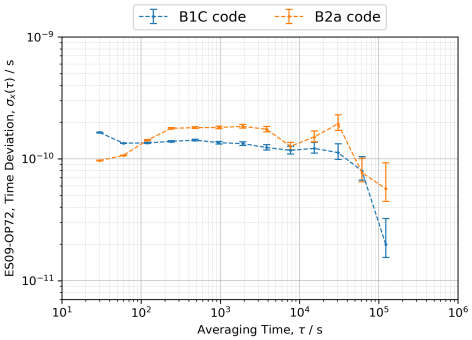


(b) TDEV of B-code delays

Figure 96: Relative calibration of ES09 with respect to OP72

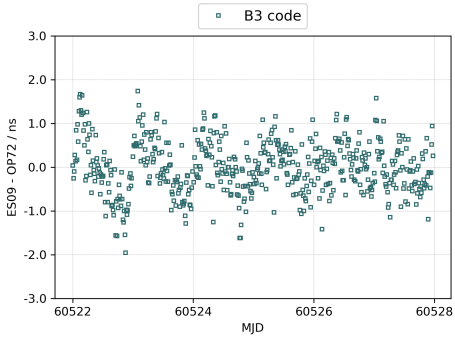


(a) B3 CV after calibration

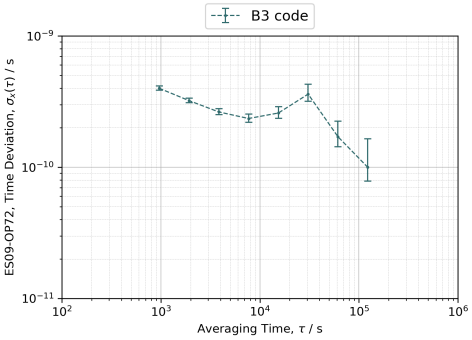


(b) TDEV of B3 CV

Figure 97: B3 CV time difference ES09 with respect to OP72

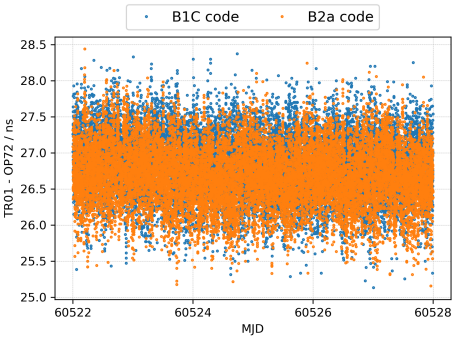


(a) B-code phase differences

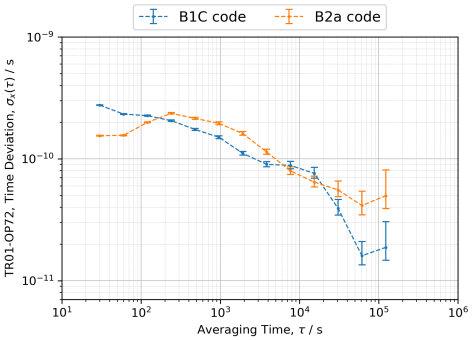


(b) TDEV of B-code delays

Figure 98: Relative calibration of TR01 with respect to OP72

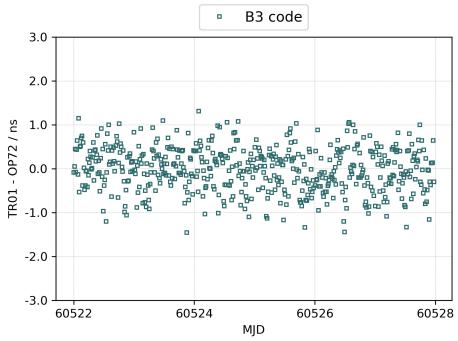


(a) B3 CV after calibration

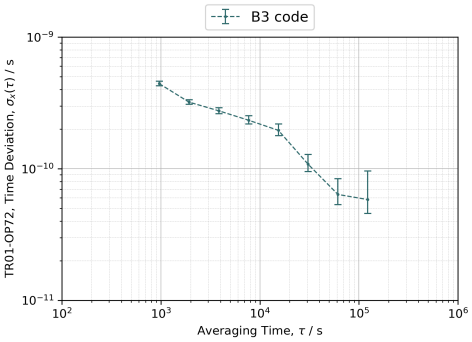


(b) TDEV of B3 CV

Figure 99: B3 CV time difference TR01 with respect to OP72

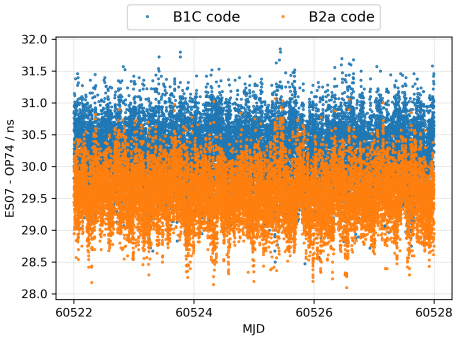


(a) B-code phase differences

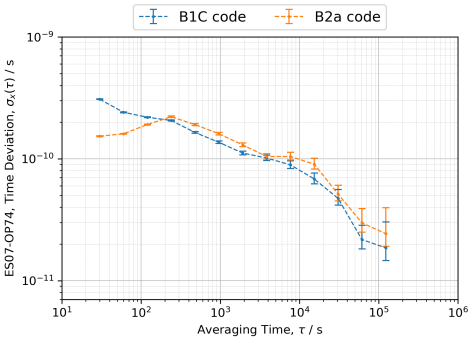


(b) TDEV of B-code delays

Figure 100: Relative calibration of ES07 with respect to OP74

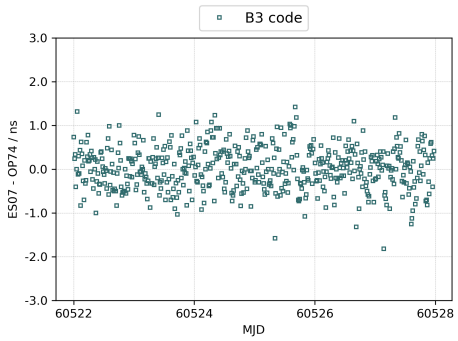


(a) B3 CV after calibration

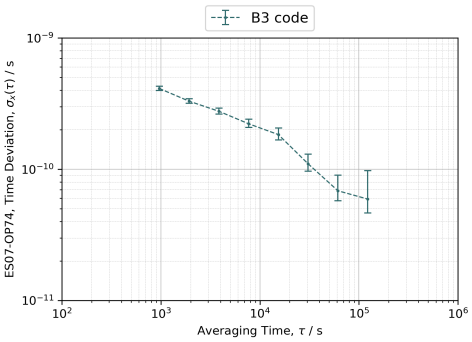


(b) TDEV of B3 CV

Figure 101: B3 CV time difference ES07 with respect to OP74

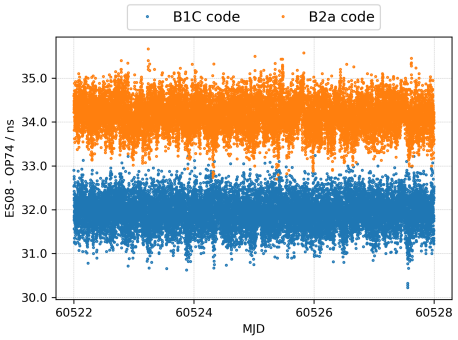


(a) B-code phase differences

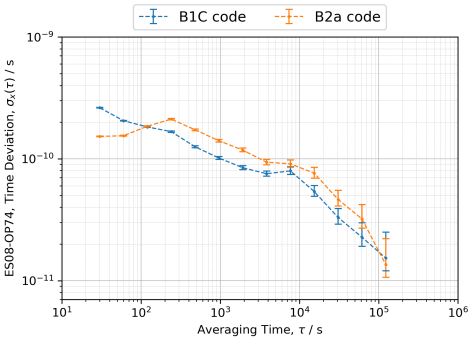


(b) TDEV of B-code delays

Figure 102: Relative calibration of ES08 with respect to OP74

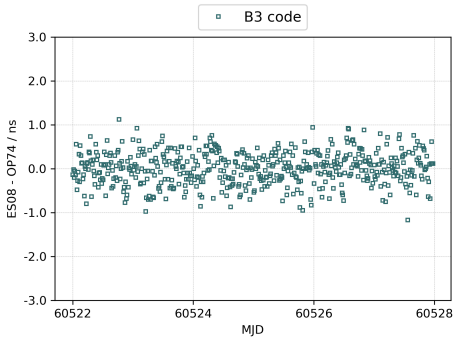


(a) B3 CV after calibration

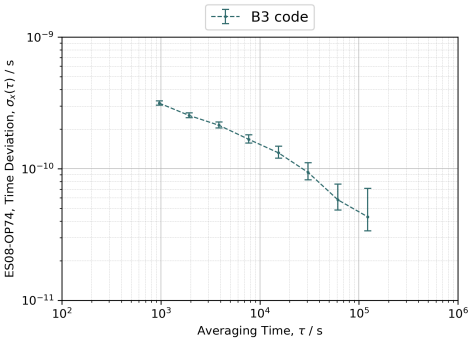


(b) TDEV of B3 CV

Figure 103: B3 CV time difference ES08 with respect to OP74

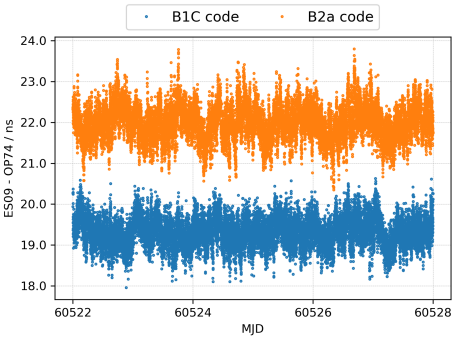


(a) B-code phase differences

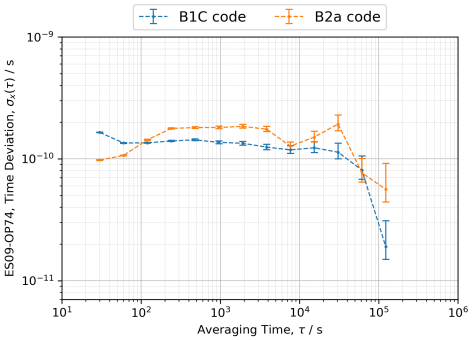


(b) TDEV of B-code delays

Figure 104: Relative calibration of ES09 with respect to OP74

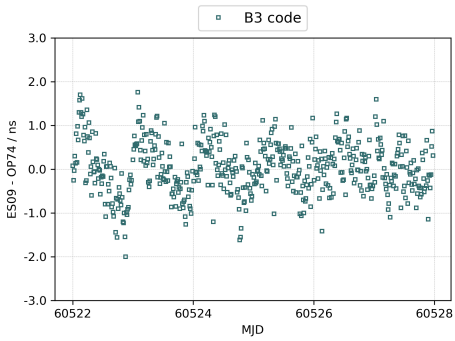


(a) B3 CV after calibration

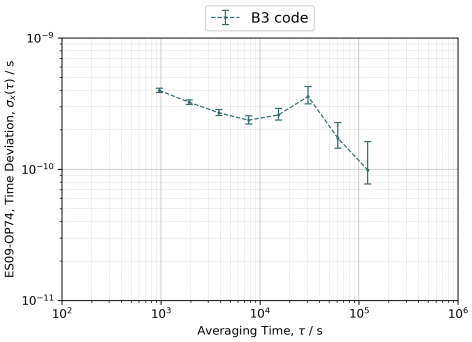


(b) TDEV of B3 CV

Figure 105: B3 CV time difference ES09 with respect to OP74

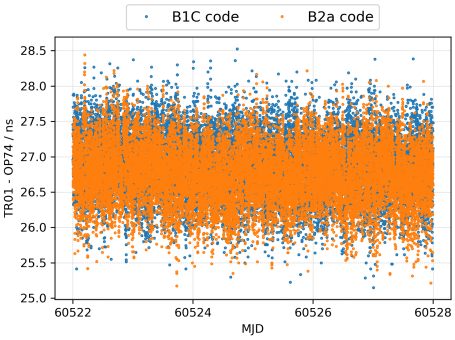


(a) B-code phase differences

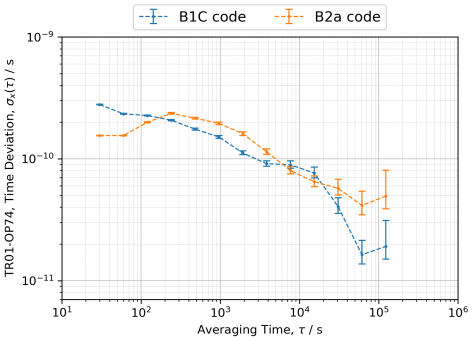


(b) TDEV of B-code delays

Figure 106: Relative calibration of TR01 with respect to OP74

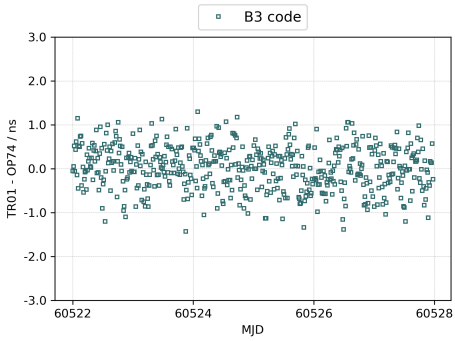


(a) B3 CV after calibration

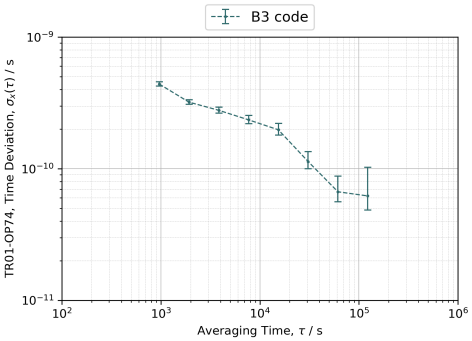


(b) TDEV of B3 CV

Figure 107: B3 CV time difference TR01 with respect to OP74

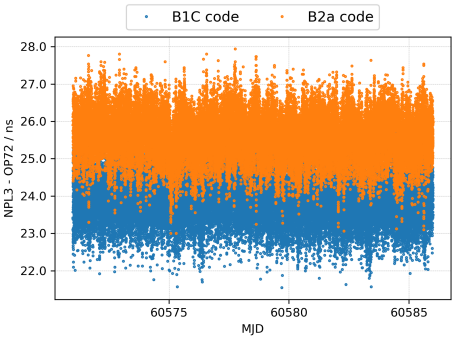


(a) B-code phase differences

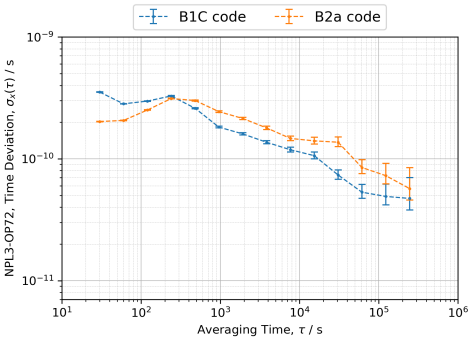


(b) TDEV of B-code delays

Figure 108: Relative calibration of NPL3 with respect to OP72

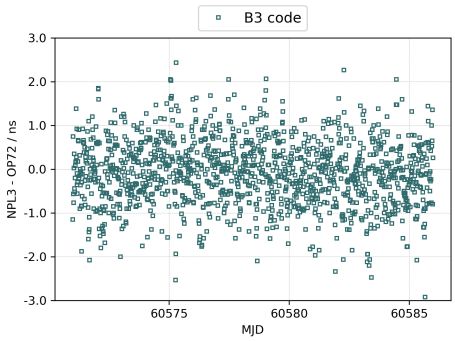


(a) B3 CV after calibration

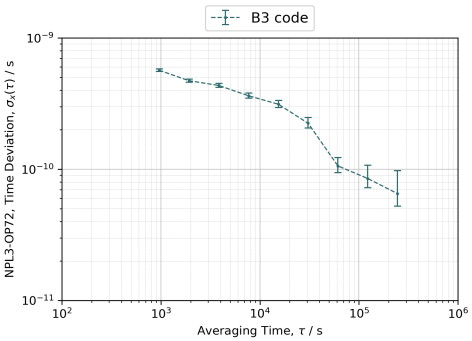


(b) TDEV of B3 CV

Figure 109: B3 CV time difference NPL3 with respect to OP72

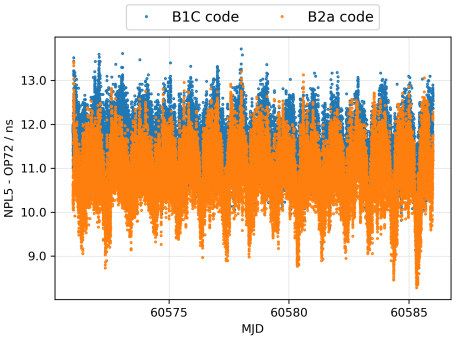


(a) B-code phase differences

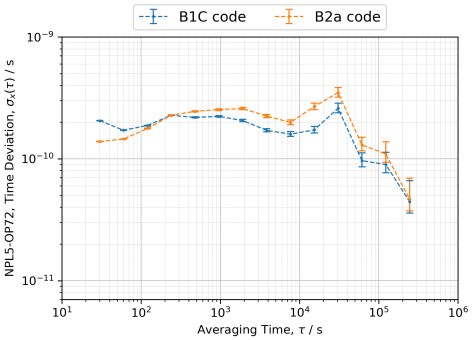


(b) TDEV of B-code delays

Figure 110: Relative calibration of NPL5 with respect to OP72

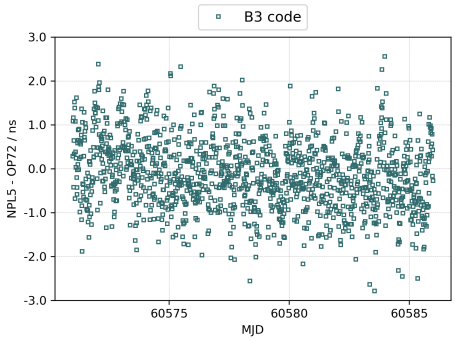


(a) B3 CV after calibration

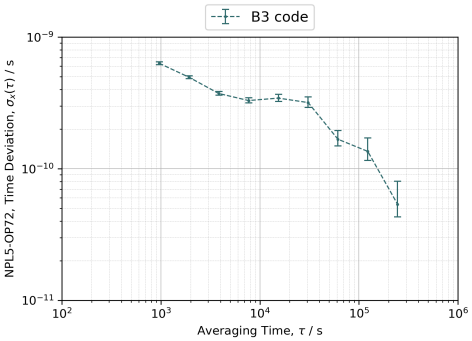


(b) TDEV of B3 CV

Figure 111: B3 CV time difference NPL5 with respect to OP72

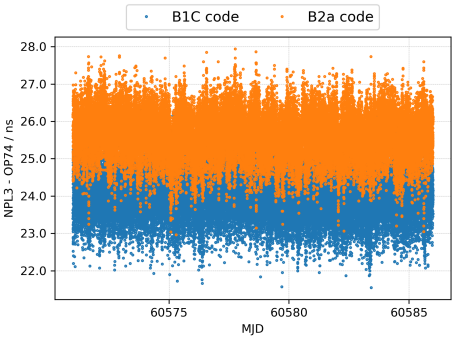


(a) B-code phase differences

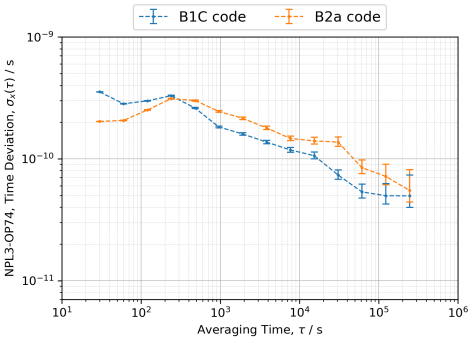


(b) TDEV of B-code delays

Figure 112: Relative calibration of NPL3 with respect to OP74

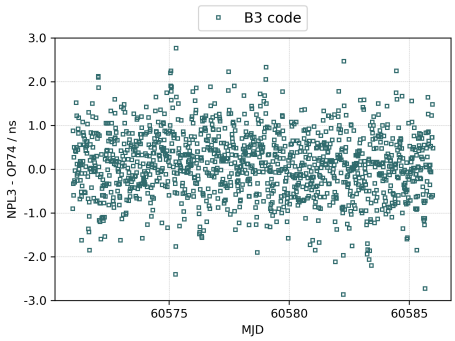


(a) B3 CV after calibration

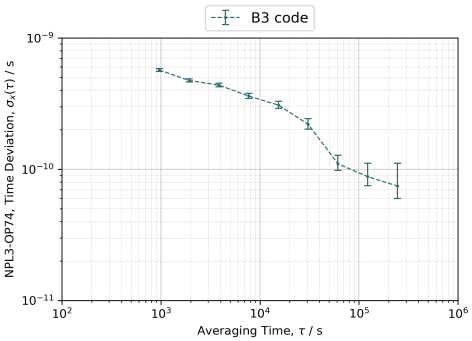


(b) TDEV of B3 CV

Figure 113: B3 CV time difference NPL3 with respect to OP74

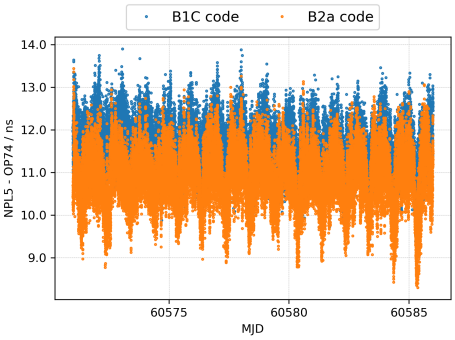


(a) B-code phase differences

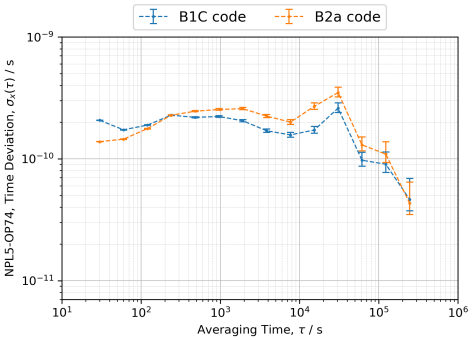


(b) TDEV of B-code delays

Figure 114: Relative calibration of NPL5 with respect to OP74


(a) B3 CV after calibration

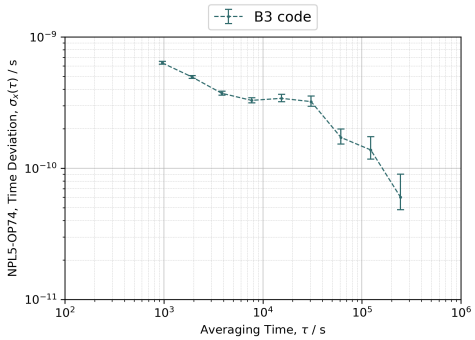


(b) TDEV of B3 CV

Figure 115: B3 CV time difference NPL5 with respect to OP74

# C Annex C: Uncertainty budget terms.

This section describes the uncertainty budget terms in the case of a calibration with a traveling equipment, including opening and closure measurement at OP.

## C.1 Type A uncertainty.

The statistical uncertainty $u_a$(A-B) for the comparison between two GNSS stations A and B and for each GNSS code is evaluated by computing the upper limit of the error bar of the TDEV at 1 d when possible, or otherwise the upper limit of the last error bar available. The sampling periods of computed calibrated offset usually lead to TDEV data available for 61 440 s and 122 880 s averaging periods. The computed $u_a$ is obtained by a linear interpolation between consecutive TDEV data at an 86 400 s averaging period. When required, a simple quadratic sum leads to the Type A uncertainty required for an uncertainty budget computation.

## C.2 Type B uncertainty.

Here are the $u_b$ uncertainties taken into account in the uncertainty budget computations, together with the way they are estimated when necessary.

- $u_{b,1}$ observed maximum misclosure. This uncertainty component is an estimation of the stability of the traveling equipment during the campaign. The misclosure $u_{b,1}$ we used here is the actual misclosure between the start and the end of the campaign.
- $u_{b,11}$ position error at reference site. The position of the center of phase of traveling antenna is estimated at opening and closure by using the NRCan PPP software, while for the OP reference station antenna the coordinates of the last G1 calibration are used. Note that this computation is achieved by using GPS data only. This might lead to a small bias on the phase center of the antenna for Galileo signals. We safely choose a conventional value of 200 ps ($\sim$ 6 cm) for the position error at the reference site.
- $u_{b,12}$ position error at visited site. At visited sites the position of the center of phase of all antennas is estimated by using the NRCan PPP software. Note that this computation is achieved by using GPS data only. This might lead to a small bias on the phase center of the antenna for Galileo signals. We safely choose a conventional value of 200 ps ($\sim$ 6 cm) for the position error at all visited sites.
- $u_{b,13}$ multipath at reference site. We assume in all cases a conventional value of 200 ps, which is in line with some experiment achieved at OP and ORB, especially when using the calibration software developed at OP, where outliers are properly averaged out. (see [2]).
- $u_{b,14}$ multipath at visited site. Same as above.
- $u_{b,21}$ REFDLY (traveling receiver at reference lab). Uncertainty of the measure of the time difference between the reference point of the traveling receiver and the local timescale. The used value is the quadratic sum of an uncertainty value attributed to the Time Interval Counter (TIC) with the standard deviation of the actual measurement (see [3]). When the REFDLY is obtained by summing several individual measurement the uncertainty is increased by quadratic sum as required. We use 220 ps as conservative conventional value.
- $u_{b,22}$ REFDLY (traveling receiver at visited lab). Same as above. This is possible because the TIC we are using for all REFDLY measurements is traveling along with the OP GNSS stations.
- $u_{b,TOT}$: Quadratic sum of all previous $u_b$.
- $u_{b,31}$ REFDLY uncertainty of the GNSS reference station to its local timescale. Computed similarly as $u_{b,21}$. This term can be set to 0 when the GNSS reference station has been recently calibrated, the uncertainty of REFDLY being already included in the conventional uncertainty decided by the CCTF WG on GNSS.
- $u_{b,32}$ REFDLY uncertainty (at visited lab) of the link of the visited station to its local UTC(k). Computed similarly as $u_{b,21}$. When this delay is measured and the $u_{b,32}$ is taken into account, the local distribution system can be modified afterwards without loosing the calibration of the local GNSS station, provided the new REFDLY is taken into account afterwards
- $u_{b,41}$ uncertainty of the antenna cable delay at reference station. The chosen value here is based on a comprehensive study which is available in reference [4].

- $u_{b,42}$ uncertainty of antenna cable delay at visited station. Same as just above. When for some reason the antenna cable of the traveling system is changed during the campaign, $u_{b,42}$ is typically obtained from the quadratic sum of the uncertainty of the antenna cable delay actually used at the visited station and the uncertainty of the antenna cable delay of the traveling equipment.

- $u_{b,SYS}$: Quadratic sum of all type B uncertainties above.

## C.3 Combined uncertainty.

- $u_{CAL0}$: Quadratic sum of $u_a$ and $u_{b,SYS}$. This uncertainty is for the link between the calibrated station and the reference station, without taking into account the uncertainty of this reference station. Note finally that, in our computation, P3 uncertainty values are not based on a linear combination of P1 and P2 uncertainty values but estimated in a similar way as for P1 and P2. And this is also the case for E3 (resp. B3) uncertainty values, which are computed in a similar way as E1 (resp.B1C) and E5a (resp. B2a) uncertainty values.